Field Theory of Disordered Elastic Interfaces at 3-Loop Order

Christoph Husemann[1] **and Kay Jörg Wiese**[2]

[1]Carl Zeiss AG, Carl Zeiss Promenade 10, D-07745 Jena, Germany

[2]CNRS-Laboratoire de Physique Thorique de l'Ecole Normale Supérieure, PSL Research University, Sorbonne Universités, UPMC, 24 rue Lhomond, 75005 Paris, France.

Abstract

We calculate the effective action for disordered elastic manifolds in the ground state (equilibrium) up to 3-loop order. This yields the renormalziation-group β-function and the critical exponents to third order in $\varepsilon = 4 - d$, in an expansion in the dimension d around the upper critical dimension $d = 4$. The calculations are performed using exact RG, and several other techniques, which allow us to treat the problems associated with the cusp of the renormalized disorder. We also obtain the full 2-point function up to order ε^2, and the correction-to-scaling exponents.

1 Introduction

Disordered systems are notoriously difficult to treat, since simple perturbation theory leads to absurd results, as exemplified by the phenomenon of dimensional reduction [1]. Two main paths out of this dilemma have been pursued: Replica symmetry breaking [2], and the functional renormalization group. The latter goes back to the work by Wilson [3] and Wegner and Houghton [4]. For disordered systems these methods were first used by Daniel Fisher [5]. However it took until 1992 that Narayan and Fisher [6, 7], shortly thereafter followed by Natterman, Stepanow, Tang and Leschhorn [8], recognized that the disorder correlator, which plays the role of the coupling constant in the functional renormalization group (FRG) treatment, has to assume a cuspy form. The physical origin of this cusp lays in the metastability of the zero-temperature states which dominate the partition function, as recognized by Balents, Bouchaud and Mézard [9] in 1996. Only in 2006 this property was given a precise meaning as an observable, which can be measured in a numerical simulation both for the statics [10, 11], the driven dynamics [12, 13], and in an experiment [14]. This was important conceptually, since the very existence of the cusp had in the early days questioned the validity of the method. Once this question of principle was solved, it remained the problems of feasibility *and* practicality: First, whether there is a controlled loop or ε-expansion, and second how to implement a method which makes sense of the cusp in this loop expansion, and more particularly of the derivatives at the cusp. The latter change sign, depending on whether the limit is taken for positive or negative argument, not to mention the additional problems arising for a higher-dimensional field [15]. While these problems were conceptually simple to solve for depinning [16], due to the Middleton-theorem [17], for the statics the question is more delicate. A consistent solution has been given at 2-loop order, based on renormalizability, recursive construction, or consistency schemes (the "sloop-algorithm" to be discussed below) [18, 19], or exact RG [20, 21, 22]. In this article, we extend these methods to 3-loop order, employing both exact RG and self-consistent schemes. As an application, we calculate to 3-loop order the roughness exponent ζ for random-bond disorder, the universal amplitude for periodic disorder, as well as the RG fixed-point functions and universal correction-to-scaling exponents. We also give the complete functional form of the universal 2-point function up to 2-loop order.

Our results are relevant for a remarkably broad set of problems, from subsequences of random permutations in mathematics [23], random matrices [24, 25] to growth models [26, 27, 28, 29, 30, 31, 32, 33, 34] and Burgers turbulence in physics [35, 36], as well as directed polymers [26, 37] and optimization problems such as sequence alignment in biology [38, 39, 40]. Furthermore, they are very useful for numerous experimental systems, each with its specific features in a variety of situations. Interfaces in magnets [41, 42] experience either short-range disorder (random bond RB), or long range (random field RF). Charge density waves (CDW) [43] or the Bragg glass in superconductors [44, 45, 46, 47, 48] are periodic objects pinned by disorder. The contact line of a meniscus on a rough substrate is governed by long-range elasticity [14, 49, 50, 51, 52]. All these systems can be parameterized by a N-component height or displacement field $u(x)$, where x denotes the d-dimensional internal coordinate of the elastic object. An interface in the 3D random field Ising model has $d = 2$, $N = 1$, a vortex lattice $d = 3$, $N = 2$, a contact-line $d = 1$ and $N = 1$. The so-called directed polymer ($d = 1$) subject to a short-range correlated disordered potential has been much studied [53] as it maps onto the Kardar-Parisi-Zhang growth model [26, 34, 31] for any N, and yields an important check for the roughness exponent, defined below, $\zeta_{\rm eq,RB}(d = 1, N = 1) = 2/3$. Another important field of applications are avalanches, in magnetic systems known as Barkhausen noise. For applications and the necessary theory see e.g. [54, 55, 56, 57, 58, 59, 60, 61, 62, 63].

2 Model and basic definitions

The equilibrium problem is defined by the partition function $\mathcal{Z} := \int \mathcal{D}[u] \, \exp(-\mathcal{H}[u]/T)$ associated to the Hamiltonian (energy)

$$\mathcal{H}[u] = \int \mathrm{d}^d x \, \frac{1}{2} \left[\nabla u(x)\right]^2 + \frac{m^2}{2} \left[u(x) - w\right]^2 + V\big(u(x), x\big) \; . \tag{2.1}$$

In order to simplify notations, we will often note

$$\int_x f(x) := \int \mathrm{d}^d x \, f(x) \; , \tag{2.2}$$

and in momentum space

$$\int_q \tilde{f}(q) := \int \frac{\mathrm{d}q^d}{(2\pi)^d} \tilde{f}(q) \; . \tag{2.3}$$

The Hamiltonian (2.1) is the sum of the elastic energy $\int_x \frac{1}{2} \left[\nabla u(x)\right]^2$ plus the confining potential $\frac{m^2}{2} \int_x \left[u(x) - w\right]^2$ which tends to suppress fluctuations away from the ordered state $u(x) = w$, and a random potential $V(u, x)$ which enhances them. w is, up to a factor of m^2, an applied external force, which is useful to measure the renormalized disorder [10, 11, 12, 13, 14, 63, 64], or properly define avalanches [12, 13, 52, 65, 66, 67, 68]. The resulting roughness exponent ζ

$$\overline{\langle [u(x) - u(x')]^2 \rangle} \sim |x - x'|^{2\zeta} \tag{2.4}$$

is measured in experiments for systems at equilibrium ($\zeta_{\rm eq}$) or driven by a force f at zero temperature (depinning, $\zeta_{\rm dep}$). Here and below $\langle \dots \rangle$ denote thermal averages and $\overline{(\dots)}$ disorder ones. In the zero-temperature limit, the partition function is dominated by the ground state, and we may drop the explicit thermal averages. In some cases, long-range elasticity appears, e.g. for a contact line by integrating out the bulk-degrees of freedom [51], corresponding to $q^2 \to |q|$ in the elastic energy. The random potential can without loss of generality [18, 19] be chosen Gaussian with second cumulant

$$\overline{V(u,x)V(u',x')} =: R_0(u-u')\delta^d(x-x') \,. \tag{2.5}$$

$R_0(u)$ takes various forms: Periodic systems are described by a periodic function $R_0(u)$, random-bond disorder by a short-ranged function, and random-field disorder of variance σ by $R(u) \simeq -\sigma|u|$ at large u. Although this paper is devoted to equilibrium statics, some comparison with dynamics will be made and it is thus useful to indicate the corresponding equation of motion. Adding a time index to the field, $u(x) \to u(x,t)$, the latter reads

$$\eta\partial_t u(x,t) = -\frac{\delta\mathcal{H}[u]}{\delta u(x,t)} = \nabla_x^2 u(x,t) + m^2[w-u(x,t)] + F\left(u(x,t),x\right) \,, \tag{2.6}$$

with friction η. The (bare) pinning force is $F(u,x) = -\partial_u V(u,x)$, with correlator

$$\Delta_0(u) = -R_0''(u) \,. \tag{2.7}$$

To average over disorder, we replicate the partition function n times, $\overline{\mathcal{Z}^n} =: \mathrm{e}^{-\mathcal{S}}$, which defines the effective action $\mathcal{S}$,

$$\mathcal{S}[u] = \sum_{a=1}^{n} \frac{1}{2T}\int_x [\nabla u_\alpha(x)]^2 + \frac{m^2}{2T}u_a(x)^2 - \frac{1}{2T^2}\int_x \sum_{a,b=1}^{n} R_0\big(u_a(x)-u_b(x)\big) \tag{2.8}$$

We used the notations introduced in Eqs. (2.2) and (2.3). In presence of external sources j_a, the n-times replicated action becomes

$$\mathcal{Z}[j] := \int \prod_{a=1}^{n} \mathcal{D}[u_a]\, \exp\left(-\mathcal{S}[u] + \int_x \sum_a j_a(x)u_a(x)\right) \,, \tag{2.9}$$

from which all static observables can be obtained. a runs from 1 to n, and the limit of zero replicas $n=0$ is implicit everywhere.

3 Summary of main results

Here we summarize the main results. Their derivation is given in the following sections.

3.1 3-loop β-function

In generalization of Eq. (3.43) of [18, 19], we obtain the following functional renormalization group equation for the renormalized, dimensionless disorder correlator $\tilde{R}(u)$,

$$\begin{aligned}
-m\partial_m \tilde{R}(u) = {} & (\varepsilon - 4\zeta)\tilde{R}(u) + \zeta u\tilde{R}'(u) + \tfrac{1}{2}\tilde{R}''(u)^2 - \tilde{R}''(u)\tilde{R}''(0) \\
& + \left(\tfrac{1}{2} + \varepsilon\,\mathcal{C}_1\right)\left[\tilde{R}''(u)\tilde{R}'''(u)^2 - \tilde{R}''(0)\tilde{R}'''(u)^2 - \tilde{R}''(u)\tilde{R}'''(0^+)^2\right] \\
& + \mathcal{C}_2\left[\tilde{R}'''(u)^4 - 2\tilde{R}'''(u)^2\tilde{R}'''(0^+)^2\right] + \mathcal{C}_3\left[\tilde{R}''(u) - \tilde{R}''(0)\right]^2\tilde{R}''''(u)^2 \\
& + \mathcal{C}_4\left[\tilde{R}''(u)\tilde{R}'''(u)^2\tilde{R}''''(u) - \tilde{R}''(0)\tilde{R}'''(u)^2\tilde{R}''''(u) - \tilde{R}''(u)\tilde{R}'''(0^+)^2\tilde{R}''''(0)\right] .
\end{aligned} \tag{3.1}$$

The coefficients are

$$\mathcal{C}_1 = \frac{1}{4} + \frac{\pi^2}{9} - \frac{\psi'(\frac{1}{3})}{6} = -0.3359768096723647... \tag{3.2}$$

$$\mathcal{C}_2 = \frac{3}{4}\zeta(3) + \frac{\pi^2}{18} - \frac{\psi'(\frac{1}{3})}{12} = 0.6085542725335131... \tag{3.3}$$

$$\mathcal{C}_3 = \frac{\psi'(\frac{1}{3})}{6} - \frac{\pi^2}{9} = 0.5859768096723648... \tag{3.4}$$

$$\mathcal{C}_4 = 2 + \frac{\pi^2}{9} - \frac{\psi'(\frac{1}{3})}{6} = 1.4140231903276352... \,. \tag{3.5}$$

The first line contains the rescaling and 1-loop terms, the second line the 2-loop terms, and the last two lines the three 3-loop terms. Note that $\mathcal{C}_1 = \frac{1}{4} - \mathcal{C}_3$, and $\mathcal{C}_4 = 2 - \mathcal{C}_3 = \sqrt{2} - 0.000190372...$

3.2 Fixed points and critical exponents

There are four generic distinct disorder classes, corresponding to random-bond, random-field, random-periodic, and generic long-ranged disorder. While we will discuss the details in section 9, we give a summary here.

3.2.1 Random-bond disorder

If the microscopic disorder potential is short-ranged, which corresponds to random-bond disorder in magnetic systems, then the roughness exponent can be calculated in an $\varepsilon = 4 - d$ expansion:

$$\zeta = \varepsilon\zeta_1 + \varepsilon^2\zeta_2 + \varepsilon^3\zeta_3 + \mathcal{O}(\varepsilon^4) \tag{3.6}$$

$$\zeta_1 = 0.2082980628(7) \tag{3.7}$$

$$\zeta_2 = 0.006857(8) \tag{3.8}$$

$$\zeta_3 = -0.01075(2)\,. \tag{3.9}$$

This series expansion has a rather large third-order coefficient. As we will discuss in the Conclusions, this is a little surprising, since one might expect the expansion to converge, contrary to φ^4-theory which has a divergent, but Borel-summable series expansion.

One can use a Padé resummation to improve the expansion. Asking that all Padé coefficients are positive singles out the (2,1)-approximant. It is given by

$$\zeta_{(2,1)} \approx \frac{0.208298\varepsilon + 0.333429\varepsilon^2}{1 + 1.56781\varepsilon} + \mathcal{O}(\varepsilon^4)\,. \tag{3.10}$$

Adding a 4-loop term, and asking that in dimension one the exact result is reproduced, i.e. $\zeta(\varepsilon = 3) = 2/3$, and choosing the Padé with positive coefficients only, leads to

$$\zeta \approx \frac{0.0021794\varepsilon^4 + 0.333429\varepsilon^2 + 0.208298\varepsilon}{1.56781\varepsilon + 1} + \mathcal{O}(\varepsilon^4)\,. \tag{3.11}$$

Details can be found in section 9.1.

3.2.2 Random-field disorder

The roughness exponent is given

$$\zeta_{\mathrm{RF}} = \frac{\varepsilon}{3} , \tag{3.12}$$

a result exact to all orders in ε. The amplitude of the 2-point function can be calculated analytically. It is given by

$$\overline{\langle \tilde u(q)\tilde u(q')\rangle} = \tilde c(d) m^{-d-2\zeta_{\mathrm{RF}}} F_d(q/m) \tag{3.13}$$

$$F_d(0) = 0 , \quad F_d(z) \simeq B(d) z^{-d-2\zeta_{\mathrm{RF}}} \text{ for } z \to \infty \tag{3.14}$$

$$\tilde c(d) \approx \frac{\varepsilon^{\frac13}\sigma^{\frac23}}{0.283721 + 0.058367\varepsilon + 0.064888\varepsilon^2} + \mathcal{O}(\varepsilon^{\frac{10}{3}}) \tag{3.15}$$

$$B(d) \approx \frac{1+0.226789\varepsilon}{1+0.560122\varepsilon} + \mathcal{O}(\varepsilon^3) . \tag{3.16}$$

An analytical result is given in Eq. (8.27) ff. We have again given the Padé approximants with only positive coefficients. Translating to position space yields

$$\frac12 \overline{\langle [u(x)-u(0)]^2\rangle} = \frac{-\Gamma(-\frac{\varepsilon}{3})\tilde c(d) B(d)}{(4\pi)^{\frac d2}\Gamma\left(\frac{d+8}{6}\right)} \left(\frac{x}{2}\right)^{\frac{2\varepsilon}{3}} \tag{3.17}$$

The renormalization-group fixed point function $R(u)$ for the disorder can in this case be calculated analytically to third order in ε. The result, together with details on the calculations is given in section 9.2.

3.2.3 Periodic disorder

For periodic disorder, the 2-point function is always a logarithm in position space, with universal amplitude, corresponding to

$$\zeta_{\mathrm{RP}} = 0 . \tag{3.18}$$

The scaling functions are defined as for RF disorder, and read

$$\overline{\langle \tilde u(q)\tilde u(q')\rangle} = \tilde c(d) m^{-d} F_d(q/m) \tag{3.19}$$

$$F_d(0) = 0 , \quad F_d(z) \simeq B(d) z^{-d} \text{ for } z \to \infty \tag{3.20}$$

$$\tilde c(d) \approx \frac{2.19325\varepsilon}{1+0.310238\varepsilon + 1.33465\varepsilon^2} + \mathcal{O}(\varepsilon^4) \tag{3.21}$$

$$B(d) \approx \frac{1+0.134567\varepsilon}{1+1.13457\varepsilon} + \mathcal{O}(\varepsilon^3) . \tag{3.22}$$

An analytical result is given in Eq. (8.28) ff. The Padé approximants are again given with only positive coefficients. Translating to position space yields, with a microscopic cutoff a

$$\frac12 \overline{\langle [u(x)-u(0)]^2\rangle} = \frac{2\tilde c(d) B(d)}{(4\pi)^{\frac d2}\Gamma(\frac d2)} \ln|x/a| . \tag{3.23}$$

Details are presented in sections 8.3 and 9.3.

3.3 Correction-to-scaling exponent

The correction-to-scaling exponent ω quantifies how an observable $\mathcal{O}$, or a critical exponent, approaches its value at the IR fixed point at length scale ℓ or at mass m

$$\mathcal{O} - \mathcal{O}_{\text{fix-point}} \sim \ell^{-\omega} \sim m^{\omega} \ . \tag{3.24}$$

For the fixed points studied above, the correction-to-scaling exponents are follows.
Random-Periodic fixed point:

$$\omega_{\text{RP}} = -\varepsilon + \frac{2\varepsilon^2}{3} - \left(\frac{4\zeta(3)}{3} + \frac{5}{9}\right)\varepsilon^3 + \mathcal{O}(\varepsilon^4) = -\varepsilon\,\frac{1 + \left[2\zeta(3) + \frac{1}{6}\right]\varepsilon}{1 + \left[2\zeta(3) + \frac{5}{6}\right]\varepsilon} + \mathcal{O}(\varepsilon^4) \ . \tag{3.25}$$

Random-Bond fixed point:

$$\omega_{\text{RB}} \approx -\varepsilon + 0.4108\varepsilon^2 + \mathcal{O}(\varepsilon^3) = -\frac{\varepsilon}{1 + 0.4108\varepsilon} + \mathcal{O}(\varepsilon^3) \ . \tag{3.26}$$

Random-Field fixed point:

$$\omega_{\text{RF}} \approx -\varepsilon + 0.1346\varepsilon^2 + \mathcal{O}(\varepsilon^3) = -\frac{\varepsilon}{1 + 0.1346\varepsilon} + \mathcal{O}(\varepsilon^3) \ . \tag{3.27}$$

Note that for the RP fixed point, we have given the solution up to 3-loop order. For the other fixed points, we have not attempted to solve the RG equations at this order, as this problem can only be tackled via shooting, which is already difficult at second order. Also, as the 2-loop result seems to be quite reliable, whereas corrections for ζ are large at 3-loop order, we expect the same to be true for ω, which justifies to stop the expansion at second order.

Finally, we can perform the same analysis at depinning, with results as follows:
Random-Field fixed point at depinning:

$$\omega_{\text{RF}}^{\text{depinning}} \approx -\varepsilon - 0.0186\varepsilon^2 + \mathcal{O}(\varepsilon^3) = -\frac{\varepsilon}{1 - 0.0186\varepsilon} + \mathcal{O}(\varepsilon^3) \ . \tag{3.28}$$

Random-Periodic fixed point at depinning:

$$\omega_{\text{RP}}^{\text{depinning}} = -\varepsilon + \frac{2\varepsilon^2}{3} + \mathcal{O}(\varepsilon^3) \ . \tag{3.29}$$

Strangely, while the RP fixed point at depinning is different, the correction-to-scaling exponent ω does not change, at least to second order.

3.4 Other results

A fixed-point function can also be constructed for generic long-ranged disorder, growing (or decaying) at large distances as $R(u) \simeq u^{\alpha}$, with $\alpha = 1$ being random-field disorder discussed above. The idea is the same, in all cases the tail for large u does not get corrected.

Let us also mention that we have analytical results for the scaling function $F_d(z)$, in an ε expansion to second order.

4 Lifting ambiguities in a non-analytic theory, summary

Ambiguities arise in a perturbative computation of the effective action if one uses a non-analytic action. To resolve this issue, several methods have been designed, of which we list the most important ones below. Some failed attempts at 2-loop order are described in Ref. [19]. In addition, the physics of the problem requires the theory to be renormalizable, potential and without super-cusp, which gives valuable checks on the values of the "anomalous" graphs.

1) Exact RG. The starting point of exact RG (ERG) methods are exact relations between functionals, for reviews see [69, 22]. A systematic but straightforward expansion in ε combines the anomalous terms from naive perturbation theory in a way that makes them automatically non-ambiguous. This method and the corresponding derivation of the β-function is discussed in Section 5.

2) Elimination of sloops. The idea, which will be explained in detail in Section 6.1 below, is as follows: Since the propagator $\langle \tilde{u}_a(k)\tilde{u}_b(-k)\rangle = T\delta_{ab}/(k^2+m^2)$ is diagonal in replica space, each contraction in a diagram reduces the number of free replica sums by at most one. Doing a contraction which does not constrain the number of replicas further counts as a factor of $T = 0$, and can thus be set to zero. Further contracting such diagrams generates a set of identities which, remarkably, is sufficient to obtain unambiguously the 2-replica projection without any further assumption. In some sense, it uses in a non-trivial way the constraint that we are working with a true $T = 0$ theory.

3) Recursive construction: An efficient method is to construct diagrams recursively. The idea is to identify in a first step parts of the diagram, which can be computed without ambiguity. This is e.g. the 1-loop chain-diagram discussed in Section 6.1. In a second step, one treats the already calculated sub-diagrams as effective vertices. In general, these vertices have the same analyticity properties, namely are derivable twice, and then have a cusp. (Compare $R(u)$ with $[R''(u) - R''(0)]R'''(u)^2 - R''(u)R'''(0^+)^2$, which is a contribution to the β-function at 2-loop order). By construction, this method ensures renormalizability, at least as long as there is only one possible path. However it is not more general than the demand of renormalizability diagram by diagram, discussed below.

4) Renormalizability diagram by diagram: Renormalizability diagram by diagram is the key to all proofs of perturbative renormalizability in field-theory, see e.g. [70, 71, 72, 73, 74, 75, 76, 77]. These methods define a subtraction operator $\mathbf{R}$. Graphically it can be constructed by drawing a box around each sub-divergence, which leads to a *forest* or *nest* of sub-diagrams (the counter-terms in the usual language), which have to be subtracted, rendering the diagram *finite*. The advantage of this procedure is that it explicitly assigns all counter-terms to a given diagram, which finally yields a proof of perturbative renormalizability. If we demand that this proof goes through for the *functional* renormalization group, the counter-terms must necessarily have the same functional dependence on $R(u)$ as the diagram itself. In general, the counter-terms are less ambiguous, and this procedure can thus be used to lift ambiguities in the calculation of the diagram itself. By construction this procedure is very similar to the recursive construction discussed under point 3, and it is build in to the ERG approach.

It has some limitations though. Indeed, if one applies this procedure to the 3-loop calculation, one finds that it renders unique all but one ambiguous diagram, namely

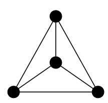 , (4.1)

which has no subdivergence. Thus there are no counter-terms which could lift the ambiguities. This diagram must therefore be computed directly and we found that it can be obtained unambiguously by the sloop elimination method. We will not give a detailed explanation of this method here, since we will not need it, and it is well documented, see section VD of [19].

5) Reparametrization invariance: From standard field theory, one knows that RG functions are not unique, but depend on the renormalization scheme. Only critical exponents are unique. This is reflected in the freedom to reparametrize the coupling constant g according to $g \longrightarrow \tilde{g}(g)$ where $\tilde{g}(g)$ is a smooth function, which has to be invertible in the domain of validity of the RG β-function.

Here we have chosen a scheme, namely defining $R(u)$ from the exact zero momentum effective action, using dimensional regularization, and a mass. One can explore the freedom in performing reparametrizations. In the functional RG framework, reparameterizations are also functional, of the form

$$R(u) \;\longrightarrow\; \hat{R}(u) = \hat{R}[R](u) \; . \tag{4.2}$$

Of course the new function $\hat{R}(u)$ does not have the same meaning as $R(u)$. Perturbatively this reads

$$R(u) \;\longrightarrow\; \hat{R}(u) = R(u) + B(R,R)(u) + O(R^3) \; , \tag{4.3}$$

where $B(R,R)$ is a functional of R. For consistency, one has to demand that $B(R,R)$ has the same analyticity properties as R, at least at the fixed point $\tilde{R} = \tilde{R}^*$, i.e. $B(R,R)$ should as R be twice differentiable and then have a cusp. Details can be found in Section 7.

As far as applicable, all methods, who are are genuinely different, give consistent results. This is strong evidence that the problem has a unique field theory, which we identify in this paper to 3-loop order. In particular, the ambiguities which arise in perturbation theory due to the cusp turn out to be superficial and are absent in our treatment. Let us now turn to actual calculations using these methods. We start with the ERG approach. We will then use renormalized field theory and a combination of the above-mentioned methods. Let us stress that these two calculations were done independently by the two authors, which serves as a non-trivial check of the RG β-function such obtained.

5 Calculation via the Exact Renormalization Group

In this section we derive the 3-loop flow equations by means of the exact renormalization group (ERG). In condensed matter this RG is sometimes called "functional RG" because it is based on exact flow equations formulated for thermodynamic functionals. To avoid possible confusions, we will use the term "functional RG" only in the sense of perturbative field theory, i.e. as a loop expansion.

5.1 Set-up of ERG equation

For each realization of the random potential V, let Z_V be the partition function. By the standard replica trick we average the logarithm of Z_V over disorder

$$\overline{\ln Z_V} = \lim_{n\to 0} \frac{1}{n} \left(\overline{Z_V^n} - 1 \right) \tag{5.1}$$

by introducing replicas of the field. The replicated partition function is written as a functional integral

$$e^{W[j]} = \mathcal{N}_0 \int \prod_x \prod_{a=1}^{n} \mathrm{d}u_a(x)\, e^{-S[u]+(j,u)} \; . \tag{5.2}$$

It depends on an external replica-dependent field $j_a(x)$ with $a = 1 \dots n$. We choose $\mathcal{N}_0 = (\overline{Z_V^n})^{-1}$ such that $e^{W[0]} = 1$. We denote $(j,u) = \sum_a \int \mathrm{d}^d x \, j_a(x) u_a(x)$ and the replicated action is given by

$$S[u] = \frac{1}{2T} \sum_a \int \mathrm{d}^d x \big[(\nabla_x u_a)^2 + m^2 u_a(x)^2\big] - \frac{1}{2T^2} \sum_{a,b} \int \mathrm{d}^d x \; R_0\big(u_a(x) - u_b(x)\big) \, . \tag{5.3}$$

Correlation functions and other observables averaged over disorder can be calculated from replica averages obtained from a polynomial expansion of $W[j]$, see Ref. [22] for details. For example, the connected 2-point correlation function is given by

$$\overline{\langle u(x)u(y)\rangle_V} - \overline{\langle u(x)\rangle_V}\,\overline{\langle u(y)\rangle_V} = \lim_{n\to 0} \Big[\langle u_1(x)u_1(y)\rangle_{\text{rep}} - \langle u_1(x)u_2(y)\rangle_{\text{rep}}\Big] \, , \tag{5.4}$$

where $\langle u_a(x)u_b(y)\rangle_{\text{rep}} = \frac{\delta^2}{\delta j_a(x)\delta j_b(y)}_{|j=0} W[j]$. Note that $\langle u_a(x)\rangle_{\text{rep}} = \frac{\delta}{\delta j_a(x)}_{|j=0} W[j] = 0$ since $S[u] = S[-u]$.

The mass $m^2 > 0$ provides an infrared regularization, and we are interested in the limit $m^2 \to 0$. The ERG is set up by successively lowering the parameter m^2, which we call RG scale. Since the action $S[u]$ depends on m only via its quadratic part in the fields, the scale derivative of $W[j]$ can be expressed by a Polchinski-type equation

$$\dot{W}[j] = \frac{\mathrm{d}}{\mathrm{d}m} W[j] = -\frac{1}{2}\left(\frac{\delta W}{\delta j}, \dot{q}\frac{\delta W}{\delta j}\right) - \frac{1}{2}\mathrm{Tr}\left[\dot{q}\frac{\delta^2 W}{\delta j^2}\right] \, . \tag{5.5}$$

Here $q_{ab}(p) = T^{-1}(p^2 + m^2)\delta_{ab}$ denotes the bare inverse thermal propagator of the action.

The second term in $S[u]$ is invariant under a shift with a replica independent field. This is expressed by the so called statistical tilt symmetry (STS)

$$W[j + \tilde{j}] = W[j] + \frac{1}{2}(\tilde{j}, g\tilde{j}) + (j, g\tilde{j}) \, , \tag{5.6}$$

where $\tilde{j}$ is a replica-independent field and $g_{ab}(q) = q_{ab}(q)^{-1}$. It follows that the thermal propagator

$$\lim_{n\to 0} \sum_a \frac{\delta^2 W}{\delta j_a(x)\delta j_b(y)}\Big|_{j=0} = \lim_{n\to 0} \sum_a g_{ab}(x,y) \tag{5.7}$$

is not renormalized.

A Legendre transform of $W[j]$ allows a more convenient expansion in loops. For this we define a functional map $u_a \mapsto J_a[u]$ such that $\frac{\delta}{\delta j_a(x)} W[j]\Big|_{j_a = J_a[u]} = u_a(x)$. This map exists, since the second functional derivative of W is positive for $m > 0$ at $j = 0$. The Legendre transform is defined as

$$\Gamma[u] = -W[J[u]] + (J[u], u) \tag{5.8}$$

and is called the effective action. Therefore $\frac{\delta}{\delta u_a(x)}\Gamma[u] = J_a[u](x)$ and $\frac{\delta^2 \Gamma}{\delta u^2} = \left(\frac{\delta^2 W}{\delta j^2}\Big|_{j=J[u]}\right)^{-1}$ is the inverse full propagator.

The Legendre transformed version of the statistical tilt symmetry reads

$$\Gamma[u + \tilde{u}] = \Gamma[u] + \frac{1}{2}(\tilde{u}, q\tilde{u}) + (u, q\tilde{u}) \tag{5.9}$$

with the field $\tilde{u}$ again being replica-independent. Because there is no thermal self-energy we write $\Gamma[u] = \frac{1}{2}(u, g^{-1}u) - \hat{\Gamma}[u]$. The flow equation for $\hat{\Gamma}$ follows from $\dot{\Gamma} = -\dot{W}$ and reads

$$\dot{\hat{\Gamma}}[u] = \frac{1}{2}\mathrm{Tr}\left[g\dot{q}\left(1 - g\frac{\delta^2\hat{\Gamma}}{\delta u^2}\right)^{-1}\right] . \tag{5.10}$$

In the limit $m \to \infty$ the effective action becomes the bare action without regularization

$$\lim_{m\to\infty} \Gamma[u] = S[u]\big|_{m=0} . \tag{5.11}$$

5.2 Replica expansion hierarchy

We expand the effective action in the number of replica sums

$$\Gamma[u] = \frac{1}{2}(u, g^{-1}u) - \frac{1}{2T^2}\sum_{a,b} R[u_{ab}] - \sum_{n\geq 3}\frac{1}{n!T^n}\sum_{a_1,\ldots a_n} S^{(n)}[u_{a_1}, \ldots u_{a_n}] \tag{5.12}$$

where we use the shorthand notation $u_{ab}(x) = u_a(x) - u_b(x)$. Due to STS the one-replica term is given by the bare inverse thermal propagator. The two-replica term is a scale-dependent functional that depends on $u_{ab}(x)$ only. The initial condition for R is local and given by the bare disorder distribution function

$$\lim_{m\to\infty} R[u] = \int \mathrm{d}^d x \; R_0(u(x)) . \tag{5.13}$$

Higher replica terms are not present in the bare action but they are generated by the RG flow. STS implies that

$$S^{(n)}[u_{a_1}, \ldots u_{a_n}] = S^{(n)}[u_{a_1} + v, \ldots u_{a_n} + v] \tag{5.14}$$

for any field $v(x)$. It follows that the two-replica term $S^{(2)}[u_a, u_b] = R[u_{ab}]$ is a functional of only one field. Because of the sum over all replica indices, we assume all n-replica terms or Γ-cumulants to be symmetric under permutation of the replica fields.

We use the following compressed notation for functional derivatives of n-replica terms to denote p_1 derivatives with respect to field u_{a_1} and similarly p_i derivatives with respect to field u_{a_i} for $i = 1, \ldots n$

$$S^{(n)}_{p_1\ldots p_n}[u_{a_1\ldots a_n}](x_1, \ldots x_{p_{\max}}) = \frac{\delta}{\delta u_{a_1}(x_1)} \cdots \frac{\delta}{\delta u_{a_1}(x_{p_1})}\frac{\delta}{\delta u_{a_2}(x_{p_1+1})} \cdots \frac{\delta}{\delta u_{a_n}(x_{p_{\max}})} S^{(n)}[u_{a_1\ldots a_n}] \tag{5.15}$$

with the total number of derivatives $p_{\max} = \sum_{i=1}^n p_i$ and the short-hand notation $S^{(n)}[u_{a_1\ldots a_n}] = S^{(n)}[u_{a_1} \ldots u_{a_n}]$. For example, using permutation symmetry, the second functional derivative of Γ is given by

$$\begin{aligned}\frac{\delta^2\hat{\Gamma}}{\delta u_a(x)\delta u_b(x)} = \sum_{n=2}^{\infty}\frac{1}{(n-1)!T^n}\sum_{a_2\ldots a_n}\Big[&S^{(n)}_{20\ldots 0}[u_a, u_{a_2}, \ldots u_{a_n}](x,y)\delta_{ab} \\ &+ \frac{1}{T}S^{(n+1)}_{110\ldots 0}[u_a, u_b, u_{a_2}, \ldots u_{a_n}](x,y)\Big] + \frac{1}{T^2}S^{(2)}_{11}[u_a, u_b](x,y) .\end{aligned} \tag{5.16}$$

Symmetrization over fields is denoted by curly brackets, that is, $\{\dots\}$ is the symmetrization of $\dots$ over all its variables. Differentiating Eq. (5.14) and using permutation symmetry implies that

$$
\begin{aligned}
0 &= \frac{\delta^2}{\delta v(x)\delta v(y)}\bigg|_{v=0} S^{(n)}[u_{a_1}+v,\dots u_{a_n}+v] \\
&= n\{S_{20\dots0}[u_{a_1}\dots u_{a_n}](x,y)\} + 2n(n-1)\{S_{110\dots0}[u_{a_1}\dots u_{a_n}](x,y)\}\ .
\end{aligned}
\tag{5.17}
$$

Because we are interested in the limit of the number of replica indices $n \to 0$, we are free to add any function that depends on $k < n$ replicas to a n-th cumulant. This "gauge invariance" will be used later to get rid of constant terms in the cumulants.

Via Legendre transformation there is a one-to-one correspondence of Γ-cumulants to cumulants obtained from a replica expansion of $W[j]$, see Ref. [22]. Therefore, the Γ-cumulants can be used to calculate observables. In particular, the exact 2-point correlation function averaged over disorder is given by

$$
\overline{\langle u(p)u(-p)\rangle_V} = \lim_{n\to 0}\left(\frac{\delta^2\Gamma}{\delta u_a(p)\delta u_b(-p)}\bigg|_{u=0}\right)^{-1}_{a=b} = \frac{T}{m^2+p^2} - \frac{1}{\left[m^2+p^2\right]^2}\frac{\delta^2 R[u]}{\delta u(p)\delta u(-p)}\bigg|_{u=0}\ ,
\tag{5.18}
$$

where, compared to leading-order perturbation theory, the second derivative of the bare function $R_0(u)$ is replaced by the second derivative of the renormalized functional $R[u]$.

In order to obtain RG equations for each Γ-cumulant, we expand the inverse in Eq. (5.10) in a geometric series

$$
\dot{\hat{\Gamma}}[u] = \frac{1}{2}\sum_{l\geq 0}\mathrm{Tr}\left[g\,\dot{q}\left(g\frac{\delta^2\hat{\Gamma}}{\delta u^2}\right)^l\right]\ ,
\tag{5.19}
$$

insert Eq. (5.16), and count the number of replica sums. The propagators g and $g\dot{q}g = -\dot{g}$ are diagonal in replica space. Replica sums arise from second derivatives of $\hat{\Gamma}$, their matrix products, and one additional sum from the trace. Therefore, in order to calculate the flow equation of the n-th cumulant, the geometric series in Eq. (5.19) does not contribute for $l > n$. On the other hand, a term in the geometric series of l-th order contributes to cumulants to all order $n \geq l$. That is, for any initial action the RG flow generates cumulants to all orders.

The term $l = 0$ and the one-replica term in $l = 1$ in Eq. (5.19) are constants and can therefore be neglected due to gauge invariance. Evaluating the two-replica contributions in the $l = 1$ and $l = 2$ terms give the flow equation

$$
\begin{aligned}
\dot{R}[u] = &\int_{x_1,x_2}\dot{g}(x_1,x_2)\left[T\mathcal{R}''[u](x_2,x_1) + S^{(3)}_{110}[0,0,-u]\right] \\
&+ \frac{1}{2}\int_{x_1,\dots,x_4}\left[\frac{\mathrm{d}}{\mathrm{d}m}g(x_1,x_2)g(x_3,x_4)\right]\mathcal{R}''[u](x_2,x_3)\mathcal{R}''[u](x_4,x_1)
\end{aligned}
\tag{5.20}
$$

where $\mathcal{R}''[u] = R''[u] - R''[0]$. The evaluation at zero field arises in terms of coinciding replica indices. We note that Eq. (5.20) is a non-linear integro-differential equation for a functional. Similar equations can be obtained for higher cumulants, $\dot{S}^{(3)}$ and $\dot{S}^{(4)}$; they are given in Appendix B.1. Due to the $l = 1$ term in Eq. (5.19) there is a contribution from $S^{(m+1)}$ to $\dot{S}^{(m)}$. Therefore, in order to obtain exact solutions for the Γ-cumulants, one has to consider the full, infinitly large hierarchy. Note that, formally, up to now no approximations were made; in particular, we do not encounter ambiguities when a cusp in the second derivative of the local disorder distribution function develops.

5.3 ε-expansion for $T = 0$

Since we cannot treat an infinite hierarchy, we perform an additional expansion in $\varepsilon = 4 - d$. To this aim we split the disorder distribution functional $R[u]$ into a local and a non-local part

$$R[u] = \int \mathrm{d}^d x\, R(u(x)) + \hat{R}[u] \,. \tag{5.21}$$

If $u(x) = u_0$ is a constant field, then $\hat{R}[u_0] = 0$, so that only the local part contributes, $R[u_0] = L^d R(u_0)$, where $L^d = \int \mathrm{d}^d x$ is the volume of the system. Note that $R[u]$ and $\hat{R}[u]$ are functionals, whereas $R(u)$ is a function. For $m \to \infty$ the disorder-distribution function has only a local part, which we assume to be *small*. That is, $R_0(u)$ and all its derivatives are uniformly bound by a small constant[1]. We also assume that the local part $R(u)$ of the renormalized disorder distribution function remains small. Then the ε-expansion can be obtained by expanding the replica expansion hierarchy in $R(u)$. From now on we set the temperature to $T = 0$. Because the rescaled temperature T becomes small for small m, the ε-expansion can also be obtained for $T > 0$ by a composite expansion in T and $R(u)$.

Suppose that $R(u) \sim \mathcal{O}(\varepsilon)$. Since for $T = 0$, Eq. (5.20) is quadratic in $\mathcal{R}''$, the non-local part of the renormalized disorder distribution function will be $\hat{R}[u] \sim \mathcal{O}(\varepsilon^2)$. A similar argument for the higher Γ-cumulants gives $S^{(n)} \sim \mathcal{O}(\varepsilon^n)$ for $n \geq 3$. The assumption that also all derivatives of the cumulants remain of the same order has to be checked; we will do so up to order ε^4, that is, 3-loop order. With this method the 2-loop order was already obtained in Ref. [22] before.

The 1-loop equation can be obtained by an expansion to second order in ε and can directly be read off from Eq. (5.20). We use that

$$R''[u](x_1, x_2) = R''\big(u(x_1)\big)\delta(x_1 - x_2) + \hat{R}''[u](x_1, x_2) \,, \tag{5.22}$$

where the second term is already $\mathcal{O}(\varepsilon^2)$ and does not contribute to Eq. (5.20) at 1-loop order. We therefore find

$$\dot{R}[u] = \frac{1}{2} \int_{x_1, x_2} \left[\frac{\mathrm{d}}{\mathrm{d}m} g(x_1, x_2)^2 \right] \mathcal{R}''\big(u(x_1)\big)\mathcal{R}''\big(u(x_2)\big) + \mathcal{O}(\varepsilon^3) \,, \tag{5.23}$$

where $\mathcal{R}''(u) := R''(u) - R''(0)$. The local part is obtained by inserting the constant field $u(x) = u_0$ and dividing by L^d

$$\dot{R}(u_0) = \frac{1}{2} \dot{I}_1 \mathcal{R}''(u_0)^2 + \mathcal{O}(\varepsilon^3) \tag{5.24}$$

where after Fourier transformation $I_1 = \int_p g(p)^2 \sim \mathcal{O}(\frac{m^{-\varepsilon}}{\varepsilon})$, and so $\dot{I}_1 \sim \mathcal{O}(1)$. The diagram I_1 is evaluated in Eq. (A.6). In order to have the simplist possible formulas, we will absorb a factor of $\varepsilon I_1|_{m=1}$ into the renormalized disorder, see Eq. (6.43). This effectively sets I_1 to $m^{-\varepsilon}/\varepsilon$. For an n-loop integral I_n we will have to evaluate the ratio I_n / I_1^n. We believe this to be the most convenient convention for obtaining standardized expressions.

[1] Due to the formation of a cusp, this consideration does not apply to derivatives at the cusp, which become infinite. We will discuss this later.

Up to rescaling Eq. (5.24) is the standard 1-loop FRG equation. The solution of this flow equation corrects $R_0(u) \sim \mathcal{O}(\varepsilon)$ to the renormalized $R(u)$ to order ε^2. The non-local part in terms of this renormalized disorder-distribution function is given by

$$\hat{R}[u] = \frac{1}{2}\int_{x_1,x_2} g(x_1,x_2)^2 \mathcal{R}''(u(x_1))\mathcal{R}''(u(x_2)) - \frac{1}{2} I_1 \int_x \mathcal{R}''(u(x))^2 + \mathcal{O}(\varepsilon^3) \tag{5.25}$$

Superficially, the ε-expansion seems to work. However, we assumed that $\hat{R}[u]$ is of order ε^2 and likewise all derivatives of $\hat{R}[u]$. In fact, the existence of the cusp in $R''(u)$ of the 1-loop solution appearing at a finite scale destroys our assumptions. Due to this cusp, $R''(u)$ is not differentiable at $u = 0$. The left- and right-sided limits of R''' exist but do not coincide $R'''(0^+) = -R'''(0^-)$. The fourth derivative $R''''(u)$ is uniformly bound for $u \neq 0$ but it is infinity at $u = 0$.

If we would only need up to two derivatives of R, the ε-expansion would work without caveats. However, even the computation of the 2-point correlation function in Eq. (5.18) requires a second derivative of the non-local part of $R[u]$, that is, a second derivative of Eq. (5.25) at zero field. There enters a third and fourth derivative of $R(u(x))$ that have to be evaluated at $u(x) = 0$. Furthermore, in the derivation of higher orders in ε, that is, higher orders in the expansion of the replica hierarchy in $R(u)$, one encounters higher derivatives as well.

For the calculation of observables via analytic continuation it suffices to evaluate derivatives of $R(u)$ at $u = 0^{\pm}$, if the left- and right-sided limits give the same result for the observable. For example, the ambiguity is avoided if odd derivatives of $R(u)$ enter the equations only squared. However, we work with fluctuating fields $u(x)$ and, for example, the second derivative of Eq. (5.25) contains a term $R'''(u(x_1))R'''(u(x_2))$. While this is a square term we have to ensure that either $u(x) \to 0^+$ or $u(x) \to 0^-$ uniformly for all x. That is, *ambiguities can be avoided if we restrict to non-crossing configurations.*

From now on, the limit of two fields $u_a(x)$ and $u_b(x)$ being equal in a Γ-cumulant is understood as

$$\lim_{u_b \to u_a} S^{(n)}[u_a, u_b, \ldots] := \lim_{u_0 \to 0^+} S^{(n)}[u_a, u_a + u_0, \ldots] \tag{5.26}$$

where u_0 is a constant field. That is, all fields are assumed to be close to a uniform configuration. We demonstrate in the next two subsections that in this weak limit the 3-loop β-function can be derived consistently. That is, it does not matter if the right limit $u_0 \to 0^+$ or left limit $u_0 \to 0^-$ are taken in Eq. (5.26).

5.4 ε-expansion to 2-loop order

As an instructive example we review the 2-loop ERG calculation done in Refs. [20, 22]. In order to obtain Eq. (5.20) to order ε^3 we have to compute $S^{(3)}_{110}[0, 0, -u]$ and $\mathcal{R}''[u](x_2, x_3)\mathcal{R}''[u](x_4, x_1)$ to this order. We first concentrate on the second term. Note that we expand in the renormalized disorder distribution function $R(u)$. This gives

$$\mathcal{R}''[u](x,y) = \mathcal{R}''(u(x))\delta(x-y) + \hat{R}''[u](x,y) - \hat{R}''[0^+](x,y) \,. \tag{5.27}$$

$\mathcal{R}''(u(x))$ is of order ε and we have to expand the non-local part $\hat{R}''$ to second order in $R(u)$, that is, we have to insert the second derivative of Eq. (5.25)

$$\hat{R}''[u](z_1,z_2) = \delta^d(z_1-z_2)\Big[\int_x g(z_1,x)^2 R''''(u(z_1))\mathcal{R}''(u(x)) - I_1 R'''(u(z_1))^2 \\ - I_1 R''''(u(z_1))\mathcal{R}''(u(z_1))\Big] + g(z_1,z_2)^2 R'''(u(z_1))R'''(u(z_2)) + \mathcal{O}(\varepsilon^3) \quad (5.28)$$

As described above, in order to calculate $\hat{R}''[0^+](z_1,z_2)$ we first insert a constant field u_0 and then take the limit $u_0 \to 0^+$ to obtain

$$\hat{R}''[0^+](z_1,z_2) = \big[g(z_1,z_2) - \delta^d(z_1-z_2)I_1\big] R'''(0^+)^2 + \mathcal{O}(\varepsilon^3)\,. \quad (5.29)$$

It is important to note that in this "weak limit" we obtain no ambiguities since $R'''(0^+)^2 = R'''(0^-)^2$ has a straightforward analytic continuation.

The feedback from $S^{(3)}$ is calculated by retaining only terms of order ε^3. The calculation is relegated to appendix B.1. The result from Eq. (B.1) is

$$\dot{S}^{(3)}[u_{abc}] = \int_{x_1,\dots,x_6} \left[\frac{\mathrm{d}}{\mathrm{d}m} g(x_1,x_2)g(x_3,x_4)g(x_5,x_6)\right] \times \\ \times \Big(3\mathcal{R}''[u_{ab}](x_2,x_3)\mathcal{R}''[u_{ac}](x_4,x_5)\mathcal{R}''[u_{ac}](x_6,x_1) \\ - \mathcal{R}''[u_{ab}](x_2,x_3)\mathcal{R}''[u_{bc}](x_4,x_5)\mathcal{R}''[u_{ac}](x_6,x_1)\Big) + \mathcal{O}(\varepsilon^4)\,. \quad (5.30)$$

To this order it integrates to

$$S^{(3)}[u_{abc}] = \big\{3\,\mathrm{tr}\big[g\mathcal{R}''_{ab}g\mathcal{R}''_{ab}g\mathcal{R}''_{ac}\big] - \mathrm{tr}\big[g\mathcal{R}''_{ab}g\mathcal{R}''_{bc}g\mathcal{R}''_{ac}\big]\big\} + \mathcal{O}(\varepsilon^4)\,, \quad (5.31)$$

where $\mathcal{R}_{ab} = \mathcal{R}[u_{ab}]$. Here the trace is over real space. The symmetrization over fields $\{\dots\}$ can be written as $S^{(3)}[u_{abc}] = \frac{1}{2}(A_1 + A_2 + A_3) + \mathcal{O}(\varepsilon^4)$ with

$$\begin{aligned} A_1 &= \mathrm{tr}\big[g\mathcal{R}''_{ab}g\mathcal{R}''_{ab}g(\mathcal{R}''_{ac}+\mathcal{R}''_{bc})\big] \\ A_2 &= \mathrm{tr}\big[g\mathcal{R}''_{ab}g(\mathcal{R}''_{ac}-\mathcal{R}''_{bc})g(\mathcal{R}''_{ac}-\mathcal{R}''_{bc})\big] \\ A_3 &= \tfrac{1}{3}\mathrm{tr}\big[g(\mathcal{R}''_{ac}+\mathcal{R}''_{bc})g(\mathcal{R}''_{ac}+\mathcal{R}''_{bc})g(\mathcal{R}''_{ac}+\mathcal{R}''_{bc})\big]\,. \end{aligned} \quad (5.32)$$

In a next step we take the functional derivatives of these terms with respect to $u_a(x)$ and $u_b(y)$. Then the limit $b \to a$ is performed by first replacing $u_b(y)$ by $u_a(x) + u_0$ and then sending $u_0 \to 0^+$. The remaining fields $u_a(x)$ only occur in the combination $u_a(x) - u_c(x)$ and can directly be set to zero. When taking the functional derivatives of Eqs. (5.32), it is helpful to remember that we set $b = a$ afterwards. Therefore A_2 does not contribute to $S^{(3)}_{110}[0,0,-v]$ and A_1 contributes only if the derivatives act on the first two $\mathcal{R}_{ab}$ in the trace. Finally, the term A_3 is a symmetric functional in u_{ac} and u_{bc} and can be symmetrically expanded in u_{ab} as outlined in the appendices of Refs. [22, 78]. Setting $u_c(x) = u(x)$, we obtain

$$S^{(3)}_{110}[0,0,-u](x_1,x_2) = 2\big[R'''(x_1)R'''(x_2) - R'''(0^+)^2\big]g(x_1,x_2)\int_y g(x_1,y)g(y,x_2)\mathcal{R}''(y) \\ + \mathcal{O}(\varepsilon^4)\,. \quad (5.33)$$

In the above equation and from now on we use the shorthand notation $R''(x) := R''(u(x))$ (and similar for higher derivatives expect for $x = 0^+$ and $x = u$). Inserting Eqs. (5.28), (5.29), and (5.33) into Eq. (5.20) we arrive at the 2-loop result

$$\begin{aligned}\dot{R}[u] = \int_{x_1,\dots,x_3} & \left[\tfrac{\mathrm{d}}{\mathrm{d}m} g(x_1,x_2) g(x_1,x_3)\right] \left[g(x_2,x_3)^2 - \delta(x_2-x_3)\right] \mathcal{R}''(x_1) \\ & \qquad\qquad\qquad \times \left[R'''(x_2)R'''(x_3) - R'''(0^+)^2\right] \\ + \int_{x_1,\dots,x_3} & \left[\tfrac{\mathrm{d}}{\mathrm{d}m} g(x_1,x_2)^2\right] \left[g(x_2,x_3)^2 - \delta(x_2-x_3)\right] \mathcal{R}''(x_1) R''''(x_2) \mathcal{R}''(x_3) \\ + \int_{x_1,\dots,x_3} & \left[\tfrac{\mathrm{d}}{\mathrm{d}m} g(x_1,x_2)^2\right] g(x_1,x_2) g(x_1,x_3) \mathcal{R}''(x_1) \left[R'''(x_2)R'''(x_3) - R'''(0^+)^2\right]\end{aligned} \tag{5.34}$$

The 2-loop β-function known from FRG calculations [18, 19] is the local contribution and is obtained by inserting a constant field and dividing by L^d

$$\dot{R}(u) = \frac{1}{2}\dot{I}_1 \mathcal{R}''(u)^2 + (\dot{I}_A - I_1\dot{I}_1)\mathcal{R}''(u)\Big[R'''(u)^2 - R'''(0^+)^2\Big] + \mathcal{O}(\varepsilon^4) \tag{5.35}$$

where

$$I_A = \int_{p_1,p_2} g(p_1)g(p_2)g(p_1+p_2)^2 \sim \frac{m^{-2\varepsilon}}{\varepsilon^2} \tag{5.36}$$

The $\mathcal{O}(\frac{1}{\varepsilon})$ term in $\dot{I}_A$ is cancelled by $I_1\dot{I}_1$, ensuring a finite β-function. The non-local part integrates to

$$\hat{R}[u] = A[u] + \int_x B(u(x)) + \mathcal{O}(\varepsilon^4) \tag{5.37}$$

with contributions

$$\begin{aligned}A[u] = \frac{1}{2}\int_{x_1,x_2} & g(x_1,x_2)^2\, \mathcal{R}''(x_1)\mathcal{R}''(x_2) + \frac{1}{2}\int_{y_1,y_2,z} g(y_1,z)^2 g(y_2,z)^2\, \mathcal{R}''(y_1)\mathcal{R}''(y_2)R''''(z) \\ + \int_{x_1,x_2,y} & g(x_1,x_2)^2 g(x_1,y)g(x_2,y)\Big[R'''(x_1)R'''(x_2) - R'''(0^+)^2\Big]\mathcal{R}''(y) \\ - I_1\int_{x_1,x_2} & g(x_1,x_2)\, \mathcal{R}''(x_1)\Big[R'''(x_2)^2 - R'''(0^+)^2 + \mathcal{R}''(x_2)R''''(x_2)\Big]\end{aligned} \tag{5.38}$$

and

$$B(u) = -\frac{1}{2}I_1\mathcal{R}''(u)^2 + (I_1^2 - I_A)\mathcal{R}''(u)\Big[R'''(u)^2 - R'''(0^+)^2\Big] + \frac{1}{2}I_1^2\mathcal{R}''(u)^2R''''(u) \tag{5.39}$$

5.5 ε-expansion to 3-loop order

In 3-loop order we have to compute $S^{(3)}_{110}[0,0,-u]$ and $\mathcal{R}''[u](x_2,x_3)\mathcal{R}''[u](x_4,x_1)$ in Eq. (5.20) to order ε^4. The flow equation for the three-replica cumulant at $T=0$, see Eq. (B.1), is given by

$$\begin{aligned}\dot{S}^{(3)}[u_{abc}] = &\int_{x_1,x_2} \dot{g}(x_1,x_2)\left\{\tfrac{3}{2}S^{(4)}_{1100}[u_{aabc}](x_1,x_2)\right\} \\ &+\int_{x_1,\ldots,x_4}\left[\tfrac{\mathrm{d}}{\mathrm{d}m}g(x_1,x_2)g(x_3,x_4)\right] \\ &\qquad\times\left\{3\mathcal{R}''[u_{ab}](x_2,x_3)\left[S^{(3)}_{110}[u_{aac}](x_4,x_1)-S^{(3)}_{110}[u_{abc}](x_4,x_1)\right]\right\} \\ &+\int_{x_1,\ldots,x_6}\left[\tfrac{\mathrm{d}}{\mathrm{d}m}g(x_1,x_2)g(x_3,x_4)g(x_5,x_6)\right] \\ &\qquad\times\left\{3\mathcal{R}''[u_{ab}](x_2,x_3)\mathcal{R}''[u_{ac}](x_4,x_5)\mathcal{R}''[u_{ac}](x_6,x_1)\right. \\ &\qquad\left.-\mathcal{R}''[u_{ab}](x_2,x_3)\mathcal{R}''[u_{bc}](x_4,x_5)\mathcal{R}''[u_{ac}](x_6,x_1)\right\}.\end{aligned} \tag{5.40}$$

Because there is a feeding term from the fourth Γ-cumulant $S^{(4)}$ we have to calculate $S^{(4)}$ to order ε^4. The only contribution in Eq. (B.2) is $S^{(4)}_4$ that integrates in this order to

$$\begin{aligned}S^{(4)}[u_{abcd}] = 3\Big\{&4\,\mathrm{tr}\Big[g\mathrm{R}''_{ab}g\mathcal{R}''_{ac}g\mathcal{R}''_{ad}g\mathcal{R}''_{ad}\Big]+2\,\mathrm{tr}\Big[g\mathcal{R}''_{ab}g\mathcal{R}''_{ac}g\mathcal{R}''_{cd}g\mathcal{R}''_{ac}\Big] \\ &-4\,\mathrm{tr}\Big[g\mathcal{R}''_{ab}g\mathcal{R}''_{ac}g\mathcal{R}''_{cd}g\mathcal{R}''_{ad}\Big]+\mathrm{tr}\Big[g\mathcal{R}''_{ab}g\mathcal{R}''_{bc}g\mathcal{R}''_{cd}g\mathcal{R}''_{ad}\Big]\Big\}+\mathcal{O}(\varepsilon^5),\end{aligned} \tag{5.41}$$

where again $\mathcal{R}''_{ab}(x,y)=\mathcal{R}''[u_{ab}](x,y)$. In order to obtain $S^{(4)}_{1100}[u_{aabc}]$ the equation has to be symmetrized over replica fields and two functional derivatives have to be taken. This lengthy but straightforward calculation is not reproduced here. The limit of identical replica fields in the first and second entry again has to be taken in the weak limit.

For brevity we introduce the symbol $\frac{\tilde{\mathrm{d}}}{\mathrm{d}m_g}$ that formally denotes a scale derivative that acts only on the propagators g that were differentiated in the initial 1PI flow equations, see Eqs. (5.20), (B.1), and (B.2). These formal "derivatives" do not act on cumulants nor on g's that arise otherwise. In this sense the 2-loop contribution to $\dot{S}^{(3)}$, see Eq. (5.30), can be written as

$$\frac{\tilde{\mathrm{d}}}{\mathrm{d}m_g}\frac{1}{2}[A_1+A_2+A_3] \tag{5.42}$$

where A_1, A_2, and A_3 are given in Eq. (5.32). This term was easily integrated in 2-loop order since a scale derivative acting on R gives an additional order of ε, that is, $\frac{\tilde{\mathrm{d}}}{\mathrm{d}m_g}$ could be replaced by $\frac{\mathrm{d}}{\mathrm{d}m}$. Here we also need the next order, so we have to calculate

$$\left(\frac{\mathrm{d}}{\mathrm{d}m}-\frac{\tilde{\mathrm{d}}}{\mathrm{d}m_g}\right)\frac{1}{2}[A_1+A_2+A_3] \tag{5.43}$$

and reinsert the 1-loop result for $\dot{R}[u]$ from Eq. (5.23) to obtain this expression to order ε^4. It is sufficient to insert the local part of R into A_1, A_2, and A_3.

Apart from the feeding from $S^{(4)}_{1100}[u_{aabc}]$, there are two more 3-loop contributions to the flow of $S^{(3)}$. One arises by inserting also non-local contributions to 1-loop order from Eq. (5.25) into A_1,

A_2, and A_3. And, finally, there is a cross term $R \times S^{(3)}$ from the third line of Eq. (5.40). Here we can insert the 2-loop solution $S^{(3)} = \frac{1}{2}(A_1 + A_2 + A_3)$ with local R's into the right-hand-side of the flow equation to obtain the complete result at 3-loop order. These 3-loop contributions are easily integrated since scale derivatives acting on cumulants would introduce additional loops. The details of this calculation and the resulting functional $S^{(3)}[u_{abc}]$ to 3-loop order are given in Appendix B.2. In order to obtain $S^{(3)}_{110}[0,0,-u]$ it is again convenient to use a symmetric replica expansion. Setting $u_a = u_b$ again requires the weak limit; in addition to potentially problematic terms $\sim R'''(0^+)^2$ we also encounter $R'''(0^+)R^{(5)}(0^+)$.

Now we turn to the term $\mathcal{R}''[u](x_2,x_3)\mathcal{R}''[u](x_4,x_1)$ in Eq. (5.20). In 3-loop order we have to insert

$$\mathcal{R}''[u](x,y) = \mathcal{R}''(u(x))\delta(x-y) + \hat{R}''[u](x,y) - \hat{R}''[0^+](x,y) \tag{5.44}$$

where $\hat{R}$ is the non-local contribution of the 2-loop solution Eq. (5.37). Taking two functional derivatives and taking the weak limit with non-crossing configurations produces anomalous terms $R'''(0^+)^2$, $R'''(0^+)R^{(5)}(0^+)$, $R''(0^+)R'''''(0^+)$, and $R''(0^+)R^{(6)}(0^+)$. Inserting the obtained expressions for $\mathcal{R}''[u](x_2,x_3)\mathcal{R}''[u](x_4,x_1)$ and $S^{(3)}_{110}[0,0,-u]$ in Eq. (5.20) allows to rearrange terms such that they are total derivatives acting on the propagators g only. In summary we obtain to 3-loop order

$$\dot{R}[u] = \beta_{\text{1loop}}[u] + \beta_{\text{2loop}}[u] + \beta_{\text{3loop}}[u] \tag{5.45}$$

with 1- and 2-loop contributions $\beta_{\text{1loop}}[u] + \beta_{\text{2loop}}[u]$ given by Eq. (5.34) and the 3-loop contribution

$$\begin{aligned}
\beta_{\text{3loop}}[u] = &\int_{x_1,x_2,y,z} \left[\tfrac{\mathrm{d}}{\mathrm{d}m} g^2_{x_1x_2} g_{x_1z} g_{x_2z} g^2_{yz}\right] \left[R'''_{x_1}R'''_{x_2} - R'''(0^+)^2\right] \mathcal{R}''_y R''''_z \\
&- 2I_1 \int_{x_1,x_2,y} \left[\tfrac{\mathrm{d}}{\mathrm{d}m} g^2_{x_1x_2} g_{x_1y} g_{x_2y}\right] \mathcal{R}''_y \Big(3\left[R'''_{x_1}R'''_{x_2}R''''_{x_2} - R'''(0^+)^2 R''''(0^+)\right] + R'''_{x_1}\mathcal{R}''_{x_2}R^{(5)}_{x_2}\Big) \\
&- I_1 \int_{x,y,z} \left[\tfrac{\mathrm{d}}{\mathrm{d}m} g^2_{xz} g^2_{yz}\right] \left[R'''^2_x - R'''(0^+)^2 + \mathcal{R}''_x R''''_x\right] \mathcal{R}''_x R''''_z \\
&+ \tfrac{1}{2} \int_{x_1,x_2,y_1,y_2} \left[\tfrac{\mathrm{d}}{\mathrm{d}m} g^2_{x_1x_2} g^2_{x_1y_1} g^2_{x_2y_2}\right] R''''_{x_1} R''''_{x_2} \mathcal{R}''(y_1)\mathcal{R}''(y_2) \\
&+ \tfrac{1}{2} I_1^2 \int_{x_1,x_2} \left[\tfrac{\mathrm{d}}{\mathrm{d}m} g^2_{x_1x_2}\right] \left[R'''^{\,2}_{x_1} - R'''(0^+)^2 + \mathcal{R}''_{x_1}R''''_{x_1}\right] \left[R'''^{\,2}_{x_2} - R'''(0^+)^2 + \mathcal{R}''_{x_2}R''''_{x_2}\right] \\
&- I_1 \int_{x_1,x_2,y} \left[\tfrac{\mathrm{d}}{\mathrm{d}m} g^2_{x_1x_2} g_{x_1y} g_{x_2y}\right] \left[R'''_{x_1}R'''_{x_2} - R'''(0^+)^2\right] \left[R'''^2_y - R'''(0^+)^2 + \mathcal{R}''_x R''''_x\right] \\
&+ \tfrac{1}{2} \int_{x_1,x_2,y_1,y_2} \left[\tfrac{\mathrm{d}}{\mathrm{d}m} g^2_{x_1x_2} g^2_{y_1y_2} g_{x_1y_1} g_{x_2y_2}\right] \left[R'''_{x_1}R'''_{x_2} - R'''(0^+)^2\right] \left[R'''_{y_1}R'''_{y_2} - R'''(0^+)^2\right] \\
&+ 4 \int_{x_1,x_2,y,z} \left[\tfrac{\mathrm{d}}{\mathrm{d}m} g_{x_1x_2} g_{yz} g_{x_1z} g^2_{x_2z} g(x_1y)\right] \left[R'''_{x_1}R'''_{x_2}R''''_z - R'''(0^+)^2 R''''(0^+)\right] \mathcal{R}''_x
\end{aligned} \tag{5.46}$$

$$
\begin{aligned}
&+\int_{x_1,x_2,y,z}\left[\tfrac{\mathrm{d}}{\mathrm{d}m}g_{x_1z}^2g_{x_2z}^2g_{x_1y}g_{x_2y}\right]\Big[R'''_{x_1}R'''_{x_2}R''''_{z}-R'''(0^+)^2R''''(0^+)\Big] \qquad (5.47)\\
&+2\int_{x,y_1,y_2,z}\left[\tfrac{\mathrm{d}}{\mathrm{d}m}g_{xz}^2g_{y_1z}^2g_{y_2z}g_{y_2x}\right]R'''_x\mathcal{R}''_{y_1}\mathcal{R}''_{y_2}R^{(5)}_z\\
&-\tfrac{1}{2}I_1\int_{y_1,y_2,z}\left[\tfrac{\mathrm{d}}{\mathrm{d}m}g_{y_1z}^2g_{y_2z}^2\right]\mathcal{R}''_{y_1}\mathcal{R}''_{y_2}\Big[3R''''^2_z+4R'''_zR^{(5)}_z+\mathcal{R}''_zR^{(6)}_z\Big]\\
&+\tfrac{1}{6}\int_{y_1,y_2,y_3,z}\left[\tfrac{\mathrm{d}}{\mathrm{d}m}g_{y_1z}^2g_{y_2z}^2g_{y_3z}^2\right]\mathcal{R}''_{y_1}\mathcal{R}''_{y_2}\mathcal{R}''_{y_3}R^{(6)}_z\\
&+\int_{x_1,x_2,y_1,y_2}\left[\tfrac{\mathrm{d}}{\mathrm{d}m}g_{x_1x_2}^2g_{x_1y_1}g_{x_1y_2}g_{x_2y_1}g_{x_2y_2}\right]R''''_{x_1}R''''_{x_2}\mathcal{R}''_{y_1}\mathcal{R}''_{y_2}\\
&+\tfrac{1}{2}\int_{x_1,x_2,x_3,x_4}\left[\tfrac{\mathrm{d}}{\mathrm{d}m}g_{x_1x_2}g_{x_3x_4}g_{x_1x_3}g_{x_1x_4}g_{x_2x_3}g_{x_2x_4}\right]\\
&\qquad\qquad\times\left\{\Big[R'''_{x_1}R'''_{x_2}-R'''(0^+)^2\Big]\Big[R'''_{x_3}R'''_{x_4}-R'''(0^+)^2\Big]-R'''(0^+)^4\right\}\\
&+\int_{x,y}\left[\tfrac{\mathrm{d}}{\mathrm{d}m}g_{xy}^2\right]\mathcal{R}''_x\Big\{(I_1^2-I_A)R''''_x\Big[R'''^2_x-R'''(0^+)^2\Big]\\
&\quad+(5I_1^2-4I_A)\Big[R'''^2_xR''''_x-R'''(0^+)^2R'''(0^+)\Big]+(3I_1^2-2I_A)\mathcal{R}''_xR''''^2_x\\
&\quad+(4I_1^2-2I_A)\mathcal{R}''_xR'''_xR^{(5)}_x+\tfrac{1}{2}I_1^2\mathcal{R}''^2_xR^{(6)}_x\Big\}
\end{aligned}
$$

Here we once again introduced shorthand notations $g_{xy} := g(x,y)$ and $R_x = R(x) = R(u(x))$ except for $x = 0^+$ and likewise for derivatives of R.

Inserting a constant field and dividing by L^d gives the 3-loop contribution to the β-function

$$
\begin{aligned}
\beta_{\text{3loop}}(u) &= \big(4\dot I_l+\dot I_m-6I_1\dot I_A+(5I_1^2-4I_A)\dot I_1\big)\Big[R'''(u)^2R''''(u)-R'''(0^+)^2R''''(0^+)\Big]\mathcal{R}''(u)\\
&\quad+\big[\dot I_j-2I_A\dot I_1\big)\big]R''''(u)^2\mathcal{R}''(u)^2 \qquad (5.48)\\
&\quad+\frac{1}{2}\Big(I_1^2\dot I_1-2I_1\dot I_A+\dot I_m+\dot I_i\Big)\Big[R'''(u)^2-R'''(0^+)^2\Big]^2-\frac{1}{2}\dot I_iR'''(0^+)^4\quad+\mathcal{O}(\varepsilon^5)
\end{aligned}
$$

with the following integrals

$$
\begin{aligned}
I_1 &= \int_p g(p)^2 \qquad (5.49)\\
I_A &= \int_{p_1,p_2} g(p_1)g(p_2)g(p_1+p_2)^2\\
I_m &= \int_{p_1,p_2,p_3} g(p_1)g(p_2)g(p_1+p_2+p_3)g(p_3)g(p_1+p_2)^2\\
I_l &= \int_{p_1,p_2,p_3} g(p_1)G(p_2)g(p_1+p_2)g(p_3)g(p_1+p_2+p_3)^2\\
I_j &= \int_{p_1,p_2,p_3} g(p_1)g(p_2)g(p_3)^2g(p_1+p_2+p_3)^2\\
I_i &= \int_{p_1,p_2,p_3} g(p_1)g(p_2)g(p_3)g(p_1+p_3)g(p_2+p_3)g(p_1-p_2)
\end{aligned}
$$

which are calculated in appendix A. It turns out that the combinations occurring in Eq. (5.48) are finite for $\varepsilon \to 0$, so our counting of orders in ε is consistent, and the theory is 3-loop renormalizable. Due to gauge invariance we can add any scale-dependent function to $R(u)$ that does *not* dependent on the fields. In this way we can drop all constants from the β-function. The constants in Eq. (5.48) arise directly from Eq. (5.46). In the derivation of the latter we neglected gauge terms in $S^{(3)}$ and $S^{(4)}$, so these constants are arbitrary.

Assuming non-crossing configurations, that is, using Eq. (5.26) for taking limits $u_a - u_b \to 0$, allows to derive all anomalous terms in the β-function without ambiguities. With this assumption, the ε-expansion is a straightforward expansion of the exact hierarchy of flow equations for the Γ-cumulants in powers of the effective local disorder distribution function $R(u)$. Presumably, this will work to all orders in ε.

Crossing configurations could not be treated and are an open problem. It is doubtful that the standard ε-expansion can be applied. This is because $R(u)$ and all its derivatives are not a small parameter suitable for an expansion if $u = 0$ cannot be avoided.

In order to make contact with the result obtained by an alternative method later in Section 6, we rescale

$$R(u) = \frac{1}{\varepsilon I_1} m^{-4\zeta} \tilde{R}(u m^{\zeta}) \tag{5.50}$$

where ζ is the roughness exponent. The rescaled function $\tilde{R}$ still depends on the RG scale m and satisfies the RG equation to 3-loop order given in Eq. (3.1).

6 Effective action and β-function via field theory

6.1 Calculation using the sloop elimination method

Here we discuss a different way to do the contractions, using "excluded replicas", which will finally lead to a rather efficient algorithm for calculating the anomalous terms.

We start by a 1-loop diagram involving two disorder vertices, after having done one Wick-contraction. For simplicity of notation we are not writing space-indices and momentum integrals, which are unimportant for the following discussion.

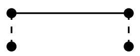

$$= \frac{1}{2T^3} \sum_{abc} R'(u_a - u_b) R'(u_a - u_c) \ . \tag{6.1}$$

At the next step, the following contractions are possible (restoring the integral)

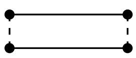 $+$ 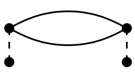 $-$  $-$ 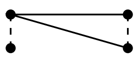

$$= \frac{1}{2T^2} \left[\sum_{ab} R''(u_a - u_b)^2 + \sum_{abc} R''(u_a - u_b) R''(u_a - u_c) - 2 \sum_{ab} R''(0) R''(u_a - u_b) \right] I_1 . \tag{6.2}$$

The second term is a 3-replica contribution (contribution to the third cumulant of the disorder), thus not of interest to us. The correction to the disorder at 1-loop order therefore consists of the first and last term, equivalent to the first and last two diagrams,

$$\delta^{(1)} R(u) = \left[\frac{1}{2} R''(u)^2 - R''(u) R''(0) \right] I_1 \ . \tag{6.3}$$

This is equivalent to the result obtained in Eq. (5.24).

An alternative approach consists in remarking that in Eq. (6.1) the terms $a = b$, and $a = c$ could be dropped, since they are constants, thus will not be contracted in the next step. We thus start from

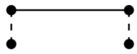

$$= \frac{1}{2T^3} \sum_{b \neq a \neq c} R'(u_a - u_b) R'(u_a - u_c) \;, \tag{6.4}$$

which after one Wick-contraction leads to

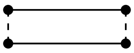 + 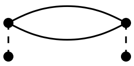

$$\begin{aligned}
&= \frac{1}{2T^2} \left[\sum_{a \neq b} R''(u_a - u_b)^2 + \sum_{b \neq a \neq c} R''(u_a - u_b) R''(u_a - u_c) \right] I_1 \\
&= \frac{1}{2T^2} \left[\sum_{ab} R''(u_a - u_b)^2 (1 - \delta_{ab}) + \sum_{abc} R''(u_a - u_b) R''(u_a - u_c)(1 - \delta_{ab})(1 - \delta_{ac}) \right] I_1 \\
&= \frac{1}{2T^2} \left[\sum_{ab} \left[R''(u_a - u_b)^2 - 2R''(u_a - u_b) R''(0) \right] + \sum_{abc} R''(u_a - u_b) R''(u_a - u_c) \right] I_1 \;. \qquad (6.5)
\end{aligned}$$

The 2-replica term (the double sum) is, as expected, the same result as obtained in Eq. (6.2). While the second line contains only excluded replica sums, there can not be any ambiguity. The latter may only appear in the ensuing projection onto non-excluded replica sums. This is indeed the case for the hat diagram $\sim R''(u) R'''(0^+)^2$, as the reader is invited to check on his own, starting from

$$\begin{aligned}
&\sum_{a,b} \delta_A^{(2)} R(u_a - u_b) \\
&= \Big[\sum_{a \neq b} R''(u_a - u_b)(R'''(u_a - u_b))^2 + \sum_{a \neq b, a \neq c} R''(u_a - u_b) R'''(u_a - u_b) R'''(u_a - u_c) \\
&\quad - \frac{1}{2} \sum_{a \neq b, a \neq c, b \neq c} R''(u_a - u_b) R'''(u_a - u_c) R'''(u_b - u_c) + \frac{3}{2} \sum_{a \neq b, a \neq c} R''(u_a - u_b) R'''(u_a - u_c)^2 \\
&\quad + \frac{1}{2} \sum_{a \neq b, a \neq c, a \neq d} R''(u_a - u_b) R'''(u_a - u_c) R'''(u_a - u_d) \Big] I_A \;. \qquad (6.6)
\end{aligned}$$

We will therefore in the following present an improved projection method, which we have termed the "sloop-elimination" method. (The name may be thought of as as "super"-partner of a normal loop, thus sloop, which cancels part of it.)

The idea of the method is very simple. Let us consider the second term on the the second line of Eq. (6.2). It is a three replica term proportional to the temperature. In a $T = 0$ theory such a diagram should not appear, thus it can identically be set to zero:

$\sum_{abc}$ 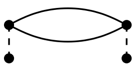

$$= \frac{1}{2T^2} \sum_{abc} R''(u_a - u_b) R''(u_a - u_c) I_1 \equiv 0 \;. \tag{6.7}$$

Projecting such terms to zero at any stage of further contractions is very natural in our present calculation (and also e.g. in the exact RG approach, where terms are constructed recursively and such forbidden terms must be projected out). It is valid only when (i) the summations over replicas are free (ii) the term inside the sum is non-ambiguous. These conditions are met for any diagram with sloops, provided the vertices have at most two derivatives. (One can in fact start from vertices which either have no derivative or exactly two.) Subtracting this term from Eq. (6.5) immediately yields the result (6.3).

While this could also have been done directly, let us illustrate the power of the procedure on an example. We want to contract the expression (6.7) with a third vertex R

$$0 = \sum_{abc}$$

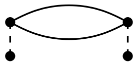

$$\sum_{de} R(u_d - u_e) \equiv \frac{1}{T^4} \sum_{a\neq b, a\neq c, d\neq e} R''(u_a - u_b) R''(u_a - u_c) R(u_d - u_e) \,. \tag{6.8}$$

where we have already dropped constant terms which will disappear after the contractions. Also note that implicitly here and in the following the vertices are at points x, y, z in that order. We will contract the third vertex twice, once with the first and once with the second , i.e. look at the term proportional to $I_A = \int_{x,y,z} g(x-y)^2 g(x-z) g(y-z)$.

Performing the first contraction between points x and z yields

$$\frac{1}{T^3}\Big[\sum_{a\neq b, a\neq c, a\neq e} R'''(u_a - u_b) R''(u_a - u_c) R'(u_a - u_e) - \sum_{a\neq b, a\neq c, b\neq e} R'''(u_a - u_b) R''(u_a - u_c) R'(u_b - u_e) \Big] \equiv 0 \,. \tag{6.9}$$

Similarly, the second contraction yields (with the standard combinatrial factor of $1/2$)

$$\begin{aligned} \frac{1}{T^2}\Big[\frac{1}{2} &\sum_{a\neq b, a\neq c, a\neq e} R'''(u_a - u_b) R'''(u_a - u_c) R''(u_a - u_e) \\ &+ \sum_{a\neq b, a\neq c} R'''(u_a - u_b) R'''(u_a - u_c) R''(u_a - u_c) \\ &+ \frac{1}{2} \sum_{a\neq b, b\neq e} R'''(u_a - u_b) R'''(u_a - u_b) R''(u_a - u_e) \\ &- \frac{1}{2} \sum_{a\neq b, a\neq c, b\neq c} R'''(u_a - u_b) R'''(u_a - u_c) R''(u_a - u_c) \Big] I_A \equiv 0 \,. \end{aligned} \tag{6.10}$$

This non-trivial identity tells us that the sum of all the terms (or diagrams) thus generated upon contractions must vanish. Stated differently: A sloop, as (6.7) as well as the sum of all its descendents vanishes. Note that this is *not* true for each single term, but only for the sum.

A property that we request from a proper p-replica term is that upon one self contraction it gives a $(p-1)$-replica term. It may also give T times a p-replica term (a sloop) but this is zero at $T = 0$, so we can continue to contract. Thus we have generated several non-trivial projection identities. The starting one is that the 2-replica part of (6.7) is zero, since (6.7) is a proper 3-replica term. This is what is meant by the symbol "$\equiv$" above and the last identity is the one we now use.

Indeed compare (6.10) with (6.6). One notices that all terms apart from the first in (6.6) appear in (6.10). They also have the same relative coefficients, apart from the third one of (6.6). Thus one can use (6.10) to simplify (6.6):

$$\sum_{a,b} \delta_A^{(2)} R(u_a - u_b) = \Big[\sum_{a\neq b} R''(u_a - u_b) R'''(u_a - u_b)^2 + \sum_{a\neq b, a\neq c} R''(u_a - u_b) R'''(u_a - u_c)^2 \Big] I_A \,. \tag{6.11}$$

The function $R'''(u)^2$, which appears in the last term, is continuous at $u = 0$. It is thus obvious how to rewrite this expression using free summations and extract the 2-replica part

$$\delta_A^{(2)} R(u) = \Big[\big(R''(u) - R''(0) \big) R'''(u)^2 - R'''(0^+)^2 R''(u) \Big] I_A \,. \tag{6.12}$$

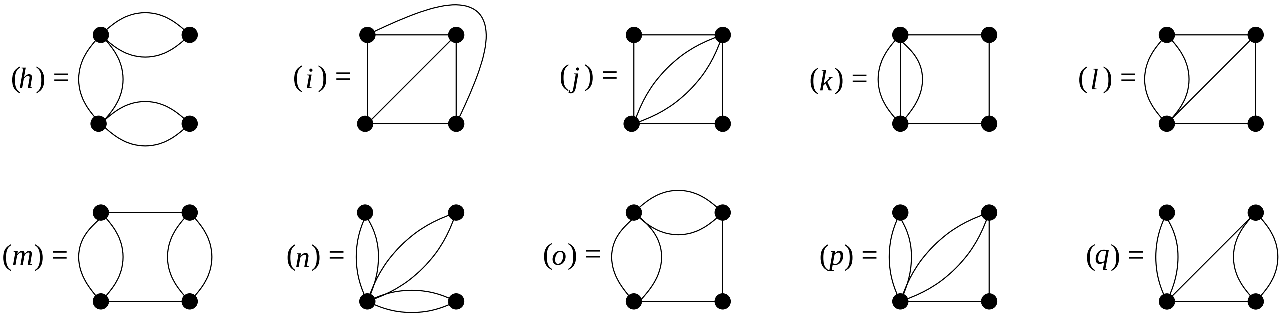

Figure 1: Diagrams at 3-loop order (without insertion of lower order counter-terms)

This coincides with the contribution of diagram A in the ERG approach, see the second term of Eq. (5.35). We can write diagrammatically the subtraction that has been performed as

$$\delta_A^{(2)} R = \quad$$ 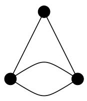 $$-$$ 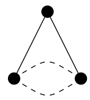 $$, \tag{6.13}$$

where the loop with the dashed line represents the sub-diagram with the sloop, i.e. the term (6.10) (with in fact the same global coefficient). The idea is that subtracting sloops is allowed since they vanish. The advantage of the method is that all intermediate results are uniquely defined.

There are other possible identities, which are descendants of other sloops. For instance a triangular sloop gives, by a similar calculation:

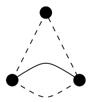

$$\begin{aligned} &= R''(0) \sum_{a \neq b} R'''(u_a - u_b)^2 + \sum_{a \neq b, a \neq c} R''(0) R'''(u_a - u_b) R'''(u_a - u_c) \\ &+ \sum_{a \neq b, b \neq c} R''(u_b - u_c) R'''(u_a - u_b)^2 + \sum_{a \neq c, b \neq c, c \neq d} R'''(u_a - u_c) R'''(u_b - u_c) R''(u_c - u_d) \, . \end{aligned} \tag{6.14}$$

This however does not prove useful to simplify $\delta_A^{(2)} R$.

Remains to calculate the 3-loop diagrams, shown on Fig 1. This is achieved in appendix C. Since the above method generates a large number of identities, one can wonder whether they are all compatible. We have checked that this is indeed so, but we have not attempted a general proof.

6.2 The effective action up to 3-loop order

Using the sloop elimination method exposed in the preceding section, we have calculated all diagrams up to 3-loop order. They are presented graphically on figure 1, and given below. The expressions intervening in the sloop-projection algorithm are collected in appendix C. Here we give the final result for the effective action, before discussing how to obtain the β-function in the next section.

The effective dimensionfull renormalized disorder to 3-loop order reads

$$R_{\text{eff}}(u) = R(u) + \delta^{(1)} R(u) + \delta^{(2)} R(u) + \delta^{(3)} R(u) + \dots \tag{6.15}$$

The 1-loop term is, noting $R''_u := R''(u)$, $R''_0 := R''(0)$, $R'''_0 := R'''(0^+)$ etc.

$$\delta^{(1)} R(u) = \frac{1}{2} \left[R''^2_u - R''_u R''_0 \right] I_1 \, . \tag{6.16}$$

The 2-loop term is

$$\delta^{(2)}R(u) = \left[R''_u R'''^2_u - R''_0 R'''^2_u - R''_u R'''^2_0\right] I_A + \frac{1}{2}\left[(R''_u - R''_0)^2 R''''_u\right] I_B \; . \tag{6.17}$$

The 3-loop terms read

$$\delta^{(3)}R(u) = (h) + (i) + (j) + (k) + (l) + (m) + (n) + (o) + (p) + (q) \tag{6.18}$$

$$(h) = \frac{1}{2}(R''_u - R''_0)^2 R''''^2_u I_h \tag{6.19}$$

$$(i) = \frac{1}{2}\left(R'''^4_u - 2R'''^2_u R'''^2_0\right) I_i \tag{6.20}$$

$$(j) = (R''_u - R''_0)^2 R''''^2_u I_j \tag{6.21}$$

$$(k) = 0 \tag{6.22}$$

$$(l) = 4\Big(R''_u R'''^2_u R''''_u - R''_0 R'''^2_u R''''_u - R''_u R'''^2_0 R''''_0\Big) I_l \tag{6.23}$$

$$(m) = \frac{1}{2}\left(R'''^4_u - 2R'''^2_u R'''^2_0\right) I_m \tag{6.24}$$

$$(n) = \frac{1}{6}\left(R''_u - R''_0\right)^3 R^{(6)}_u I_n \tag{6.25}$$

$$(o) = \left(R''_u R''''_u R'''^2_u - R''_0 R''''_u R'''^2_u - R''_u R'''^2_0 R''''_0\right) I_o \tag{6.26}$$

$$(p) = 2(R''_u - R''_0)^2 R'''_u R^{(5)}_u I_p \tag{6.27}$$

$$(q) = (R''_u - R''_0) R''''_u \left(R'''^2_u - R'''^2_0\right) I_q \; . \tag{6.28}$$

6.3 Derivation of the RG-equation to 3-loop order

Let us now discuss in general the strategy to renormalize theories, whose interaction is not a single coupling-constant, but a whole function, here the disorder-correlator $R(u)$. We denote by R_0 the bare disorder – this is the object in which perturbation theory is carried out – and by R the renormalized disorder, i.e. the corresponding term in the effective action Γ.

We define the dimensionless bilinear 1-loop, trilinear 2-loop and quadrilinear 3-loop functions

$$\delta^{(1)}(R,R) := \delta^{(1)}R \tag{6.29}$$

$$\delta^{(2)}(R,R,R) := \delta^{(2)}R \tag{6.30}$$

$$\delta^{(3)}(R,R,R,R) := \delta^{(3)}R \tag{6.31}$$

where if all arguments are the same, we only give this one argument, e.g. $\delta^{(1)}(R) = \delta^{(1)}(R,R)$, $\delta^{(2)}(R) = \delta^{(2)}(R,R,R)$ and $\delta^{(3)}(R) = \delta^{(3)}(R,R,R,R)$. For different arguments we use the multilinear formulas

$$
\begin{aligned}
f(x,y) &:= \frac{1}{2}\Big[f(x+y)-f(x)-f(y)\Big] && (6.32)\\
g(x,y,z) &:= \frac{1}{6}\Big[g(x+y+z)-g(x+y)-g(y+z)\\
&\qquad -g(x+z)+g(x)+g(y)+g(z))\Big] && (6.33)\\
h(w,x,y,z) &:= \frac{1}{24}\Big[h(w+x+y+z)-h(w+x+y)-h(w+x+z)-h(w+y+z)\\
&\qquad -h(x+y+z)+h(w+x)+h(w+y)+h(w+z)+h(x+y)+h(x+z)\\
&\qquad +h(y+z)-h(w)-h(x)-h(y)-h(z)\Big] && (6.34)
\end{aligned}
$$

Schematically, the renormalized disorder is

$$
R = R_0 + \delta^{(1)}R(R_0) + \delta^{(2)}R(R_0) + \delta^{(3)}R(R_0) + O(R_0^5)\ , \tag{6.35}
$$

calculated in the preceding section (where we had not explicitly written an index 0 to indicate the bare disorder). The inversion of relation (6.35) is

$$
\begin{aligned}
R_0 = R &- \delta^{(1)}(R) - \delta^{(2)}(R) + 2\delta^{(1)}(R,\delta^{(1)}(R))\\
&-\delta^{(3)}(R) + 3\delta^{(2)}(R,R,\delta^{(1)}(R)) + 2\delta^{(1)}(R,\delta^{(2)}(R))\\
&-\delta^{(1)}(\delta^{(1)}(R)) - 4\delta^{(1)}(R,\delta^{(1)}(R,\delta^{(1)}(R))) + O(R^5)\ .
\end{aligned} \tag{6.36}
$$

Since an n-loop integral scales like $m^{-n\varepsilon}$ the β-function is directly read off from (6.35),

$$
-\, m\partial_m R\Big|_{R_0} = \varepsilon\Big[\delta^{(1)}(R_0) + 2\delta^{(2)}(R_0) + 3\delta^{(3)}(R_0)\Big] + O(R_0^5)\ . \tag{6.37}
$$

However, we need the β-function in terms of R, for which we replace R_0 by R, using Eq. (6.36),

$$
\begin{aligned}
-m\partial_m R\Big|_{R_0} = \varepsilon\Big[&\delta^{(1)}(R) + 2\delta^{(2)}(R) - 2\delta^{(1)}(R,\delta^{(1)}(R))\\
&+3\delta^{(3)}(R) - 6\delta^{(2)}(R,R,\delta^{(1)}(R)) - 2\delta^{(1)}(R,\delta^{(2)}(R))\\
&+\delta^{(1)}(\delta^{(1)}(R),\delta^{(1)}(R)) + 4\delta^{(1)}(R,\delta^{(1)}(R,\delta^{(1)}(R)))\Big] + O(R^5)\ .
\end{aligned} \tag{6.38}
$$

Using the results from Eqs. (6.16), (6.17) and (6.18), this is, printing one diagram and its counter-terms (as dictated by the renormalization group $\mathbf{R}$-operation) per line:

$$
\begin{aligned}
-m\partial_m R_u = & \left(\tfrac{1}{2}R_u''^2 - R_u''R_0''\right)(\varepsilon I_1) \\
& + \left(R_u''R_u'''^2 - R_0''R_u'''^2 - R_u''R_0'''^2\right)\varepsilon\left(2I_A - I_1^2\right) \\
& + \left((R_u''-R_0'')^2 R_u''''\right)\varepsilon\left(I_B - I_1^2\right) \\
& +(R_u''-R_0'')^2(R_u'''')^2\varepsilon\left(\tfrac{3}{2}I_h - 6I_1I_B + \tfrac{9}{2}I_1^3\right) \\
& +\tfrac{3}{2}\left(R_u'''^4 - 2R_u'''^2R_0'''^2\right)(\varepsilon I_i) \\
& +(R_u''-R_0'')^2R_u''''^2\varepsilon\left(3I_j - 2I_AI_1\right) \\
& +\left(R_u''R_u'''^2R_u'''' - R_0''R_u'''^2R_u'''' - R_u''R_0'''^2R_0''''\right)\varepsilon\left(12I_l - 12I_1I_A + 4I_1^3\right) \\
& + \left(R_u'''^4 - 2R_u'''^2R_0'''^2\right)\varepsilon\left(\tfrac{3}{2}I_m + \tfrac{1}{2}I_1^3 - 2I_1I_A\right) \\
& + \left(R_u''-R_0''\right)^3 R_u^{(6)}\varepsilon\tfrac{1}{2}\left(I_n - 3I_1I_B + 2I_1^3\right) \\
& +\left(R_u''R_u''''R_u'''^2 - R_0''R_u''''R_u'''^2 - R_u''R_0'''^2R_0''''\right)\varepsilon(3I_o - 4I_1I_A + I_1I_B) \\
& +(R_u''-R_0'')^2R_u'''R_u^{(5)}\varepsilon 6(I_p - I_1I_A - I_1I_B + I_1^3) \\
& +(R_u''-R_0'')R_u''''\left(R_u'''^2 - R_0'''^2\right)\varepsilon(3I_q - 3I_1I_A - 2I_1I_B + 2I_1^3)
\end{aligned}
\tag{6.39}
$$

On this form, one can explicitly check renormalizability. Since we kept the amplitudes of sub-divergences, as for instance that of the 2-loop bubble-chain diagram, one can exactly see, where these terms come from. Actually the form given above is unique, even though several diagrams have the same functional dependence on R.

Let us now proceed to simplify the above equation. In order to do so, we have to choose a renormalization-scheme. We calculate the 3 leading terms in the ε-expansion of each diagram, i.e. up to order $1/\varepsilon$ for the 3-loop diagrams, up to order ε^0 for the 2-loop diagrams and up to order ε for the 1-loop diagram. In order to have the final result as simple as possible, we absorb a factor of εI_1 into R. This means that an n-loop integral has to be normalized by $(\varepsilon I_1)^n$. It is with this normalization that the amplitudes are given in appendix A. The advantage of this procedure is that integrals take the most simple form, and there are no spurious terms like $\psi(1)$ or $\zeta(2)$. By this way, the 1-loop diagram is automatically subtracted completely and one never has to worry about its finite parts. However, we have a choice of how to subtract diagrams at 2-loop order. The most common choice is to subtract the divergent part only. The advantage of this procedure is that the 2-loop β-function takes the simplest form, with the combination of $\varepsilon(2I_A - I_1^2)$ in the second line of (6.39) replaced by $\frac{1}{2}$. The disadvantage is that then diagrams like (q) do not vanish, but have an amplitude proportional to (see last line of (6.39)) $I_q - I_1I_A$ (since $I_B = I_1^2$, and in our normalizations this is exact in any subtraction scheme). Now if at second order, we only subtract the diverging part of I_A this combination becomes

$$
\begin{aligned}
& I_q - I_1 \times \text{diverging part of } I_A \\
& \qquad = I_1 \times \text{fintite part of } I_A = O\left(\frac{1}{\varepsilon}\right) .
\end{aligned}
\tag{6.40}
$$

We therefore chose to always subtract the diagram exactly. At order 3 at which we are working here, this means that we have to keep the finite part of I_A. This is sufficient, since the 1-loop integral is normalized to have no finite part, and since from the 3-loop integrals one only needs the diverging part anyway. Let us now use that

$$\begin{aligned} I_B &= I_I^2 \\ I_h &= I_n = I_1^3 \\ I_p &= I_q = I_1 I_A \end{aligned} \tag{6.41}$$

to restate the β-function:

$$\begin{aligned} -m\partial_m R_u = & \left(\tfrac{1}{2}R_u''^2 - R_u''R_0''\right)(\varepsilon I_1) \\ & + \left(R_u''R_u'''^2 - R_0''R_u'''^2 - R_u''R_0'''^2\right)\varepsilon\left(2I_A - I_1^2\right) \\ & + \tfrac{3}{2}\left(R_u'''^4 - 2R_u'''^2R_0'''^2\right)(\varepsilon I_i) \\ & + (R_u'' - R_0'')^2 R_u''''^2 \varepsilon\left(3I_j - 2I_AI_1\right) \\ & + \left(R_u''R_u'''^2R_u'''' - R_0''R_u'''^2R_u'''' - R_u''R_0'''^2R_0''''\right)\varepsilon\left(12I_l - 12I_1I_A + 4I_1^3\right) \\ & + \left(R_u'''^4 - 2R_u'''^2R_0'''^2\right)\varepsilon\left(\tfrac{3}{2}I_m + \tfrac{1}{2}I_1^3 - 2I_1I_A\right) \\ & + \left(R_u''R_u''''R_u'''^2 - R_0''R_u''''R_u'''^2 - R_u''R_0'''^2R_0''''\right)\varepsilon(3I_o - 4I_1I_A + I_1^3)\,. \end{aligned} \tag{6.42}$$

Finally, we go to the dimensionless renormalized disorder $\tilde{R}$, defined in Eq. (5.50) by

$$R(u) =: \frac{m^{-4\zeta}}{\varepsilon I_1}\tilde{R}(um^\zeta) \equiv \frac{m^{\varepsilon-4\zeta}}{\varepsilon \tilde{I}_1}\tilde{R}(um^\zeta) \tag{6.43}$$

and group together alike terms. This yields our final expression for the 3-loop β-function given in Eq. (3.1). The coefficients $\mathcal{C}_1$ to $\mathcal{C}_4$, already given in Eqs. (3.2)–(3.5) are constructed from the diagrams via

$$\begin{aligned} \mathcal{C}_1 &= \frac{2I_A}{(\varepsilon I_1)^2} - \frac{1}{\varepsilon^2} - \frac{1}{2\varepsilon} = \frac{9 + 4\pi^2 - 6\psi'(\frac{1}{3})}{36} \\ &= -0.3359768096723647 \end{aligned} \tag{6.44}$$

$$\begin{aligned} \mathcal{C}_2 &= \varepsilon\left(\frac{3}{2}I_1 + \frac{3}{2}I_m + \frac{1}{2}I_1^3 - 2I_1I_A\right)(\varepsilon I_1)^{-3} \\ &= \frac{3}{4}\zeta(3) + \frac{\pi^2}{18} - \frac{\psi'(\frac{1}{3})}{12} = 0.6085542725335131 \end{aligned} \tag{6.45}$$

$$\begin{aligned} \mathcal{C}_3 &= \varepsilon(3I_j - 2I_1I_A)(\varepsilon I_1)^{-3} = \frac{\psi'(\frac{1}{3})}{6} - \frac{\pi^2}{9} \\ &= 0.5859768096723648 \end{aligned} \tag{6.46}$$

$$\begin{aligned} \mathcal{C}_4 &= \varepsilon\left(12I_l - 16I_1I_A + 5I_1^3 + 3I_o\right)(\varepsilon I_1)^{-3} \\ &= 2 + \frac{\pi^2}{9} - \frac{\psi'(\frac{1}{3})}{6} = 1.4140231903276352\,. \end{aligned} \tag{6.47}$$

These constants are closely related to each other analytically.

7 Reparametrization invariance

It is known in standard field theory, that one can perform a change of variables, and thus formally change the β-function, while all observables remain unchanged. In the context of a functional RG, this reparametrization invariance is much larger. The function $R(u)$ can be changed into an arbitrary functional of $f[R]$. The most useful such reparametrizations involve functionals $f[R]$, which have the same structure as corrections to R, obtained perturbatively. Especially, when the field u has dimension ζ, and R times the 1-loop integral has dimension -4ζ, this means that on dimensional grounds for each additional power of R in $f[R]$, there should be 4 derivatives. Also we do not want $R(u)$ to have different analyticity properties, i.e. if $R(u)$ has a r.h.s. Taylor-expansion with a missing linear term (absence of a super-cusp) then $f[R]$ should have the same properties. The most suggesting such functional is the 1-loop contribution itself, which we study now.

The 2-loop RG-equation for the renamed disorder correlator $\tilde{R}_u$ reads

$$\begin{aligned} -m\partial_m \tilde{R}_u &\equiv \beta[\tilde{R}](u) \\ &= (\varepsilon - 4\zeta)\,\tilde{R}_u + u\zeta \tilde{R}'_u + \frac{1}{2}\tilde{R}''^2_u - \tilde{R}''_u \tilde{R}''_0 + \frac{1}{2}\left(\tilde{R}''_u \tilde{R}'''^2_u - \tilde{R}''_0 \tilde{R}'''^2_u - \tilde{R}''_u \tilde{R}'''^2_0\right) . \end{aligned} \tag{7.1}$$

Consider the following change of variables

$$\tilde{R}_u \equiv f[R](u) = R_u - \lambda\left(\frac{1}{2}R''^2_u - R''_u R''_0\right) + \mathcal{O}(R^3) . \tag{7.2}$$

Varying m yields

$$-m\partial_m \tilde{R}_u = -m\partial_m\left[R_u - \lambda\left(\frac{1}{2}R''^2_u - R''_u R''_0\right)\right] . \tag{7.3}$$

This is equivalent to stating that

$$\beta[\tilde{R}](u) = \beta[R](u) - \lambda\Big\{R''(u)\beta[R]''(u) - R''(0)\beta[R]''(u) - R''(u)\beta[R]''(0)\Big\} . \tag{7.4}$$

Solving this equation perturbatively yields the β-function for R_u

$$\begin{aligned} \beta[R](u) = (\varepsilon - 4\zeta)R_u + \zeta u R'_u + \left[\frac{1}{2}R''^2_u - R''_u R''_0\right](1+\lambda\varepsilon) + \frac{1}{2}\left(R''_u \tilde{R}'''^2_u - R''_0 R'''^2_u - R''_u R'''^2_0\right) \\ + \mathcal{O}(\varepsilon^4) \end{aligned} \tag{7.5}$$

This equations tells us nothing more than that adding a coefficient of order ε to the second-order term does not change universal results at 2-loop order. (The reader may want to verify this surprising result for the slope of the β-function at 2-loop order in a scalar field-theory.)

Suppose now that $\beta[R](u) = 0$. Then this also holds for its derivatives and multiples thereof. Therefore, we can add terms of the form

$$R''(u)\beta[R]''(u) - R''(0)\beta[R]''(u) - R''(u)\beta[R]''(0) . \tag{7.6}$$

Note that these are the same terms, which appeared in equation (7.4).

In the following, we chose $\zeta = 0$, since this yields the simplest relations. We will comment on the more general case later. Expression (7.6) then reads

$$\varepsilon\left(R''^2_u - 2R''_u R''_0\right) + \left(R''_u R'''^2_u - R''_0 R'''^2_u - R''_u R'''^2_0\right) + \left(R''_u - R''_0\right)^2 R''''(u) . \tag{7.7}$$

Adding $-1/2$ times (7.7) to the β-function (7.5) and choosing there $\lambda = -1/2$ to eliminate the additional 1-loop order term gives

$$0 = \varepsilon R_u + \left[\frac{1}{2} R_u''^2 - R_u'' R_0''\right] - \frac{1}{2} \left(R_u'' - R_0''\right)^2 R''''(u) + \mathcal{O}(\varepsilon^4) \; . \tag{7.8}$$

In this equation, we have traded the term proportional to $R'' R'''^2$ for a term of the form $R'''' R''^2$. Since the latter is uniquely defined, this allows again to fix the anomalous terms associated to $R'' R'''^2$.

It would be satisfactory, to have a similar result for the case $\zeta \neq 0$. The above construction however yields terms of the form

$$\left(\zeta u R_u'\right)'' R_u'' \tag{7.9}$$

plus the respective anomalous terms. Although one can of course solve differential equations involving these terms, and thus e.g. check the numerical solution of the fixed point equation to be discussed later, we have found no way to eliminate these terms, without generating even more "unusual" ones. Our search comprised rescalings of R_u, of the field u, adding $u\beta[R]'(u)$ to both the variable transformation and the β-function itself, and adding multiples of the β-function. On the other hand, one can first write the β-function without rescaling, then do the non-trivial transformations given above, and finally perform the rescaling. This will simply give the standard rescaling terms.

Let us also comment on the power of reparametrization invariance at 3-loop order. While it proves to be a powerful tool for many diagrams, it is at least not applicable to fix all anomalous terms. This can be anticipated from the difference between diagrams (o) and (q) (see appendices C.3.8 and C.3.10), which is proportional to

$$(o) - (q) \sim R_0'''^2 \left(R_u'' R_u^{(4)} - R_0'' R_u^{(4)} - R_u'' R_0^{(4)}\right) \; . \tag{7.10}$$

While (o) and (q) have the same normal terms, their difference is proportional to $R'''(0^+)^2$, thus the anomalous terms are different.

8 2-point correlation function

As a prototype physical observable we calculate the 2-point correlation function to 2-loop order in an ε-expansion. The Fourier transform of Eq. (5.18) reads

$$\overline{\langle u(x) u(y)\rangle}_V = T g(x,y) - \int_{z,z'} g(x,z) g(y,z') R''[0^+](z,z'). \tag{8.1}$$

Because of the limit $n \to 0$ in Eq. (5.18), where n is the number of replica fields, this is an exact expression; in particular, there are no contributions of three- or higher-replica terms to the 2-point function. As in Sec. 5, the expression $R''[0^+](z,z')$ denotes the second functional derivative of $R[u]$ with respect to $u(z)$ and $u(z')$ that is evaluated in a weak limit $u(x) \approx \text{const.} \to 0$. A precise definition of the weak limit is given in Eq. (5.26).

8.1 2-loop expression

For the expansion in the renormalized local disorder function $R(u)$ with a constant field u we again use that

$$R''[0^+](z,z') = R''(0^+)\delta(z-z') + \tilde{R}''[0^+](z,z'), \tag{8.2}$$

where the non-local part $\tilde{R}''[0^+](z,z')$ has to be expanded to 2-loop order, like in the derivation of the 3-loop β-function. Taking two derivatives of Eq. (5.37), evaluated at a constant field u, and sending $u \to 0^+$ we find

$$\begin{aligned}\tilde{R}''[0^+](z_1,z_2) = \delta_{z_1 z_2}\Big[&- I_1 R'''(0^+)^2 + (5I_1^2 - 4I_A) R'''(0^+)^2 R''''(0^+)\Big] \\ &+ g(z_1,z_2)^2 \Big[R'''(0^+)^2 - 6 I_1 R'''(0^+)^2 R''''(0^+)\Big] \\ &+ 2 g(z_1,z_2) R'''(0^+)^2 R''''(0^+) \int_x g(x,z_1) g(x,z_2) \big[g(x,z_1) + g(x,z_2)\big] \\ &+ R'''(0^+)^2 R''''(0^+) \int_x g(x,z_1)^2 g(x,z_2)^2 .\end{aligned} \tag{8.3}$$

Of course, the limit $u \to 0^-$ would yield the same result. Inserting into Eq. (8.1) and taking the Fourier transform gives at $T=0$ yields

$$\begin{aligned} g(q)^{-2}\overline{\langle u(q)u(-q)\rangle}_V = -R''(0^+) + R'''(0^+)^2 \big[I_1 - I_1(q)\big] \\ - R'''(0^+)^2 R''''(0^+) \big[(I_1 - I_1(q))^2 + 4\Phi_{2,\varepsilon}(q)\big] .\end{aligned} \tag{8.4}$$

As before $I_1 = I_1(0)$, $I_A = I_A(0)$, and $\Phi_{2,\varepsilon}(q) = I_A(q) - I_A + I_1^2 - I_1 I_1(q)$ with

$$I_1(q) = \quad$$ 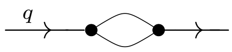 $$\quad = \int_p g(p) g(p+q) \tag{8.5}$$

$$I_A(q) = \quad$$ 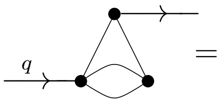 $$\quad = \int_{p_1,p_2} g(p_1) g(p_2) g(p_1+p_2) g(p_1+q). \tag{8.6}$$

The first line in Eq. (8.4) is the tree and 1-loop contribution, already calculated in [19]. The second line is the 2-loop contribution, again with a non-vanishing limit $R'''(0^+)^2$. Note that the momentum could go through the non-trivial 2-loop diagram I_A in two different ways, but only the one in Eq. (8.6) contributes to the 2-point function.

8.2 Integrals

Let us start out with the normalization factors used throughout this work. Consider the 1-loop integral

$$\tilde{I}_1 = \quad$$ 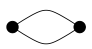 $$\Big|_{m=1} = \int_k g(k)^2 \Big|_{m=1} = \int \frac{\mathrm{d}^d k}{(2\pi)^d} \frac{1}{(k^2+1)^2} \tag{8.7}$$

Using a Feynman-representation for the propagator yields

$$\tilde{I}_1 = \int \frac{\mathrm{d}^d k}{(2\pi)^d} \int_0^\infty \mathrm{d}\alpha\, \alpha\, \mathrm{e}^{-\alpha(k^2+1)} = \int \frac{\mathrm{d}^d k}{(2\pi)^d} \mathrm{e}^{-k^2} \times \int_0^\infty \mathrm{d}\alpha\, \alpha^{1-d/2}\, \mathrm{e}^{-\alpha} \tag{8.8}$$

Let us note, with $d = 4 - \varepsilon$

$$\mathcal{N} := \int \frac{\mathrm{d}^d k}{(2\pi)^d} \mathrm{e}^{-k^2} = \frac{1}{(4\pi)^{\frac{d}{2}}} , \tag{8.9}$$

$$\int_0^\infty \mathrm{d}\alpha\, \alpha^{1-d/2}\, \mathrm{e}^{-\alpha} = \Gamma(2 - \tfrac{d}{2}) = \Gamma(\tfrac{\varepsilon}{2}) = \frac{2}{\varepsilon}\Gamma(1 + \tfrac{\varepsilon}{2}) \tag{8.10}$$

This yields

$$\varepsilon\tilde{I}_1 = \mathcal{N}\times 2\Gamma(1+\tfrac{\varepsilon}{2}) = \mathcal{N}\times\left[2-\gamma_{\rm E}\varepsilon+\frac{1}{24}(6\gamma_{\rm E}^2+\pi^2)\varepsilon^2+\mathcal{O}(\varepsilon^3)\right] . \tag{8.11}$$

There are therefore two convenient choices for normalizations: Either we normalize everything by $\varepsilon\tilde{I}_1$: then $\tilde{I}_1$ will be effectively $1/\varepsilon$, without higher loop corrections. Or we normalize by $\mathcal{N}$, which takes out the factor from the Gauss integration. We use whatever is more convenient.

We now turn to the evaluation of $I_1(q)$ and $I_A(q)$. The 1-loop integral in presence of an external momentum can be parameterized by $I_1(q) = \frac{1}{m^{\varepsilon}}\tilde{I}_1(\frac{q}{m})$ with

$$\tilde{I}_1(z) = \tilde{I}_1(0)\ {}_2F_1(2-d/2,1,3/2,-z^2/4) \tag{8.12}$$

$$= \tilde{I}_1(0)\int_0^1 \mathrm{d}y\ \left[1+y(1-y)z^2\right]^{-\frac{\varepsilon}{2}} . \tag{8.13}$$

Using the series expansion of the hypergeometric function in Eq. (8.12) or an expansion in ε of the integrand in Eq. (8.13), we find

$$\begin{aligned}\tilde{I}_1(z) = \tilde{I}_1(0)\Bigg\{&1+\varepsilon\left(1-\frac{\sqrt{4+z^2}}{z}\operatorname{asinh}(z/2)\right)\\ &+\varepsilon^2\Bigg[1+\frac{\sqrt{4+z^2}}{4z}\bigg(\mathrm{Li}_2\Big(\tfrac{1}{2}-\tfrac{z}{2\sqrt{z^2+4}}\Big)-\mathrm{Li}_2\Big(\tfrac{1}{2}+\tfrac{z}{2\sqrt{z^2+4}}\Big)+\big(\ln(z^2{+}4){-}4\big)\operatorname{asinh}(z/2)\bigg)\Bigg]\\ &+\mathcal{O}(\varepsilon^3)\Bigg\}\end{aligned} \tag{8.14}$$

All singular contributions of $\tilde{I}_1(z)$ are present for $z=0$, where $\tilde{I}_1(0)=\mathcal{N}[\frac{2}{\varepsilon}-\gamma_{\rm E}+\mathcal{O}(\varepsilon)]$. Thus, the difference $I_1 - I_1(q)$ is finite in the limit of $\varepsilon\to 0$. The asymptotics for large z is given by

$$\begin{aligned}\tilde{I}_1(z)\simeq\tilde{I}_1(0)\Big\{&1+\varepsilon\left[1-\ln z+\mathcal{O}(\tfrac{1}{z}\ln z)\right]+\varepsilon^2\left[\frac{1}{2}(\ln z)^2-\ln(z)+1-\frac{\pi^2}{24}+\mathcal{O}(\tfrac{1}{z}\ln z)\right]\\ &+\mathcal{O}(\varepsilon^3)\Big\}\end{aligned} \tag{8.15}$$

The second term $\Phi_{2,\varepsilon}(q) = \frac{1}{m^{2\varepsilon}}\tilde{\Phi}_{2,\varepsilon}(\frac{q}{m})$ is more complicated and treated in App. D. It also has a finite limit $\varepsilon\to 0$, which we can only state as an integral. A Taylor expansion for small z gives

$$\tilde{\Phi}_{2,0}(z)\approx\mathcal{N}^2\big(0.03821z^2+0.00169z^4-0.00039z^6+0.00007z^8+\dots\big) \tag{8.16}$$

For large z we find

$$\tilde{\Phi}_{2,0}(z)\simeq\mathcal{N}^2\big[2(\ln z)^2-6\ln z+\alpha_0+\mathcal{O}(\tfrac{1}{z}\ln z)\big] . \tag{8.17}$$

Thus the full 2-loop contribution to the 2-point function has the asymptotic form

$$\big[\tilde{I}_1(z)-\tilde{I}_1(0)\big]^2+4\tilde{\Phi}_{2,0}(z)\simeq\mathcal{N}^2\big[12(\ln z)^2-32\ln z+4+4\alpha_0+\mathcal{O}(\tfrac{1}{z}\ln z)+\mathcal{O}(\varepsilon)\big] . \tag{8.18}$$

The constant $\alpha_0\approx 6.17$ was calculated numerically.

8.3 Scaling function (for arbitrary ζ)

We parameterize the 2-point correlation function as

$$\overline{\langle u(q)u(-q)\rangle} = m^{-d-2\zeta}\tilde{c}(d)F_d(\tfrac{|q|}{m}) \tag{8.19}$$

with universal amplitude $\tilde{c}(d)$ and scaling function F_d with $F_d(0)=1$. At momentum zero the higher loop terms do not contribute to the 2-point correlation function such that to all orders in ε

$$\tilde{c}(d) = m^{d+2\zeta}\langle u(0)u(0)\rangle = -\frac{1}{\varepsilon\tilde{I}_1}\tilde{R}''(0). \tag{8.20}$$

Using Eq. (8.4) and the rescaled renormalized disorder $\tilde{R}$, defined in Eq. (5.50), the scaling function is given by

$$\begin{aligned} F_d(z) = \frac{-1}{\tilde{R}''(0)}\frac{1}{(1+z^2)^2}\Big\{&-\tilde{R}''(0)+\tilde{R}'''(0^+)^2\frac{1}{\varepsilon\tilde{I}_1}\left[\tilde{I}_1-\tilde{I}_1(z)\right] \\ &-\tilde{R}'''(0^+)^2\tilde{R}''''(0^+)\frac{1}{(\varepsilon\tilde{I}_1)^2}\left[\left(\tilde{I}_1-\tilde{I}_1(z)\right)^2+4\tilde{\Phi}_{2,\varepsilon}(z)\right]+\mathcal{O}(\varepsilon^4)\Big\}. \end{aligned} \tag{8.21}$$

At a fix-point there are a number of consistency relations for the third and fourth derivatives of the disorder distribution at $u=0^+$ in an ε-expansion. Taking two field-derivatives of the fix-point equation, that is, evaluating $0=\frac{\partial}{\partial m}\tilde{R}''(0^+)$ gives

$$0 = (\varepsilon-2\zeta)\tilde{R}''(0^+)+\tilde{R}'''(0^+)^2+2\tilde{R}'''(0^+)^2\tilde{R}''''(0^+)+\mathcal{O}(\varepsilon^4). \tag{8.22}$$

Similarly, $0=\frac{\partial}{\partial m}\tilde{R}'''(0^+)$ gives the identity

$$0 = R'''(0^+)\big[-\zeta+\varepsilon+3R''''(0^+)+\mathcal{O}(\varepsilon^2)\big]. \tag{8.23}$$

Regardless of the sign of the prefactor, the bracket has to vanish. Therefore, evaluation at $u=0^-$ would lead to the same result, namely $\tilde{R}''''(0^+) = -\frac{\varepsilon-\zeta}{3}+\mathcal{O}(\varepsilon^2)$, which can be inserted into Eq. (8.22) to obtain

$$\tilde{R}'''(0^+)^2 = -(\varepsilon-2\zeta)\tilde{R}''(0^+)\left[1+\tfrac{2}{3}(\varepsilon-\zeta)\right]+\mathcal{O}(\varepsilon^4) \tag{8.24}$$

$$\tilde{R}'''(0^+)^2\tilde{R}''''(0^+) = \tfrac{1}{3}(\varepsilon-2\zeta)(\varepsilon-\zeta)\tilde{R}''(0^+)+\mathcal{O}(\varepsilon^4). \tag{8.25}$$

Substituting these expressions into Eq. (8.21) gives

$$\begin{aligned} F_d(z) = \frac{1}{(1+z^2)^2}\Big\{&1+(\varepsilon-2\zeta)\big[1+\tfrac{2}{3}(\varepsilon-\zeta)\big]\frac{1}{\varepsilon\tilde{I}_1}\big(\tilde{I}_1-\tilde{I}_1(z)\big) \\ &+\tfrac{1}{3}(\varepsilon-2\zeta)(\varepsilon-\zeta)\frac{1}{(\varepsilon\tilde{I}_1)^2}\left[\left(\tilde{I}_1-\tilde{I}_1(z)\right)^2+4\tilde{\Phi}_{2,\varepsilon}(z)\right]\Big\}+\mathcal{O}(\varepsilon^3). \end{aligned} \tag{8.26}$$

For large $z=\frac{|q|}{m}$ the asymptotic behavior of the scaling function is, with α_0 given after Eq. (8.18),

$$\begin{aligned} F_d(z) \simeq \frac{1}{(1+z^2)^2}\Big\{&1+(\ln z-1)(\varepsilon-2\zeta)+\left(\frac{1}{2}(\ln z)^2-\ln z\right)(\varepsilon-2\zeta)^2 \\ &+(\varepsilon-2\zeta)\left[\left(\frac{\alpha_0-1}{3}-1+\frac{\pi^2}{24}\right)\varepsilon-\frac{\alpha_0-1}{3}\zeta\right]\Big\}+\mathcal{O}(\varepsilon^3)+\mathcal{O}(\tfrac{1}{z}\ln z). \end{aligned} \tag{8.27}$$

Assuming the following behavior for large z

$$F_d(z) \simeq \left[1 + b_1\varepsilon + b_2\varepsilon^2 + \mathcal{O}(\varepsilon^3)\right] z^{\varepsilon-2\zeta-4} \tag{8.28}$$

the coefficients b_1 and b_2 are

$$b_1 = -(1-2\zeta_1) \tag{8.29}$$

$$b_2 = 2\zeta_2 + (1-2\zeta_1)\left[\frac{\alpha_0-1}{3}(1-\zeta_1) - 1 + \frac{\pi^2}{24}\right] \tag{8.30}$$

In the massless limit, that is $|q| \gg m$, the amplitude of the 2-point correlation function is given by

$$\langle u(q)u(-q)\rangle \sim |q|^{-(d+2\zeta)} c(d) \tag{8.31}$$

with propagator

$$c(d) = [1 + b_1\varepsilon + b_2\varepsilon^2 + \mathcal{O}(\varepsilon^3)]\tilde{c}(d). \tag{8.32}$$

We also note that transforming to real space we have

$$\begin{aligned}\frac{1}{2}\overline{\langle[u(x)-u(0)]^2\rangle} &= c(d)\int\frac{\mathrm{d}^d q}{(2\pi)^d}\,(1-\mathrm{e}^{iqx})|q|^{-d-2\zeta}\\ &= \frac{-\Gamma(-\zeta)c(d)}{(4\pi)^{\frac{d}{2}}\Gamma\left(\frac{d}{2}+\zeta\right)}\left(\frac{x}{2}\right)^{2\zeta}\ .\end{aligned} \tag{8.33}$$

This expression breaks down for $\zeta \geq 1$. Having in mind the RF fixed point in $d=1$ which has $\zeta = 1$, we consider a finite system of size L and periodic boundary conditions,

$$\begin{aligned}\int\frac{\mathrm{d}q}{2\pi}\,(1-\mathrm{e}^{iqx})|q|^{-3} &\to \frac{2}{L}\sum_{n=1}^{\infty}\frac{1-\cos(\frac{2\pi n x}{L})}{(\frac{2\pi n}{L})^3}\\ &= -\frac{L^2}{8\pi^3}\left[\mathrm{Li}_3\left(\mathrm{e}^{-\frac{2i\pi x}{L}}\right) + \mathrm{Li}_3\left(\mathrm{e}^{\frac{2i\pi x}{L}}\right) - 2\zeta_{\mathrm{R}}(3)\right]\\ &= \frac{x^2\left[3 + 2\log\left(\frac{L}{2\pi x}\right)\right]}{4\pi} + \mathcal{O}(x^3)\ .\end{aligned} \tag{8.34}$$

To avoid confusion, we have added an index R to the Riemann ζ-function. When $\zeta > 1$, the correlation function (8.33) will grow quadratically with the distance x, with an L-dependent prefactor scaling as $L^{2\zeta-1}$, even though the Fourier-transform has a pure power-law.

$$\begin{aligned}\int\frac{\mathrm{d}q}{2\pi}\,(1-\mathrm{e}^{iqx})|q|^{-1-2\zeta} &\to \frac{L^{2\zeta+1}}{(2\pi)^{2(\zeta+1)}}\left[2\zeta_{\mathrm{R}}(2\zeta+1) - \mathrm{Li}_{2\zeta+1}\left(e^{-\frac{2i\pi x}{L}}\right) - \mathrm{Li}_{2\zeta+1}\left(e^{\frac{2i\pi x}{L}}\right)\right]\\ &= \frac{L^{2\zeta-1}}{(2\pi)^{2\zeta}}\zeta_{\mathrm{R}}(2\zeta-1)x^2 - \frac{x^{2\zeta}\cos(\pi\zeta)\Gamma(-2\zeta)}{2\pi^2} + \ldots\end{aligned} \tag{8.35}$$

The best studied example is depinning, where $\zeta = \frac{5}{4}$ (possibly exactly [79]). As an example we mention Fig. 1 of Ref. [80], where one sees that the structure factor, i.e. Fourier transform of the 2-point function, is a power-law over almost three decades.

9 Fix-point analysis

Irrespective of the precise form of the initial disorder distribution function R_0 in the bare action, we identify different fix-point classes of the RG equation. Although our description may not be complete, the analysis of fix-point solutions gives insight into possible physical realizations of our simple model [Eq. (2.1)]. We study a universality class where R_0 is periodic and in the non-periodic case we distinguish whether R_0 is short range (random bond disorder) or long range (random field disorder). This chapter follows closely Ref. [19] but generalizes the results to 3-loop order.

In terms of the rescaled disorder distribution function

$$\tilde{R}(u) = (\varepsilon \tilde{I}_1) m^{-\varepsilon+4\zeta} R(u m^{-\zeta}) \tag{9.1}$$

the β- function up to 3-loop order reads

$$\begin{aligned} -m\frac{\partial}{\partial m}\tilde{R}(u) &= (\varepsilon - 4\zeta)\tilde{R}(u) + u\zeta \tilde{R}'(u) + \tfrac{1}{2}\tilde{R}''(u)^2 - \tilde{R}''(u)\tilde{R}''(0^+) \\ &\quad + (\tfrac{1}{2} + \mathcal{C}_1\varepsilon)\big[\tilde{R}''(u)\big[\tilde{R}'''(u)^2 - \tilde{R}'''(0^+)^2\big] - \tilde{R}''(0^+)\tilde{R}'''(u)^2\big] \\ &\quad + \mathcal{C}_4\big[\tilde{R}''(u)\big[\tilde{R}'''(u)^2\tilde{R}''''(u) - \tilde{R}'''(0^+)^2\tilde{R}''''(0^+)\big] - \tilde{R}''(0^+)\tilde{R}'''(u)^2\tilde{R}''''(u)\big] \\ &\quad + \mathcal{C}_3\big[\tilde{R}''(u) - \tilde{R}''(0^+)\big]^2\tilde{R}''''(u)^2 + \mathcal{C}_2\big[\tilde{R}'''(u)^4 - 2\tilde{R}'''(u)^2\tilde{R}'''(0^+)^2\big]\,. \end{aligned} \tag{9.2}$$

with coefficients $\mathcal{C}_1, \ldots, \mathcal{C}_4$ given in Eqs. (3.2) ff.

9.1 Random-bond disorder

In order to describe short-range disorder caused by random bonds we look for a fix-point solution that decays exponentially fast for large fields u. To this end we numerically solve the fix-point equation

$$-m\frac{\partial}{\partial m}\tilde{R}(u) = 0 \tag{9.3}$$

order by order in ε. We make the Ansatz

$$\tilde{R}(u) = \varepsilon r_1(u) + \varepsilon^2 r_2(u) + \varepsilon^3 r_3(u) + \mathcal{O}(\varepsilon^4) \tag{9.4}$$

and assume that higher orders in ε do not contribute to field derivatives of lower orders. Also the roughness exponent is expanded in ε

$$\zeta = \varepsilon\zeta_1 + \varepsilon^2\zeta_2 + \varepsilon^3\zeta_3 + \mathcal{O}(\varepsilon^4)\,. \tag{9.5}$$

If $\tilde{R}(u)$ is a fix-point solution of Eq. (9.2) then $\xi^4\tilde{R}(u/\xi)$ is a fix-point solution as well for any ξ. Thus, without loss of generality, it is possible to normalize $\tilde{R}(0) = \varepsilon$, that is, we set $r_1(0) = 1$ and $r_2(0) = r_3(0) = 0$.

Inserting the Ansatz into the fix-point equation we find to lowest, that is, second order in ε

$$0 = (1 - 4\zeta_1)r_1(u) + \zeta_1 u r_1'(u) + \frac{1}{2}r_1''(u)^2 - r_1''(u)r_1''(0)\,. \tag{9.6}$$

Together with $r_1(0) = 1$ this differential equation has a solution for any ζ_1. But for only one specific value of ζ_1 the solution does not change sign and decays exponentially fast for large u. Since $R(u) = R(-u)$ we only consider positive values of u.

Numerically, we adopt the following iterative procedure: First, we guess a value for ζ_1 and compute the corresponding $r_1(u)$. Then we evaluate r_1 at a large value $u_{\max}$. This is repeated until $r_1(u_{\max}) = 0$. The guessing of ζ_1 is improved by calculating $r_1(u_{\max})$ for many values of ζ_1 and interpolating to zero. In order to circumvent numerical problems at small u we approximate $r_1(u)$ by its Taylor expansion up to a finite order for $|u|$ smaller than a gluing point u_{glue}. We find

$$\zeta_1 = 0.2082980628(7) \tag{9.7}$$

for $u_{\max} = 25$. Below $u_{\text{glue}} = 0.01$ a Taylor expansion of order 30 was used. The result does not depend on the order if high enough, also a reasonable variation of the glueing point $u_{\text{glue}} < 2$ is within error tolerances (that is, does not change the digits shown here). Of course, the result does depend on $u_{\max}$, but choosing $u_{max} > 25$ gives results within error tolerances (checked up to $u_{\max} = 50$).

For the higher loop contributions we also need derivatives of r_1. Instead of solving the corresponding differential equations we simply take numerical derivatives. This is possible since r_1 is a smooth function away from zero. Using the obtained ζ_1, $r_1(u)$, and its derivatives, we can solve for the 2-loop contribution

$$\begin{aligned} 0 = {} & r_2(u) - 4\zeta_2 r_1(u) - 4\zeta_1 r_2(u) + u\zeta_2 r_1'(u) + u\zeta_1 r_2'(u) + r_1''(u) r_2''(u) - r_1''(0) r_2''(u) \\ & - r_1''(u) r_2''(0) + \frac{1}{2}\left(r_1''(u) - r_1''(0)\right) r_1'''(u)^2 - \frac{1}{2} r_1''(u) r_1'''(0^+)^2 \end{aligned} \tag{9.8}$$

with $r_2(0) = 0$. This equation is solved for $r_2(u)$ for different values of ζ_2. With an analogous iterative procedure we adjust ζ_2 such that $r_2(u)$ decays exponentially. The best value is

$$\zeta_2 = 0.006857(8) \tag{9.9}$$

as found in [19]. Again, derivatives of $r_2(u)$ are computed numerically and put into the 3-loop contribution

$$\begin{aligned} 0 = {} & r_3(u) - 4\zeta_3 r_1(u) - 4\zeta_2 r_2(u) - 4\zeta_1 r_3(u) + u\big[\zeta_3 r_1'(u) + \zeta_2 r_2'(u) + \zeta_1 r_3'(u)\big] \\ & - r_2''(0) r_2''(u) + \tfrac{1}{2} r_2''(u)^2 - r_1''(u) r_3''(0) - r_1''(0) r_3''(u) + r_1''(u) r_3''(u) - \mathcal{C}_1 r_1''(u) r_1'''(0)^2 \\ & - \tfrac{1}{2} r_2''(u) r_1'''(0)^2 - \mathcal{C}_1 r_1''(0) r_1'''(u)^2 + \mathcal{C}_1 r_1''(u) r_1'''(u)^2 - \tfrac{1}{2} r_2''(0) r_1'''(u)^2 + \tfrac{1}{2} r_2''(u) r_1'''(u)^2 \\ & - 2\mathcal{C}_2 r_1'''(0)^2 r_1'''(u)^2 + \mathcal{C}_2 r_1'''(u)^4 - r_1''(u) r_1'''(0) r_2'''(0) - r_1''(0) r_1'''(u) r_2'''(u) + r_1''(u) r_1'''(u) r_2'''(u) \\ & - \mathcal{C}_4 r_1''(u) r_1'''(0)^2 r_1''''(0) - \mathcal{C}_4 r_1''(0) r_1'''(u)^2 r_1''''(u) + \mathcal{C}_4 r_1''(u) r_1'''(u)^2 r_1''''(u) + \mathcal{C}_3 r_1''(0)^2 r_1''''(u)^2 \\ & - 2\mathcal{C}_3 r_1''(0) r_1''(u) r_1''''(u)^2 + \mathcal{C}_3 r_1''(u)^2 r_1''''(u)^2 \end{aligned} \tag{9.10}$$

with normalization $r_3(0) = 0$. With the iterative procedure described above an approximate exponential decay of $r_3(u)$ is found for

$$\zeta_3 = -0.01075(2)\,. \tag{9.11}$$

The force correlator $-R''(u)$ of the fix-point is plotted on the left side in Fig. 2 for $d = 3$, that is, $\varepsilon = 1$ in a one-, two-, and 3-loop approximation. There are further renormalizations of the cusp, in particular, the 3-loop contribution seems to counteract the 2-loop contribution such that the 3-loop results is close to the 1-loop result.

The dimensional dependence of the roughness exponent is shown in the right graph of Fig. 2. The corrections in 3-loop order are substantial, for $\varepsilon > 1$ they are so large that the ε-expansion is bound to fail. Correspondingly, while the 2-loop results seem to reproduce exact ($d = 1$) [81] and

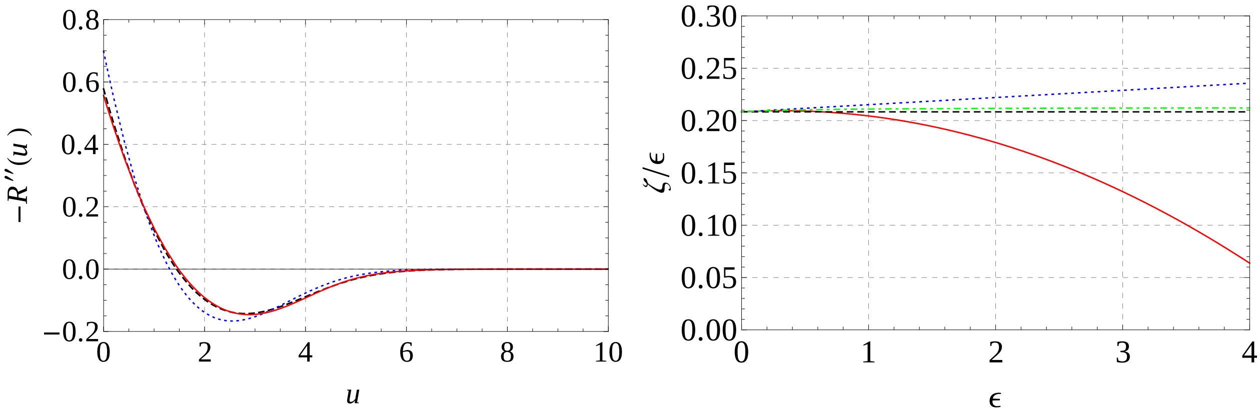

Figure 2: Comparison of results for random bond disorder in 1-loop (black, dashed), 2-loop (blue, dotted), and 3-loop (red, solid) order. Left: Fix point disorder correlator for $d = 3$. Right: Dimensional dependence of the roughness exponent normalized with ε. The (2,1)-Padé approximant is plotted in a green dash-dotted line.

ζ_{eq}	one loop	two loop	three loop	Padé-(2,1)	simulation and exact
$d = 3$	0.208	0.215	0.204	0.211	0.22 ± 0.01 [82]
$d = 2$	0.417	0.444	0.358	0.423	0.41 ± 0.01 [82]
$d = 1$	0.625	0.687	0.396	0.636	2/3 [81]

Figure 3: Roughness exponent for random bond disorder obtained by an ε-expansion in comparison with exact results and numerical simulations. In the fourth column is an estimate value using a (2,1)-Padé approximant of the 3-loop result.

simulation results ($d = 2, 3$) [82], the 3-loop results are worse throughout in this comparison, see Fig. 3. Surprisingly, the (2,1)-Padé-approximant of the 3-loop ε-expansion, which is given by

$$\zeta_{(2,1)} \approx \frac{0.208298\varepsilon + 0.333429\varepsilon^2}{1 + 1.56781\varepsilon}, \tag{9.12}$$

is again very close to the 1-loop result but agrees even better with the reference data. Unfortunately, the third order of a series does not allow to make statements of its asymptotic behavior.

9.2 Random-field disorder

We consider a class of long-range fix-point solutions with $\tilde{R}(u) \sim -\sigma|u|$ for large u. Due to the linear behavior, second and higher derivatives of $\tilde{R}$ do not contribute in the limits $u \to \pm\infty$. Subsequently, all loop corrections to the tail vanish and the reparameterisation terms give $\zeta = \frac{\varepsilon}{3}$ for the roughness exponent to all orders as a prerequisite for the existence of such a fix-point solution.

Following closely the 2-loop calculation [19], we consider $y(u) = -\frac{3}{\varepsilon}\tilde{R}''(u)$ and normalize $y(0) = 1$. Rewriting the fix-point equation in terms of y and integrating over the interval $[0^+, u]$ gives (without loss of generality we consider $u > 0$)

$$0 = B_1 + B_2\varepsilon + B_3\varepsilon^2 + \mathcal{O}(\varepsilon^4) \tag{9.13}$$

This is equivalent to taking one derivative of the β function (3.1), and expressing it in terms of y. The coefficients are B_1, B_2 and B_3 are the 1-, 2-, and 3-loop contributions, given by

$$B_1 = uy + (1-y)y', \tag{9.14}$$

$$B_2 = \frac{1}{6}\left[y'^2(y-1)\right]' - \frac{1}{6}y'y'(0)^2 \tag{9.15}$$

and

$$\begin{aligned} B_3 =& \frac{1}{9}y'(0)^2\left[(C_4 y''(0) - 3C_1)y + 2C_2 y'^2\right]' \\ &+ \frac{1}{9}\left[-C_2 y'^4 - C_3(1-y)^2 y''^2 + (1-y)y'^2(C_4 y'' - 3C_1)\right]' . \end{aligned} \tag{9.16}$$

These equations can be solved analytically, expressing u as a function of y. For the 1-loop equation, the solution reads

$$\frac{u^2}{2} = y - 1 - \ln y, \tag{9.17}$$

which features the cusp. Higher-loop contributions are obtained by making an ansatz; to 3-loop order we need

$$\frac{u^2}{2} = y - 1 - \ln y - \frac{\varepsilon}{3}F_2(y) - \frac{\varepsilon^2}{6}F_3(y) + \mathcal{O}(\varepsilon^3) , \qquad u > 0 . \tag{9.18}$$

The inverse function of $u(y)$, $u > 0$, is $y(u)$. We make use of the known 2-loop solution [19]

$$F_2(y) = 2y - 1 - \frac{1}{2}\ln y + \frac{y}{1-y}\ln y + \mathrm{Li}_2(1-y) \tag{9.19}$$

with boundary conditions up to 2-loop order

$$\begin{aligned} y'(0) &= -1 - \frac{2}{9}\varepsilon + \mathcal{O}(\varepsilon^2) \\ y''(0) &= \frac{2}{3} + \frac{19}{54}\varepsilon + \mathcal{O}(\varepsilon^2) \\ y'''(0) &= -\frac{1}{6} - \frac{71}{360}\varepsilon + \mathcal{O}(\varepsilon^2). \end{aligned} \tag{9.20}$$

Differentiating the ansatz (9.18), with respect to u gives an ε-expansion for $y'(u)$

$$y'(u) = -\frac{uy(u)}{1-y(u)} - \frac{1}{3}\frac{y(u)y'(u)}{1-y(u)}\left[\varepsilon\frac{\mathrm{d}}{\mathrm{d}y}F_2(y)\Big|_{y=y(u)} + \frac{1}{2}\varepsilon^2\frac{\mathrm{d}}{\mathrm{d}y}F_3(y)\Big|_{y=y(u)}\right] + \mathcal{O}(\varepsilon^3). \tag{9.21}$$

We now insert this expression into Eq. (9.13), replacing for the moment only B_1 by its explicit form (9.14). Then the fix-point condition reads

$$0 = \varepsilon\left[B_2 - \frac{1}{3}y(u)y(u)'F_2'(y(u))\right] + \varepsilon^2\left[B_3 - \frac{1}{6}y(u)y'(u)F_3'(y(u))\right] + \mathcal{O}(\varepsilon^3). \tag{9.22}$$

The two terms, each enclosed by square brackets, are dealt with separately. We integrate the first term with respect to u and then again insert Eq. (9.21) to shift the occurrence of $y'(u)$ to a higher order in ε. Since F_2 determines the 2-loop fixed point, the expression is of order ε

$$\int_{0^+}^{\overline{u}} \mathrm{d}u \left[B_2 - \frac{1}{3} y(u) y(u)' F_2'(y(u))\right] =: u_1(y(\overline{u}), \overline{u})\varepsilon + \mathcal{O}(\varepsilon^2). \tag{9.23}$$

The function F_3 can now be determined by considering the ε^2-contribution to Eq. (9.22),

$$B_3 - \frac{1}{6} F_3'(y(u)) y'(u) y(u) + \frac{\mathrm{d}}{\mathrm{d}u} u_1(y(u), u) = 0 \tag{9.24}$$

and $F_3(1) = 0$. Dividing by $y(u)$ and integrating over u we find

$$F_3(y(u)) = 6 \int^u \mathrm{d}u \frac{1}{y(u)} \left[B_3 + \frac{\mathrm{d}}{\mathrm{d}u} u_1(y(u), u)\right] . \tag{9.25}$$

(The lower bounds from the left and right-hand side cancel.) The integral on the right-hand-side is evaluated by first integrating

$$\Psi(u) = \int^u \mathrm{d}u \left[B_3 + \frac{\mathrm{d}}{\mathrm{d}u} u_1(y(u), u)\right] \tag{9.26}$$

and then replacing $y'(u)$ and $y''(u)$ by Eq. (9.21) and u^2 by Eq. (9.18) to zeroth order in ε. The remaining integral

$$\int \mathrm{d}u \frac{1}{y(u)} \frac{\mathrm{d}}{\mathrm{d}u} \Psi(u) = \tilde{F}_3(y(u)) \tag{9.27}$$

can be evaluated with the help of Mathematica and is a function of $y(u)$ only. We find

$$F_3(y) = \tilde{F}_3(y) - \tilde{F}_3(1) = f_0 + f_1 \ln y + f_2 (\ln y)^2 + f_3 \ln y \ln(1-y), \tag{9.28}$$

where

$$\begin{aligned} f_0 = {} & \frac{4 + \frac{4\pi^2}{9} - \frac{2}{3}\gamma_{\frac{1}{3}} - 2\zeta(3)}{(1-y)^2} - \frac{48 - \pi^2 - 30\zeta(3)}{9(1-y)} - \frac{1}{18}\Big[6 - 3\gamma_{\frac{1}{3}} + (57 + 8\pi^2)\zeta(3)\Big] \\ & + (1-y)\Big[-\frac{4}{9}\pi^2 + \frac{2}{3} + \frac{2}{3}\gamma_{\frac{1}{3}} + 4\zeta(3)\Big] + \frac{2}{3}\left(4\zeta(3) - \frac{2-y}{1-y}\right)\mathrm{Li}_2(y) - \frac{2}{3}\mathrm{Li}_3(1-y) \end{aligned} \tag{9.29}$$

with $\gamma_{\frac{1}{3}} = \psi'(\frac{1}{3})$. Furthermore,

$$\begin{aligned} f_1 = {} & \frac{23}{18} - \frac{38\pi^2}{81} + \frac{19}{27}\gamma_{\frac{1}{3}} + \frac{4}{27}\frac{-2\pi^2 + 3(9 + \gamma_{\frac{1}{3}} - 15\zeta(3))}{1-y} - \frac{2}{27}\frac{180 + 4\pi^2 - 6\gamma_{\frac{1}{3}} - 117\zeta(3)}{(1-y)^2} \\ & + \frac{8 + \frac{8\pi^2}{9} - \frac{4}{3}\gamma_{\frac{1}{3}} - 4\zeta(3)}{(1-y)^3} + 2\zeta(3) \end{aligned} \tag{9.30}$$

$$f_2 = \frac{4 + \frac{4\pi^2}{9} - \frac{2}{3}\gamma_{\frac{1}{3}} - 2\zeta(3)}{(1-y)^4} - \frac{8 + \frac{8\pi^2}{27} - \frac{4}{9}\gamma_{\frac{1}{3}} - \frac{16}{3}\zeta(3)}{(1-y)^3} + \frac{4 - \frac{4\pi^2}{27} + \frac{2}{9}\gamma_{\frac{1}{3}} - 4\zeta(3)}{(1-y)^2} + \frac{2}{3}\zeta(3) \tag{9.31}$$

$$f_3 = -\frac{2}{3} - \frac{\frac{2}{3}}{1-y} + \frac{8}{3}\zeta(3). \tag{9.32}$$

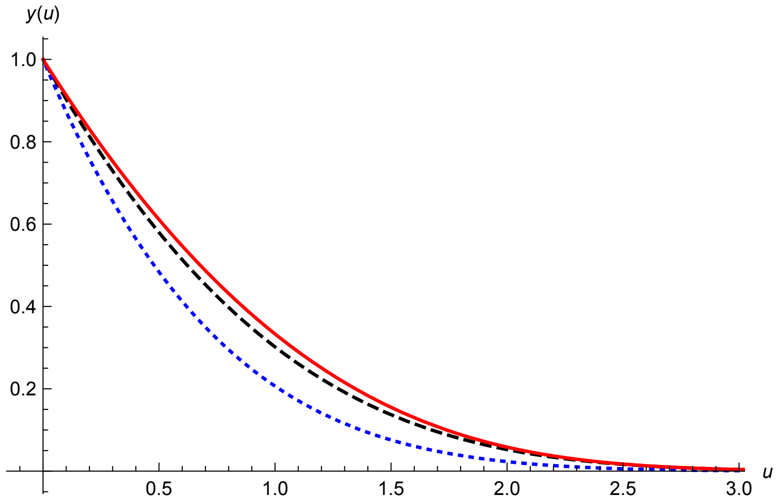

Figure 4: Fix-point solution $y(u) = -\frac{3}{\varepsilon}\tilde{R}''(u)$ for $\varepsilon = 1$ in the case of random-field disorder. Comparison of 1-loop (dashed black), 2-loop (blue dotted), and 3-loop (red line).

The functions F_2 and F_3 correct the cusp without destroying it, since both have a finite Taylor expansion around $y = 1$

$$
\begin{aligned}
F_2(y) =& \frac{2}{3}(1-y)^2 + \frac{13}{36}(1-y)^3 + \frac{19}{80}(1-y)^4 + \frac{13}{75}(1-y)^5 + \frac{17}{126}(1-y)^6 + \frac{43}{392}(1-y)^7 \\
&+ \frac{53}{576}(1-y)^8 + \frac{32}{405}(1-y)^9 + \frac{19}{275}(1-y)^{10} + \mathcal{O}(1-y)^{11} \qquad (9.33)\\
F_3(y) =& -2.08216(1-y)^2 - 0.949217(1-y)^3 - 0.541283(1-y)^4 - 0.350724(1-y)^5 \\
&- 0.247215(1-y)^6 - 0.185059(1-y)^7 - 0.144938(1-y)^8 - 0.117575(1-y)^9 \\
&- 0.0980832(1-y)^{10} + \mathcal{O}(1-y)^{11} \qquad (9.34)
\end{aligned}
$$

Both Taylor-expansions seems to be convergent in the whole range of y. The 3-loop contribution has the opposite sign as the 2-loop contribution. For $\varepsilon = 1$ the 3-loop result corrects the 1-loop result in a different direction than the 2-loop result, see Fig. 4. The 3-loop contribution is larger than the 2-loop contribution, and the 3-loop result is closer to the 1-loop result.

If $\tilde{\Delta}(u) := -\tilde{R}''(u) = \frac{\varepsilon}{3}y(u)$ is a fix-point solution, then

$$
\tilde{\Delta}(u) = -\tilde{R}''(u) = \frac{\varepsilon}{3}\xi^2 y(\tfrac{u}{\xi}) \qquad (9.35)
$$

is a fix-point solution for any ξ as well. We choose ξ to set the normalization of the fix-point function such that $\tilde{R}(u) \sim -\tilde{\sigma}|u|$ for large u, where $\tilde{\sigma} = (\varepsilon\tilde{I}_1)\sigma$. This ensures $R(u) = \frac{1}{\varepsilon\tilde{I}_1}m^{\varepsilon-4\zeta}\tilde{R}(um^{\zeta}) \sim -\sigma|u|$, with $\zeta = \frac{\varepsilon}{3}$. The constant ξ is determined by

$$
\tilde{\sigma} \stackrel{!}{=} -\int_0^\infty \mathrm{d}u\, \tilde{R}''(u) = \frac{\varepsilon}{3}\xi^3 \int_0^\infty \mathrm{d}u\, y(u) = \frac{\varepsilon}{3}\xi^3 \int_0^1 \mathrm{d}y\, u(y) = \frac{\varepsilon}{3}\xi^3 \mathcal{I}_y \qquad (9.36)
$$

The (implicit) solution $u(y)$ is given by the ansatz (9.18). Numerically, the integral is given by

$$
\mathcal{I}_y = \int_0^1 \mathrm{d}y\, u(y) \approx 0.775304 - 0.139455\varepsilon + 0.17420\varepsilon^2 + \mathcal{O}(\varepsilon^3). \qquad (9.37)
$$

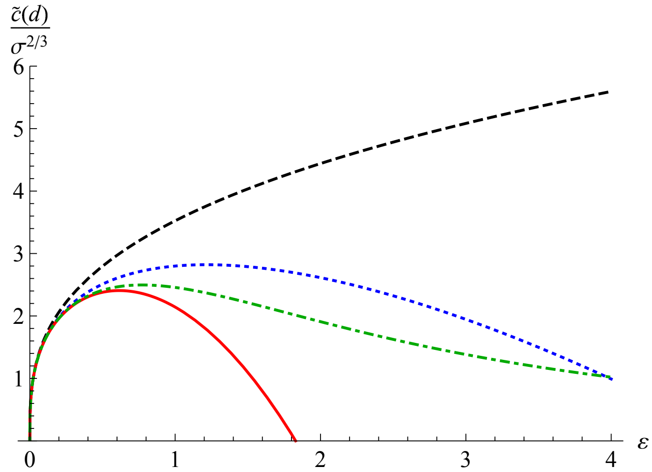

Figure 5: Dimensional dependence of the universal amplitude for random-field disorder. Comparison of 1-loop (dashed black), 2-loop (blue dotted), and 3-loop (red line). The green dot-dashed line is the (0,2)-Padé approximant of the 3-loop solution.

With this fix-point solution, we calculate the universal amplitude as

$$\tilde{c}(d) = m^{d+2\zeta}\langle u(0)u(0)\rangle = -\frac{1}{\varepsilon\tilde{I}_1}\tilde{R}''(0) = \frac{1}{(\varepsilon\tilde{I}_1)^{\frac{1}{3}}}\left(\frac{\varepsilon}{3}\right)^{\frac{1}{3}}\sigma^{\frac{2}{3}}\mathcal{I}_y^{-\frac{2}{3}} . \tag{9.38}$$

Using formulas (8.9)–(8.11), we obtain

$$\tilde{c}(d) \approx \varepsilon^{\frac{1}{3}}\sigma^{\frac{2}{3}}\left[3.52459 - 0.72508\varepsilon - 0.65692\varepsilon^2 + \mathcal{O}(\varepsilon^3)\right] . \tag{9.39}$$

For $\varepsilon < 0.5$ the 3-loop solution is relatively close to the 2-loop contribution. For larger ε it deviates substantially and even changes sign for $\varepsilon \approx 1.83$, see Fig.5.

The comparison with the exact result in $d = 0$ dimensions [83] may be far fetched in an $\varepsilon = 4-d$ expansion. The 1- and 3-loop results are far off from the exact result, but the 2-loop result comes surprisingly close, see Fig. 6. More convincingly and even closer to the exact result is the (0,2)-Padé approximant of the 3-loop result, taking out the prefactor of $\varepsilon^{1/3}$, which is the unique approximant with only positive coefficients,

$$\tilde{c}(d)_{(0,2)} \approx \frac{\varepsilon^{\frac{1}{3}}\sigma^{\frac{2}{3}}}{0.283721 + 0.058367\varepsilon + 0.064888\varepsilon^2} . \tag{9.40}$$

9.3 Periodic systems

In order to allow for a periodic solution of the fix-point equation we set $\zeta = 0$. Further we assume a period one; we can use the reparametrization invariance in Eq. (9.35) to adjust to other periods. The ansatz

$$\tilde{R}(u) = (a_1\varepsilon + a_2\varepsilon^2 + a_3\varepsilon^3 + \ldots) + (b_1\varepsilon + b_2\varepsilon^2 + b_3\varepsilon^3 + \ldots)u^2(1-u)^2 + \mathcal{O}(\varepsilon^4) \tag{9.41}$$

$\tilde{c}(d)\sigma^{-\frac{2}{3}}$	one loop	two loop	three loop	Padé-(0,2)	exact
$d=3$	3.525	2.800	2.143	2.457	
$d=2$	4.441	2.614	-0.697	1.909	
$d=1$	5.083	1.946	-6.581	1.383	
$d=0$	5.595	0.991	-15.694	1.021	≈ 1.054 [83]

Figure 6: Universal amplitude for random field disorder obtained by an ε-expansion in comparision with the exact result. In the fourth column is the estimated value using a (0,2)-Padé approximant of the 3-loop result.

works to all orders in ε. This can be seen from the following observations: Each further order in a loop-expansion has one more factor of $R(u)$, and 4 more derivatives. So the RG-equations close for a polynomial up to order u^4, and no higher-order terms in u are needed. This leaves us with 5 terms, u^i, with $0 \leq i \leq 4$. The function must further be even under the transformation $u \to 1-u$. This leaves space in Eq. (9.41) for one additional term, $cu(1-u)$, where the constant c may depend on ε. However, each term in the β-function except the first one $\varepsilon R(u)$ has at least 2 derivatives, so this term would only appear in $\varepsilon R(u)$, and thus must vanish. (It can appear at depinning for different reasons, see [16].)

This leads to the fix-point function

$$\tilde{R}^*(u) = \frac{\varepsilon}{2592} + \frac{\varepsilon^2}{7776} + \varepsilon^3\left(-\frac{1}{46656} + \frac{\pi^2}{23328} - \frac{\psi'(\frac{1}{3})}{15552} + \frac{\zeta(3)}{15552}\right) \\ - (1-u)^2u^2\left(\frac{\varepsilon}{72} + \frac{\varepsilon^2}{108} + \varepsilon^3\frac{9+2\pi^2-3\psi'(\frac{1}{3})-18\zeta(3)}{1944}\right) + \mathcal{O}(\varepsilon^4) \tag{9.42}$$

With numerical coefficients, the function reads

$$\tilde{R}(u) \approx 0.000385802\varepsilon + 0.000128601\varepsilon^2 - 0.000170212\varepsilon^3 \\ - (0.0138889\varepsilon + 0.00925926\varepsilon^2 - 0.0119262\varepsilon^3)(1-u)^2u^2 + \mathcal{O}(\varepsilon^4)\,. \tag{9.43}$$

Similarly to the case of random-field disorder we obtain the universal amplitude as

$$\tilde{c}(d) = -\frac{1}{\varepsilon\tilde{I}_1}\tilde{R}''(0) \approx 2.19325\varepsilon - 0.680427\varepsilon^2 - 2.71612\varepsilon^3 + \mathcal{O}(\varepsilon^4)\,. \tag{9.44}$$

This is the 2-point correlation function at zero momentum. There is a large contribution in 3-loop order with a larger coefficient than at 2-loop order. For $\varepsilon > 0.72$ the 3-loop expansion becomes negative (as does the 2-loop expansion for $\varepsilon > 3.22$). This makes the ε-expansion questionable in this case, although the (1,2)-Padé approximant remains positive,

$$\tilde{c}(d)_{(1,2)} \approx \frac{2.19325\varepsilon}{1+0.310238\varepsilon+1.33465\varepsilon^2} + \mathcal{O}(\varepsilon^4) \tag{9.45}$$

The results from different truncations in the loop order and the (1,2)-Padé approximant are plotted in Fig. 7. The propagator in the massless limit is given by

$$c(d) \approx 2.19325\varepsilon - 2.87367\varepsilon^2 + 0.45(1)\varepsilon^3 + \mathcal{O}(\varepsilon^4) \tag{9.46}$$

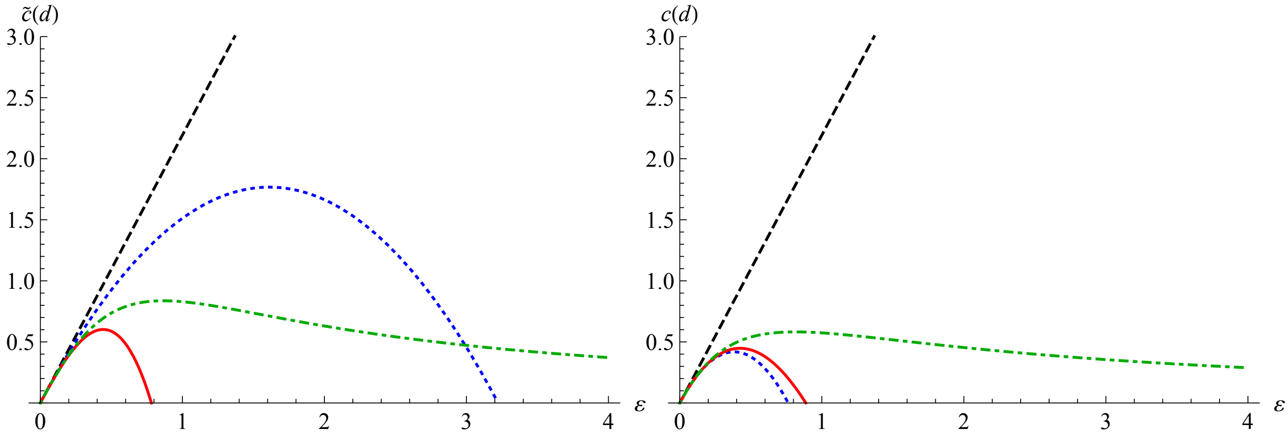

Figure 7: Left: Dimensional dependence of the universal amplitude $\tilde{c}(d)$ in the periodic case. Comparison of 1-loop (dashed black), 2-loop (blue dotted), and 3-loop (red line). The green line corresponds to a (1,2)-Padé approximant of the 3-loop solution. Right: ibid for $c(d)$.

with a 3-loop coefficient not as large as the 2-loop coefficient. Here, however, already the 2-loop solution leads to negative values for $\varepsilon > 0.76$. The probably best extrapolations is obtained from the (1,2)-Padé approximant

$$c(d)_{(1,2)} \approx \frac{2.19325\varepsilon}{1 + 1.31024\varepsilon + 1.510(6)\varepsilon^2} + \mathcal{O}(\varepsilon^4) . \tag{9.47}$$

10 The correction-to-scaling exponent ω

The correction-to-scaling exponent ω controls what happens when a fixed point, here a functional fixed point, is perturbed. In particular, for a fixed point $\Delta^*(u) = -\partial_u^2 R^*(u)$ with $\beta[\Delta^*] = 0$ we consider linear perturbations. Their eigenvalue ω is determined from the $\mathcal{O}(\kappa)$-term in the equation

$$\beta[\Delta^* + \kappa z](u) = \omega\kappa\, z(u) + \mathcal{O}(\kappa^2) . \tag{10.1}$$

Since observables, and also scaling functions which determine the critical exponents, in general depend analytically on the coupling constants, a deviation of a critical exponent from the fix-point value scales linearly with the deviation of the coupling constant, or coupling function, from its value at the critical point. In formulas, an observable $\mathcal{O}$ or exponent α scales with a length scale ℓ as

$$\mathcal{O} - \mathcal{O}_{\text{fix-point}} \sim \alpha - \alpha_{\text{fix-point}} \sim R(u) - R_{\text{fix-point}}(u) \sim \ell^{-\omega} \tag{10.2}$$

This is important for numerical simulations, where ℓ is the system size.

For disordered elastic manifolds, this problem has been considered in Ref. [84]. There it was concluded, that two cases have to be distinguished:

(a) There is the freedom to rescale the field u while at the same time rescaling the disorder correlator. This includes the random-bond and random-field interface models.

(b) There is no such freedom, since the period is fixed by the microscopic disorder. This is the case for a charge density wave (random periodic problem), but also for the random-field bulk problem, in its treatment via a non-linear sigma model.

In case (a), the two leading eigenvalues and eigenfunctions to linear order in ε are [84]

$$z_{\rm red}(u) = u\Delta'(u) - 2\Delta(u) \ , \qquad \omega_{\rm red} = 0 \ , \tag{10.3}$$

$$z_1(u) = \zeta u\Delta'(u) + (\varepsilon - 2\zeta)\Delta(u) \ , \qquad \omega_1 = -\varepsilon \ . \tag{10.4}$$

The first eigenvalue and eigenfunction $z_{\rm red}(u)$ are a consequence of the reparametrization invariance $\Delta(u) \to \kappa^2\Delta(u/\kappa)$, and are therefore exact. $z_{\rm red}(u)$ is a *redundant* operator. $z_1(u)$ and ω_1 are the dominant eigenfunction and eigenvalue entering into Eq. (10.2). Both eigenfunctions are given as perturbations of the fixed point $\Delta(u)$ of the force-force correlator. At least for random-field disorder, is was argued [84] that there cannot be any other eigenvalues and eigenfunctions.

In case (b) we can at 1-loop order identify two perturbations, written here as perturbations for the potential-potential correlator $R(u)$:

$$z_{\rm red}(u) = 1 \ , \qquad \omega_{\rm red} = \varepsilon \tag{10.5}$$

$$z_1(u) = R(u) \ , \qquad \omega_1 = -\varepsilon \tag{10.6}$$

10.1 The correction-to-scaling exponent ω to 2-loop order: General formulas

The 2-loop β-function is

$$-m\partial_m\tilde\Delta(u) = (\varepsilon - 2\zeta)\Delta(u) + \zeta u\Delta'(u) + f_1[\Delta,\Delta](u) + f_2[\Delta,\Delta,\Delta](u) + ... \tag{10.7}$$

Both $f_1[\Delta] \equiv f_1[\Delta,\Delta]$ and $f_2[\Delta] \equiv f_2[\Delta,\Delta,\Delta]$ are completely symmetric functionals acting locally on the functions $\Delta(u) - \Delta(0)$. More explicitly, we have

$$f_1[\Delta] = -\frac{1}{2}\left[(\Delta(u) - \Delta(0))^2\right]'' \tag{10.8}$$

$$f_2[\Delta] = \frac{1}{2}\left[(\tilde\Delta(u) - \tilde\Delta(0))\tilde\Delta'(u)^2\right]'' - \frac{1}{2}\tilde\Delta'(0^+)^2\tilde\Delta''(u) \tag{10.9}$$

For different arguments we use the multilinear formulas (6.32).

Consider now $\tilde\Delta^*(u)$, solution of Eq. (10.7) with $-m\partial_m\tilde\Delta^*(u) = 0$. Setting $\tilde\Delta(u) = \tilde\Delta^*(u) + \kappa z(u)$, we study the flow of the term linear in κ. Its eigenmodes $z(u)$ with eigenvalues ω describe the behavior close to the critical point. The eigenvalue-equation to be solved is

$$o(u) := \left[\varepsilon - 2\zeta - \omega\right]z(u) + \zeta u z'(u) + 2f_1[z,\Delta](u) + 3f_2[z,\Delta,\Delta](u) = 0 \tag{10.10}$$

There are several possible simplifications. First note that if $\Delta(u)$ is a fixed point, also $\kappa^{-2}\Delta(\kappa u)$ is a fixed point. Varying in Eq. (10.7) the fixed-point condition $-m\partial_m\Delta(u) = 0$ around $\kappa = 1$ yields the *redundant* or *rescaling mode* $r(u)$,

$$\begin{aligned} r(u) = {} & (\varepsilon - 2\zeta)\left(u\Delta'(u) - 2\Delta(u)\right) + \zeta u\left(u\Delta'(u) - 2\Delta(u)\right)' \\ & + 2f_1\left(\Delta(u), u\Delta'(u) - 2\Delta(u)\right) + 3f_2\left(\Delta(u),\Delta(u),u\Delta'(u) - 2\Delta(u)\right) = 0 \end{aligned} \tag{10.11}$$

This equation, as well as a multiple of the vanishing β-function (10.7), can be added to Eq. (10.10). This leaves some freedom to obtain a simpler equation.

We now want to know how the physically relevant correction-to-scaling exponent $\omega = -\varepsilon$ changes to 2-loop order. To this aim we do a loop expansion, starting from what we know,

$$\Delta(u) = \varepsilon\Delta_1(u) + \varepsilon^2\Delta_2(u) + \ldots \tag{10.12}$$
$$z(u) = \varepsilon z_1(u) + \varepsilon^2 z_2(u) + \ldots \tag{10.13}$$
$$z_1(u) = \zeta_1 u\Delta_1'(u) + (1-2\zeta_1)\Delta_1(u) \tag{10.14}$$
$$\zeta = \zeta_1\varepsilon + \zeta_2\varepsilon^2 + \ldots \tag{10.15}$$
$$\omega = -\varepsilon + \omega_2\varepsilon^2 + \ldots \tag{10.16}$$

The 1- and 2-loop orders of the β-function are given by $\beta = \varepsilon\beta_1 + \varepsilon^2\beta_2 + \mathcal{O}(\varepsilon^3)$ with

$$\beta_1 = (1-2\zeta_1)\Delta_1(u) + \zeta_1 u\Delta_1'(u) + f_1(\Delta_1)(u) = 0 \tag{10.17}$$
$$\beta_2 = (1-2\zeta_1)\Delta_2(u) + \zeta_1 u\Delta_2'(u) - 2\zeta_2\Delta_1(u) + \zeta_2 u\Delta_1'(u) + 2f_1(\Delta_1,\Delta_2) + f_2(\Delta_1)(u) \tag{10.18}$$

There are many ways a relatively simple differential relation for $\delta z_2(u)$ can be written. We start with the ansatz

$$z_2(u) = cu\Delta_1'(u) + d\Delta_1(u) + eu\Delta_2'(u) + f\Delta_2(u) + \delta z_2(u)\ , \tag{10.19}$$

and consider the following combination

$$o(u) - \beta(u)(2+\varepsilon(4b+2d)) - r(u)(\zeta_1 + b\varepsilon) - g\beta_2(u)\varepsilon^3 = 0\ . \tag{10.20}$$

For

$$b = c = \frac{2\zeta_2}{1-2\zeta_1}\ , \quad d = -\omega_2\ , \quad e = \zeta_1\ , \quad f = 2-2\zeta_1\ , \quad g = 1\ , \tag{10.21}$$

we get

$$2\left(1-\zeta_1\right)\delta z_2(u) + \zeta_1 u\delta z_2'(u) + 2f_1\left[\Delta_1(u),\delta z_2(u)\right] - \omega_2\Delta_1(u) + \Delta_2(u) = 0\ . \tag{10.22}$$

This is the simplest equation we have been able to find.

At 3-loop order, the problem becomes more complicated. The best equation we found was

$$\begin{aligned}
&2f_1\Big(\Delta_1(u),\delta z_3(u)\Big) + 2f_1\Big(\Delta_2(u),\delta z_2(u)\Big) + 3f_2\Big(\Delta_1(u),\Delta_1(u),\delta z_2(u)\Big)\\
&+\left(\frac{4\zeta_2\omega_2}{1-2\zeta_1} - \omega_2^2 + \omega_3\right) f_1\Big(\Delta_1(u),\Delta_1(u)\Big) + \left(\frac{4\zeta_2}{1-2\zeta_1} - 3\omega_2\right)\Delta_2(u) + 2\Delta_3(u)\\
&-\left(2\zeta_2+\omega_2\right)\delta z_2(u) + \zeta_2 u\delta z_2'(u) + \zeta_1 u\delta z_3'(u) - 2(\zeta_1-1)\delta z_3(u) = 0
\end{aligned} \tag{10.23}$$

For the lack of use in applications (the 3-loop order for the roughness exponent is rather large), we did not try to solve this equation.

We now specify to the main cases of interest.

10.2 Correction to scaling exponent at the random-field fixed point

Using shooting, we find $\omega_2 = 0.1346$, thus

$$\omega \approx -\varepsilon + 0.1346\varepsilon^2 + \mathcal{O}(\varepsilon^3) = -\frac{\varepsilon}{1+0.1346\varepsilon} + \mathcal{O}(\varepsilon^3)\ . \tag{10.24}$$

The corresponding function $\delta z_2(u)$ and $z(u)$ at $\varepsilon = 3$ are plotted on figure 8. In $d=1$ this gives

$$\omega = -1.97(20)\ , \qquad d = 1\ . \tag{10.25}$$

where the error-estimate comes from the deviation of the direct expansion as compared to the Padé approximant.

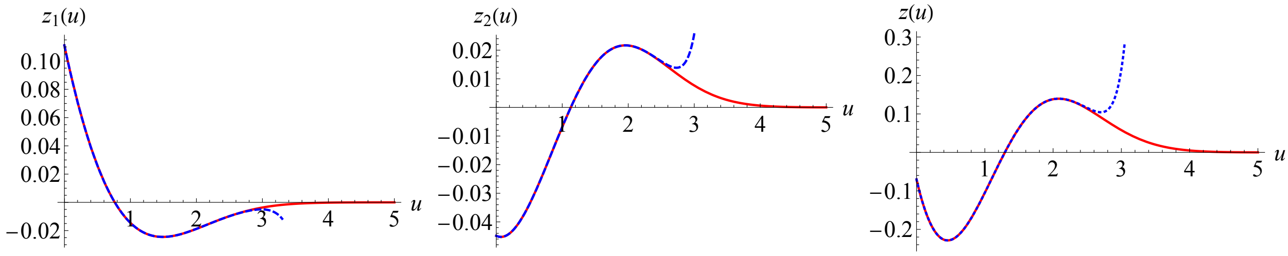

Figure 8: $z_1(u)$, $z_2(u)$ and $z(u)_{\varepsilon=3}$ for RF, statics. Red (solid) is the numerical solution, blue (dashed) the Taylor expansion around $u = 0$.

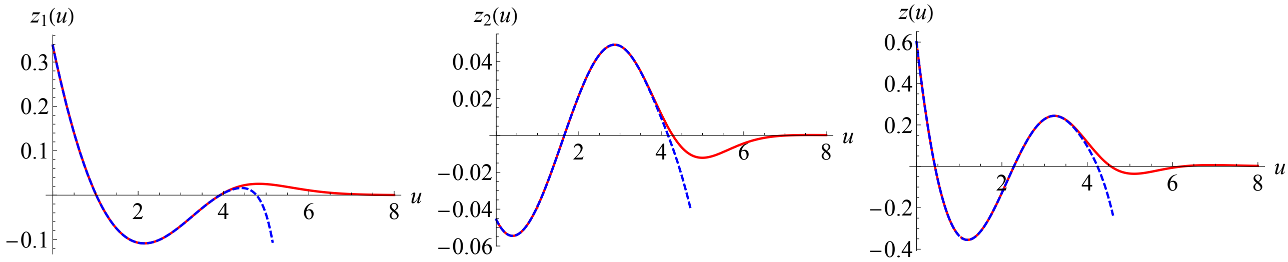

Figure 9: $z_1(u)$, $z_2(u)$ and $z(u)|_{\varepsilon=3}$ for RB, statics. Red (solid) is the numerical solution, blue (dashed) Taylor expansion.

10.3 Correction to scaling exponent at the random-bond fixed point

We find via shooting

$$\omega \approx -\varepsilon + 0.4108(1)\varepsilon^2 + \mathcal{O}(\varepsilon^3) = -\frac{\varepsilon}{1 + 0.4108(1)\varepsilon} + \mathcal{O}(\varepsilon^3)\ . \tag{10.26}$$

In $d = 1$ this gives using the Padé approximant (the direct ε expansion is not monotonous)

$$\omega \approx -1.344\ , \qquad d = 1\ . \tag{10.27}$$

We have checked that the numerical solutions, given on figure 9, integrate to 0 within numerical accuracy, as necessary for a RB fixed point.

10.4 Correction to scaling exponent for charge-density waves (random-periodic fixed point)

We find that the leading-order perturbation for the random-periodic fix-point (9.42) closes in the same space spanned by 1 and $[u(1-u)]^2$. The correction-to-scaling exponent becomes

$$\omega_{\rm RP} = -\varepsilon + \frac{2\varepsilon^2}{3} - \left(\frac{4\zeta(3)}{3} + \frac{5}{9}\right)\varepsilon^3 + \mathcal{O}(\varepsilon^4) = -\varepsilon\,\frac{1 + \left[2\zeta(3) + \frac{1}{6}\right]\varepsilon}{1 + \left[2\zeta(3) + \frac{5}{6}\right]\varepsilon} + \mathcal{O}(\varepsilon^4)\ . \tag{10.28}$$

Curiously, all contributions proportional to π^2 and $\psi'(1/3)$, present in the coefficients $\mathcal{C}_1, \ldots, \mathcal{C}_4$ have canceled. The corresponding eigenfunction, normalized to $R(0) = 1$ is

$$\delta R(u) = 1 - 36[u(1-u)]^2\left[1 + \frac{\varepsilon}{2} + \varepsilon^2\frac{8 - 30\zeta(3) + 3\psi'(\frac{1}{3}) - 2\pi^2}{18} + \mathcal{O}(\varepsilon^3)\right] \tag{10.29}$$

Up to 2-loop order, the exponent ω is the same for depinning.

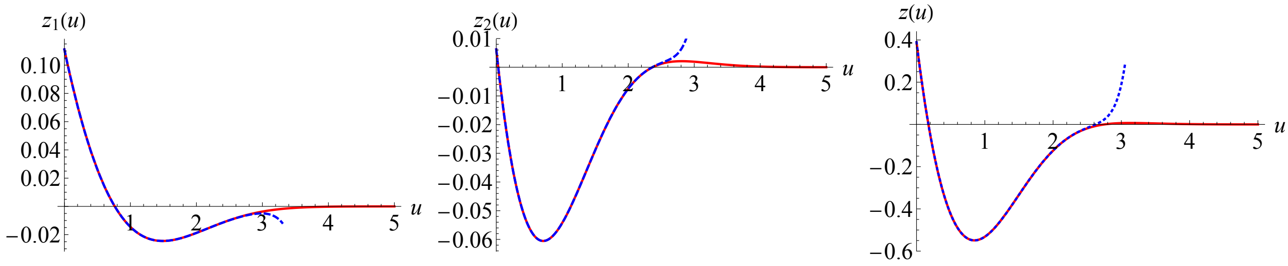

Figure 10: $z_1(u)$, $z_2(u)$ and $z(u)|_{\varepsilon=3}$ for RF, depinning. Red (solid) is the numerical solution, blue (dashed) the Taylor expansion.

10.5 Correction to scaling exponent for depinning (random-field fixed point)

For completeness and usefulness in applications, we also give the correction to scaling exponent at depinning, using the β-function of [16, 18]. Via shooting, we find $\omega_2 = -0.0186$, thus

$$\omega \approx -\varepsilon - 0.0186\varepsilon^2 + \mathcal{O}(\varepsilon^3) = -\frac{\varepsilon}{1-0.0186\varepsilon} + \mathcal{O}(\varepsilon^3) \ . \tag{10.30}$$

The corresponding function $\delta z_2(u)$ and $z(u)$ at $\varepsilon = 3$ are plotted on figure 10. In $d = 1$ this gives

$$\omega = -3.17(1) \ , \qquad d = 1 \ . \tag{10.31}$$

where the error-estimate comes from the difference of the Padé approximant to the direct expansion.

11 Conclusions and open problems

In this article, we have obtained the functional renormalization-group flow equations for the equilibrium properties of elastic manifolds in quenched disorder up to 3-loop order. This allowed us to obtain several critical exponents, especially the roughness exponent, to 3-loop accuracy, for random-bond, random-field, and periodic disorder. For an elastic string in a random-bond environment, for which we know the exact value $\zeta = \frac{2}{3}$, the corrections turn out to be quite large. This suggests that convergence of the ε-expansion is plagued by the typical problem of renormalized field theory, namely that the perturbation expansion in the coupling is not convergent, but only Borel-summable. In φ^4-theory the physical reason for a only Borel-summable series is that the theory with the opposite sign of the coupling is unstable, thus the perturbative expansion cannot be convergent. For the case at hand, this is not evident: Since averaging over disorder leads to attractive inter-replica interactions, making the latter repulsive should make the problem even better defined: a self-attractive polymer is unstable, whereas a self-repelling one has a well-defined fixed point, the self-avoiding polymer fixed point. The second point which makes us doubt that the theory is only Borel-summable is that when the interaction behaves as $\int_x g\varphi^{2\alpha}(x)$, then the standard instanton analysis yields that $\left<\exp(-\int_x g\varphi^{2\alpha}(x))\right> = \sum_{n=0}^{\infty} \frac{(-g)^n}{n!} \left<\left[\int_x \varphi^{2\alpha}(x)\right]^n\right>$, with $\left<\left[\int_x \varphi^{2\alpha}(x)\right]^n\right> \simeq (n!)^\alpha$ for a total of the n-th order term being $(n!)^{\alpha-1}$. The exponent α in the last formula is extracted from the large φ behavior of the interaction. For the problem at hand, $R(u)$ has a Gaussian tail, thus the perturbative expansion should converge! This does however not say anything about the result at a given order, here $n = 3$. It would be interesting to find an exact solution in some limit, which could shed light on this issue. In some cases, large N (with N being the number of components) provides such a limit. It has however been shown in [85, 86] that the β-function at leading order in $1/N$ is as obtained in 1-loop order. For the order $1/N$-corrections [87], the same problem appears.

Another interesting question is how the formalism derived here can be extended to $N > 1$ components. It had been shown in Ref. [15] that there is an ambiguity in the 2-point function already at 1-loop order. This allowed the authors of [15] to still conclude on the β-function at 2-loop order. The problem becomes more severe at 3-loop order, and despite considerable efforts in this direction we have not been able to lift this ambiguity, present in some of the graphs.

Acknowledgements

We would like to thank Pierre Le Doussal for the many years of stimulating collaboration in which some of the tools used here were developed. We also thank him for useful discussions which helped us to properly set up the exact RG equations. We thank Andreas Ludwig and Boris Kastening for their help in calculating the loop-integrals. We acknowledge discussions with Pascal Chauve at an early stage of this work.

A Loop integrals for all diagrams up to 3 loops

A.1 General formulae, strategy of calculation, and conventions

We make use of the Schwinger parameterization

$$\frac{1}{A^n} = \frac{1}{\Gamma(n)} \int_0^\infty \mathrm{d}u\; u^{n-1} e^{-uA} \tag{A.1}$$

and the d-dimensional momentum integration

$$\int \frac{\mathrm{d}^d p}{(2\pi)^d} \mathrm{e}^{-ap^2} \equiv \int_p e^{-ap^2} = \frac{1}{a^{d/2}} \int_p \mathrm{e}^{-p^2} = \frac{1}{a^{d/2}} \frac{1}{(4\pi)^{d/2}} \tag{A.2}$$

In order to avoid cumbersome appearances of factors like $\frac{1}{(4\pi)^{d/2}}$, we will write explicitly the last integral, and will only calculate ratios compared to the leading 1-loop diagram I_1, given in the next section.

We will frequently use the decomposition trick

$$\frac{1}{k^2+1} = \frac{1}{k^2} - \frac{1}{k^2(k^2+1)} \tag{A.3}$$

which works well for dimension $d \leq 4$. The reason for the utility of this decomposition is that it allows one to replace the massive propagator by a massless one, which is easier to integrate over, and a term converging faster for large k, which finally renders the integration finite.

Special functions which appear are

$$\psi(x) := \frac{\Gamma'(x)}{\Gamma(x)} \tag{A.4}$$

$$\psi'(x) = \frac{\mathrm{d}}{\mathrm{d}x}\psi(x) \tag{A.5}$$

A.2 The 1-loop integral I_1

The integral I_1 is defined as

$I_1 :=$ 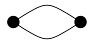

$$= \int_k \frac{1}{(k^2+m^2)^2}\,, \tag{A.6}$$

and is calculated as follows:

$$\begin{aligned} I_1 &= \int_k \int_0^\infty \mathrm{d}\alpha\,\alpha\,\mathrm{e}^{-\alpha(k^2+m^2)} \\ &= \left(\int_k \mathrm{e}^{-k^2}\right) \int_0^\infty \mathrm{d}\alpha\,\alpha^{1-\frac{d}{2}}\,\mathrm{e}^{-\alpha m^2} \\ &= \left(\int_k \mathrm{e}^{-k^2}\right) m^{-\varepsilon}\Gamma\left(\frac{\varepsilon}{2}\right) \end{aligned} \tag{A.7}$$

We will also denote the dimensionless integral

$$\tilde{I}_1 = I_1\Big|_{m=1}\,. \tag{A.8}$$

This gives us the normalization-constant for higher-loop calculations

$$(\varepsilon I_1) = m^{-\varepsilon}\left(\int_k \mathrm{e}^{-k^2}\right)\varepsilon\Gamma\left(\frac{\varepsilon}{2}\right) = m^{-\varepsilon}\left(\int_k \mathrm{e}^{-k^2}\right)2\,\Gamma\left(1+\frac{\varepsilon}{2}\right) \tag{A.9}$$

A.3 2-loop diagram I_A

The non-trivial 2-loop integral can be written as

$I_A =$ 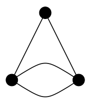

$$= \int_{p_1,p_2} G(p_1)G(p_2)^2G(p_1+p_2) = \frac{\Gamma(\varepsilon)}{m^{2\varepsilon}}\tilde{J}_A \tag{A.10}$$

with

$$\tilde{J}_A = \int_0^\infty \mathrm{d}x\,\mathrm{d}y\,f_A(x,y) = J_1 + J_2 + J_3 \tag{A.11}$$

$$f_A(x,y) = \frac{y}{(x+y+xy)^{2-\frac{\varepsilon}{2}}(1+x+y)^{\varepsilon}} \tag{A.12}$$

$$J_1 = \int_0^1 \mathrm{d}y \int_0^\infty \mathrm{d}x f_A(x,y) \tag{A.13}$$

$$J_2 = \int_1^\infty \mathrm{d}y \int_0^\infty \mathrm{d}x\,\frac{1}{(1+x)^{2-\frac{\varepsilon}{2}}}\frac{1}{y^{1+\frac{\varepsilon}{2}}} = \frac{4}{(2-\varepsilon)\varepsilon} \tag{A.14}$$

$$J_3 = \int_1^\infty \mathrm{d}y \int_0^\infty \mathrm{d}x\,\left[f_A(x,y) - \frac{1}{(1+x)^{2-\frac{\varepsilon}{2}}}\frac{1}{y^{1+\frac{\varepsilon}{2}}}\right] \tag{A.15}$$

The integrals J_1 and I_1 were solved by expanding the integrand in ε to order ε

$$\frac{I_A}{(\varepsilon I_1)^2} = \frac{1}{2\varepsilon^2} + \frac{1}{4\varepsilon} + \frac{1}{72}\left[9 + 4\pi^2 - 6\psi'(\tfrac{1}{3})\right] + \mathcal{O}(\varepsilon) \tag{A.16}$$

The result agrees with the one obtained by the subtraction method.

A.4 2-loop integral I_B

The trivial 2-loop diagram is

$I_B :=$ 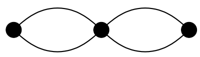 $= I_1^2$ (A.17)

A.5 I_i

$I_i =$ 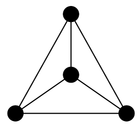 (A.18)

$$\frac{I_i}{(\varepsilon I_1)^3} = \frac{1}{(\varepsilon I_1)^3}\int_{p_1,p_2,p_3} G(p_1)G(p_2)G(p_3)G(p_1+p_3)G(p_2+p_3)G(p_1-p_2)$$
$$= \frac{\zeta(3)}{2\varepsilon} + \mathcal{O}(\varepsilon) \tag{A.19}$$

A.6 I_j

$I_j =$ 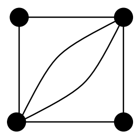 (A.20)

$$\frac{I_j}{(\varepsilon I_1)^3} = \frac{1}{(\varepsilon I_1)^3}\int_{p_1,p_2,p_3} G(p_1)G(p_2)G(p_3)^2G(p_1+p_2+p_3)^2 = \sum_{i=1}^{3} I_i^j \tag{A.21}$$
$$I_1^j = \frac{1}{(\varepsilon I_1)^3}\int_{p_1,p_2,p_3} \frac{1}{p_1^2p_2^2}G(p_3)^2G(p_1+p_2+p_3)^2 = \frac{1}{3\varepsilon^3} + \frac{1}{6\varepsilon^2} + \frac{1}{12\varepsilon} + \mathcal{O}(1) \tag{A.22}$$
$$I_2^j = -2\frac{1}{(\varepsilon I_1)^3}\int_{p_1,p_2,p_3} \frac{1}{p_1^2p_2^2}G(p_1)G(p_3)^2G(p_1+p_2+p_3)^2 = \mathcal{O}(1) \tag{A.23}$$
$$I_3^j = \frac{1}{(\varepsilon I_1)^3}\int_{p_1,p_2,p_3} \frac{1}{p_1^2p_2^2}G(p_1)G(p_2)G(p_3)^2G(p_1+p_2+p_3)^2 = \mathcal{O}(1) \tag{A.24}$$

A.7 I_l

$I_l =$ 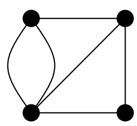 (A.25)

$$\frac{I_l}{(\varepsilon I_1)^3} = \frac{1}{(\varepsilon I_1)^3}\int_{p_1,p_2,p_3} G(p_1)G(p_2)G(p_1+p_2)G(p_3)G(p_1+p_2+p_3)^2 = \sum_{i=1}^{4} I_i^l \tag{A.26}$$

$$\begin{aligned} I_1^l &= \frac{1}{(\varepsilon I_1)^3}\int_{p_1,p_2,p_3} \frac{1}{p_1^2p_2^2(p_1+p_2)^2}G(p_3)G(p_1+p_2+p_3)^2 \\ &= \frac{1}{6\varepsilon^3}+\frac{1}{4\varepsilon^2}+\frac{7}{24\varepsilon}+\mathcal{O}(1) \end{aligned} \tag{A.27}$$

$$\begin{aligned} I_2^l &= \frac{1}{(\varepsilon I_1)^3}\int_{p_1,p_2,p_3} \frac{1}{p_1^2p_2^2(p_1+p_2)^2}G(p_1+p_2)G(p_3)G(p_1+p_2+p_3)^2 \\ &= -\frac{4\pi^2+3\psi'(\frac{1}{3})-3\psi'(\frac{5}{6})}{216\varepsilon}+\mathcal{O}(1) = I_2^m+\mathcal{O}(1) \end{aligned} \tag{A.28}$$

$$I_3^l = \frac{1}{(\varepsilon I_1)^3}\int_{p_1,p_2,p_3} \frac{1}{p_1^2p_2^2}G(p_2)G(p_1+p_2)G(p_3)G(p_1+p_2+p_3)^2 = \mathcal{O}(1) \tag{A.29}$$

$$I_4^l = \frac{1}{(\varepsilon I_1)^3}\int_{p_1,p_2,p_3} \frac{1}{p_1^2p_2^2}G(p_1)G(p_2)G(p_1+p_2)G(p_3)G(p_1+p_2+p_3)^2 = \mathcal{O}(1) \tag{A.30}$$

$$\frac{I_l}{(\varepsilon I_1)^3} = \frac{1}{6\varepsilon^3}+\frac{1}{4\varepsilon^2}+\frac{1}{\varepsilon}\left[-\frac{\pi^2}{54}+\frac{7}{24}-\frac{1}{72}\left(\psi'(\tfrac{1}{3})-\psi'(\tfrac{5}{6})\right)\right] \tag{A.31}$$

A.8 I_m

$I_m =$ 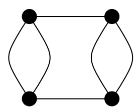 (A.32)

$$\frac{I_m}{(\varepsilon I_1)^3} = \frac{1}{(\varepsilon I_1)^3}\int_{p_1,p_2,p_3} G(p_1)G(p_2)G(p_1+p_2+p_3)G(p_3)G(p_1+p_2)^2 = \sum_{i=1}^{4} I_i^m \tag{A.33}$$

$$\begin{aligned} I_1^m &= \frac{1}{(\varepsilon I_1)^3}\int_{p_1,p_2,p_3} \frac{1}{p_1^2p_2^2(p_1+p_2+p_3)^2}G(p_3)G(p_1+p_2)^2 \\ &= I_{1,1}^m + I_{1,2}^m \end{aligned} \tag{A.34}$$

$$I_{1,1}^m = \frac{1}{(\varepsilon I_1)^3}\int_{p_1,p_2,p_3} \frac{1}{p_1^2p_2^2(p_1+p_2+p_3)^2}\frac{1}{p_3^2}G(p_1+p_2)^2 = \frac{1}{3\varepsilon^3}+\frac{1}{3\varepsilon^2}+\frac{2+\pi^2}{12\varepsilon} \tag{A.35}$$

$$I_{1,2}^m = -\frac{1}{(\varepsilon I_1)^3}\int_{p_1,p_2,p_3} \frac{1}{p_1^2p_2^2(p_1+p_2+p_3)^2}\frac{1}{p_3^2}G(p_3)G(p_1+p_2)^2 = -\frac{\pi^2}{24\varepsilon} \tag{A.36}$$

$$\begin{aligned} I_2^m &= -\frac{1}{(\varepsilon I_1)^3}\int_{p_1,p_2,p_3} \frac{1}{p_1^2p_2^2(p_1+p_2+p_3)^2}G(p_1+p_2+p_3)G(p_3)G(p_1+p_2)^2 \\ &= -\frac{4\pi^2+3\psi'(\frac{1}{3})-3\psi'(\frac{5}{6})}{216\varepsilon}+\mathcal{O}(1) \end{aligned} \tag{A.37}$$

$$I_3^m = -2\frac{1}{(\varepsilon I_1)^3}\int_{p_1,p_2,p_3} \frac{1}{p_1^2p_2^2}G(p_2)G(p_1+p_2+p_3)G(p_3)G(p_1+p_2)^2 = -\frac{\pi^2}{12\varepsilon}+\mathcal{O}(1)\,. \tag{A.38}$$

Finally,

$$I_4^m = \frac{1}{(\varepsilon I_1)^3}\int_{p_1,p_2,p_3}\frac{1}{p_1^2p_2^2}G(p_1)G(p_2)G(p_1+p_2+p_3)G(p_3)G(p_1+p_2)^2 = I_{4,0}^m + I_{4,1}^m \tag{A.39}$$

$$\begin{aligned} I_{4,0}^m &= I_1(0)\frac{1}{(\varepsilon I_1)^3}\int \mathrm{d}^2p \frac{1}{p_1^2p_2^2}G(p_1)G(p_2)G(p_1+p_2)^2 \\ &= \frac{5\pi^2 - 3\psi'(\frac{1}{3}) + 3\psi'(\frac{5}{6})}{216\varepsilon} + \mathcal{O}(1) \end{aligned} \tag{A.40}$$

$$I_{4,1}^m = \frac{1}{(\varepsilon I_1)^3}\int \mathrm{d}^2p(I_1(p_1+p_2) - I_1(0))\frac{1}{p_1^2p_2^2}G(p_1)G(p_2)G(p_1+p_2)^2 = \mathcal{O}(1)\ . \tag{A.41}$$

All in all

$$\begin{aligned} \frac{I_m}{(\varepsilon I_1)^3} &= \frac{1}{3\varepsilon^3} + \frac{1}{3\varepsilon^2} - \frac{4\pi^2 - 18 + \psi'(\frac{1}{3}) - \psi'(\frac{5}{6})}{108\varepsilon} + \mathcal{O}(1) \\ &= \frac{1}{3\varepsilon^3} + \frac{1}{3\varepsilon^2} + \frac{3 + 2\pi^2 - 3\psi'(\frac{1}{3})}{18\varepsilon} + \mathcal{O}(1) \end{aligned} \tag{A.42}$$

where two PolyGamma-identities were used

$$\psi'(\tfrac{1}{3}) + \psi'(\tfrac{5}{6}) = 4\psi'(\tfrac{2}{3}) \tag{A.43}$$

$$\psi'(\tfrac{1}{3}) + \psi'(\tfrac{2}{3}) = \frac{4\pi^2}{3}\ . \tag{A.44}$$

B Complimentary Material for Section 5

B.1 Functional RG Equations for $S^{(3)}$ and $S^{(4)}$

The flow equation of the third Γ-cumulant in the ERG hierachy is given by

$$\begin{aligned} \dot{S}^{(3)}[u_{abc}] &= \int \mathrm{d}^2x\ \dot{g}(x_1,x_2)\left\{-3TS^{(3)}_{110}[u_{abc}](x_1,x_2) + \frac{3}{2}S^{(4)}_{1100}[u_{aabc}](x_1,x_2)\right\} \\ &+ \int \mathrm{d}^4x\left[\frac{\mathrm{d}}{\mathrm{d}m}g(x_1,x_2)g(x_3,x_4)\right]\left\{\frac{3T}{2}\mathcal{R}''[u_{ab}](x_2,x_3)\mathcal{R}''[u_{ac}](x_4,x_1)\right. \\ &\qquad \left. +3\mathcal{R}''[u_{ab}](x_2,x_3)\left[S^{(3)}_{110}[u_{aac}](x_4,x_1) - S^{(3)}_{110}[u_{abc}](x_4,x_1)\right]\right\} \\ &+ \int \mathrm{d}^6x\left[\frac{\mathrm{d}}{\mathrm{d}m}g(x_1,x_2)g(x_3,x_4)g(x_5,x_6)\right] \\ &\qquad \{3\mathcal{R}''[u_{ab}](x_2,x_3)\mathcal{R}''[u_{ac}](x_4,x_5)\mathcal{R}''[u_{ac}](x_6,x_1) \\ &\qquad -\mathcal{R}''[u_{ab}](x_2,x_3)\mathcal{R}''[u_{bc}](x_4,x_5)\mathcal{R}''[u_{ac}](x_6,x_1)\} \end{aligned} \tag{B.1}$$

We split the flow equation for the fourth Γ-cumulant

$$\dot{S}^{(4)}[u_{abcd}] = \dot{S}^{(4)}_1[u_{abcd}] + \dot{S}^{(4)}_2[u_{abcd}] + \dot{S}^{(4)}_3[u_{abcd}] + \dot{S}^{(4)}_4[u_{abcd}] \tag{B.2}$$

into four parts

$$S_1^{(4)}[u_{abcd}] = 2\int \mathrm{d}^2x\ \dot{g}(x_1,x_2)\left\{-3TS^{(4)}[u_{abcd}](x_2,x_1) + S^{(5)}[u_{aabcd}](x_2,x_1)\right\} \tag{B.3}$$

$$\begin{aligned} S_2^{(4)}[u_{abcd}] = 6T\int \mathrm{d}^4x \left[\frac{\mathrm{d}}{\mathrm{d}m} g(x_1,x_2)g(x_3,x_4)\right] &\left\{\mathcal{R}''[u_{ab}](x_2,x_3)S_{200}^{(3)}[u_{acd}](x_4,x_1)\right\} \\ + 6\int \mathrm{d}^4x \left[\frac{\mathrm{d}}{\mathrm{d}m} g(x_1,x_2)g(x_3,x_4)\right] &\left\{\mathcal{R}''[u_{ab}](x_2,x_3)S_{1100}^{(4)}[u_{aacd}](x_4,x_1)\right. \\ &- \mathcal{R}''[u_{ab}](x_2,x_3)S_{1100}^{(4)}[u_{abcd}](x_4,x_1) \\ + S_{200}^{(3)}[u_{abc}](x_2,x_3)S_{110}^{(3)}[u_{aad}](x_4,x_1) &+ \left. S_{110}^{(3)}[u_{abc}](x_2,x_3)S_{110}^{(3)}[u_{bad}](x_4,x_1)\right\} \end{aligned} \tag{B.4}$$

$$\begin{aligned} S_3^{(4)}[u_{abcd}] = 4T\int \mathrm{d}^6x &\left[\frac{\mathrm{d}}{\mathrm{d}m} g(x_1,x_2)g(x_3,x_4)g(x_5,x_6)\right] \\ &\left\{\mathcal{R}''[u_{ab}](x_2,x_3)\mathcal{R}''[u_{ac}](x_4,x_5)\mathcal{R}''[u_{ad}](x_6,x_1)\right\} \\ + 6\int \mathrm{d}^6x &\left[\frac{\mathrm{d}}{\mathrm{d}m} g(x_1,x_2)g(x_3,x_4)g(x_5,x_6)\right] \\ &\left\{2\mathcal{R}''[u_{ab}](x_2,x_3)\mathcal{R}''[u_{ac}](x_4,x_5)S_{110}^{(3)}[u_{aad}](x_6,x_1)\right. \\ &- 2\mathcal{R}''[u_{ab}](x_2,x_3)\mathcal{R}''[u_{ac}](x_4,x_5)S_{110}^{(3)}[u_{acd}](x_6,x_1) \\ &- 2\mathcal{R}''[u_{ac}](x_2,x_3)\mathcal{R}''[u_{ab}](x_4,x_5)S_{110}^{(3)}[u_{acd}](x_6,x_1) \\ &+ 2\mathcal{R}''[u_{bc}](x_2,x_3)\mathcal{R}''[u_{ab}](x_4,x_5)S_{110}^{(3)}[u_{acd}](x_6,x_1) \\ &+ \left.\mathcal{R}''[u_{ab}](x_2,x_3)\mathcal{R}''[u_{ab}](x_4,x_5)S_{110}^{(3)}[u_{acd}](x_6,x_1)\right\} \end{aligned} \tag{B.5}$$

$$\begin{aligned} S_4^{(4)}[u_{abcd}] = 3\int \mathrm{d}^8x &\left[\frac{\mathrm{d}}{\mathrm{d}m} g(x_1,x_2)g(x_3,x_4)g(x_5,x_6)g(x_7,x_8)\right] \\ &\left\{4\mathcal{R}''[u_{ab}](x_2,x_3)\mathcal{R}''[u_{ac}](x_4,x_5)\mathcal{R}''[u_{ad}](x_6,x_7)\mathcal{R}''[u_{ad}](x_8,x_1)\right. \\ &+ 2\mathcal{R}''[u_{ab}](x_2,x_3)\mathcal{R}''[u_{ac}](x_4,x_5)\mathcal{R}''[u_{cd}](x_6,x_7)\mathcal{R}''[u_{ac}](x_8,x_1) \\ &- 4\mathcal{R}''[u_{ab}](x_2,x_3)\mathcal{R}''[u_{ac}](x_4,x_5)\mathcal{R}''[u_{cd}](x_6,x_7)\mathcal{R}''[u_{ad}](x_8,x_1) \\ &+ \left.\mathcal{R}''[u_{ab}](x_2,x_3)\mathcal{R}''[u_{bc}](x_4,x_5)\mathcal{R}''[u_{cd}](x_6,x_7)\mathcal{R}''[u_{ad}](x_8,x_1)\right\} \end{aligned} \tag{B.6}$$

B.2 Third Γ-cumulant $S^{(3)}$ to 3-loop order

In total there are four contributions to the flow of $S^{(3)}$ in 3-loop order

$$\dot{S}^{(3)}[u_{abc}] = \frac{\tilde{\mathrm{d}}}{\mathrm{d}m_g}\sum_{i=1}^{4} u_i[u_{abc}] + \mathcal{O}(\varepsilon^5) \tag{B.7}$$

where the first contribution is known from the the 2-loop calculation and reads

$$u_1 = \frac{1}{2}(A_1 + A_2 + A_3) \sim \mathcal{O}(\varepsilon^3) \tag{B.8}$$

where only the local part of $R[v]$ is inserted, so u_1 is of order ε^3. The second contribution comes from inserting the non-local part of $R[v]$ to second order, that is Eq. (5.25), into $\frac{1}{2}(A_1 + A_2 + A_3)$.

$$u_2 = u_{2,1} + u_{2,2} + u_{2,3} \sim \mathcal{O}(\varepsilon^4) \tag{B.9}$$

where we split the contributions according to different types of integrals. This is not the shortest way to write but better comprehensible. The same is done in the contributions from the $RS^{(3)}$ term

$$u_3 = u_{3,1} + u_{3,2} \sim \mathcal{O}(\varepsilon^4) \tag{B.10}$$

where u_1 was used for $S^{(3)}$ on the right hand side. Finally

$$u_4 = u_{4,1} + u_{4,2} \sim \mathcal{O}(\varepsilon^4) \tag{B.11}$$

is the feeding term from $S^{(4)}$, where we insert Eq. (5.41).

Eq. (B.7) integrates to

$$S^{(3)}[u_{abc}] = \sum_{i=1}^{5} u^{(3),i}[u_{abc}] + \mathcal{O}(\varepsilon^5) \tag{B.12}$$

with the 2-loop result $u^{(3),1}[u_{abc}] = u_1[u_{abc}]$ and

$$\begin{aligned}
u^{(3),2}[u_{abc}] = \int^m (u_{2,1} - T) = -\frac{1}{2} I_1 \int \mathrm{d}^3x\, g(x_1,x_2) g(x_2,x_3) g(x_3,x_1) \\
\times \Bigg(\Big(2\mathcal{R}''_{ab}(x_1) \Big[\mathcal{R}''_{ac}(x_2) + \mathcal{R}''_{bc}(x_2)\Big] + \Big[\mathcal{R}''_{ac}(x_1) - \mathcal{R}''_{bc}(x_1)\Big]\Big[\mathcal{R}''_{ac}(x_2) - \mathcal{R}''_{bc}(x_2)\Big]\Big) \\
\times \Big[R''''_{ab}(x_3)\mathcal{R}''_{ab}(x_3) + R'''_{ab}(x_3)^2 - R'''(0^+)^2 \Big] \\
+ \Big(\mathcal{R}''_{ab}(x_1)\mathcal{R}''_{ab}(x_2) + \Big[\mathcal{R}''_{ac}(x_1) + \mathcal{R}''_{bc}(x_1)\Big]\Big[\mathcal{R}''_{ac}(x_2) + \mathcal{R}''_{bc}(x_2)\Big]\Big) \\
\times \Big[R''''_{ac}(x_3)\mathcal{R}''_{ac}(x_3) + R''''_{bc}(x_3)\mathcal{R}''_{bc}(x_3) + R'''_{ac}(x_3)^2 + R'''_{bc}(x_3)^2 - 2R'''(0^+)^2 \Big] \\
+ 2\mathcal{R}''_{ab}(x_1)\Big[\mathcal{R}''_{ac}(x_2) - \mathcal{R}''_{bc}(x_2)\Big]\Big[R''''_{ac}(x_3)\mathcal{R}''_{ac}(x_3) - R''''_{bc}(x_3)\mathcal{R}''_{bc}(x_3) \\
+ R'''_{ac}(x_3)^2 - R'''_{bc}(x_3)^2 \Big] \Bigg)
\end{aligned} \tag{B.13}$$

$$\begin{aligned}
u^{(3),3}[u_{abc}] = \int^m (u_{2,2} + u_{3,1}) = \frac{1}{2} \int \mathrm{d}^4x\, g(x_1,x_2) g(x_1,x_4) g(x_2,x_4) g(x_3,x_4)^2 \\
\times \Bigg(\Big(2\mathcal{R}''_{ab}(x_1) \Big[\mathcal{R}''_{ac}(x_2) + \mathcal{R}''_{bc}(x_2)\Big] + \Big[\mathcal{R}''_{ac}(x_1) - \mathcal{R}''_{bc}(x_1)\Big]\Big[\mathcal{R}''_{ac}(x_2) - \mathcal{R}''_{bc}(x_2)\Big]\Big) \\
\times \mathcal{R}''_{ab}(x_3) R''''_{ab}(x_4) \\
+ \Big(\mathcal{R}''_{ab}(x_1)\mathcal{R}''_{ab}(x_2) + \Big[\mathcal{R}''_{ac}(x_1) + \mathcal{R}''_{bc}(x_1)\Big]\Big[\mathcal{R}''_{ac}(x_2) + \mathcal{R}''_{bc}(x_2)\Big]\Big) \\
\times \Big[\mathcal{R}''_{ac}(x_3) R''''_{ac}(x_4) + \mathcal{R}''_{bc}(x_3) R''''_{bc}(x_4) \Big] \\
+ 2\mathcal{R}''_{ab}(x_1)\Big[\mathcal{R}''_{ac}(x_2) - \mathcal{R}''_{bc}(x_2)\Big]\Big[\mathcal{R}''_{ac}(x_3) R''''_{ac}(x_4) - \mathcal{R}''_{bc}(x_3) R''''_{bc}(x_4) \Big] \Bigg)
\end{aligned} \tag{B.14}$$

$$
\begin{aligned}
u^{(3),4}[u_{abc}] = \int^m (u_{2,3}+u_{4,2}) = \int \mathrm{d}^2x\mathrm{d}^2y\ g(y_1,y_2)^2 g(x_1,x_2)g(x_1,y_1)g(x_2,y_2)\\
\times \Bigg\{ \Big\{ \mathcal{R}''_{ab}(x_1)\Big[\mathcal{R}''_{ac}(x_2)+\mathcal{R}''_{bc}(x_2)\Big] + \frac{1}{2}\Big[\mathcal{R}''_{ac}(x_1)-\mathcal{R}''_{bc}(x_1)\Big]\Big[\mathcal{R}''_{ac}(x_2)-\mathcal{R}''_{bc}(x_2)\Big]\Big\}\\
\times \Big[R'''_{ab}(y_1)R'''_{ab}(y_2) - R'''(0^+)^2\Big]\\
+\frac{1}{2}\Big\{\mathcal{R}''_{ab}(x_1)\mathcal{R}''_{ab}(x_2) + \Big[\mathcal{R}''_{ac}(x_1)+\mathcal{R}''_{bc}(x_1)\Big]\Big[\mathcal{R}''_{ac}(x_2)+\mathcal{R}''_{bc}(x_2)\Big]\Big\}\\
\times\Big[R'''_{ac}(y_1)R'''_{ac}(y_2)+R'''_{bc}(y_1)R'''_{bc}(y_2)-2R'''(0^+)^2\Big]\\
+\mathcal{R}''_{ab}(x_1)\Big[\mathcal{R}''_{ac}(x_2)-\mathcal{R}''_{bc}(x_2)\Big]\Big[R'''_{ac}(y_1)R'''_{ac}(y_2)-R'''_{bc}(y_1)R'''_{bc}(y_2)\Big]\Bigg\}
\end{aligned}
\tag{B.15}
$$

$$
\begin{aligned}
u^{(3),5}[u_{abc}] = \int^m (u_{3,2}+u_{4,1}) = \frac{1}{2}\int \mathrm{d}^2x\mathrm{d}^2y\ g(y_1,y_2)g(x_1,y_1)g(x_1,y_2)g(x_2,y_1)g(x_2,y_2)\\
\times\Bigg\{\Big[\mathcal{R}''_{ab}(x_1)\mathcal{R}''_{ab}(x_2)+\mathcal{R}''_{bc}(x_1)\mathcal{R}''_{bc}(x_2)+\mathcal{R}''_{ac}(x_1)\mathcal{R}''_{ac}(x_2)\Big]\\
\times\Big[R'''_{ab}(y_1)R'''_{ac}(y_2)+R'''_{ac}(y_1)R'''_{bc}(y_2)-R'''_{ab}(y_1)R'''_{bc}(y_2)\Big]\\
+2\mathcal{R}''_{ab}(x_1)\mathcal{R}''_{ac}(x_2)\Big[R'''_{ab}(y_1)R'''_{ab}(y_2)+R'''_{ab}(y_1)R'''_{ac}(y_2)+R'''_{ab}(y_1)R'''_{bc}(y_2)\\
-R'''_{ac}(y_1)R'''_{bc}(y_2)+R'''_{ac}(y_1)R'''_{ac}(y_2)-R'''(0^+)^2\Big]\\
+2\mathcal{R}''_{ab}(x_1)\mathcal{R}''_{bc}(x_2)\Big[R'''_{ab}(y_1)R'''_{ab}(y_2)-R'''_{ab}(y_1)R'''_{ac}(y_2)-R'''_{ab}(y_1)R'''_{bc}(y_2)\\
-R'''_{ac}(y_1)R'''_{bc}(y_2)+R'''_{bc}(y_1)R'''_{bc}(y_2)-R'''(0^+)^2\Big]\\
+2\mathcal{R}''_{ac}(x_1)\mathcal{R}''_{bc}(x_2)\Big[R'''_{bc}(y_1)R'''_{bc}(y_2)-R'''_{ab}(y_1)R'''_{ac}(y_2)+R'''_{ab}(y_1)R'''_{bc}(y_2)\\
+R'''_{ac}(y_1)R'''_{bc}(y_2)+R'''_{ac}(y_1)R'''_{ac}(y_2)-R'''(0^+)^2\Big]\Bigg\}
\end{aligned}
\tag{B.16}
$$

C Systematic treatment of diagrams up to 3 loops: sloops and recursive construction

We present a systematic procedure to obtain (relatively) simple results for diagrams at up to 3 loops. The idea is to write the diagram, and then to consider all possible sloops which lead to the same diagram. Subtracting them with the right weight leads to results which are much simpler than those obtained by trying to reduce expressions term by term. The notation used throughout this section is

$$
\begin{aligned}
h_{ab} := R''_{ab}(1-\delta_{ab}) \qquad g_{ab} := R'''_{ab}(1-\delta_{ab}) \qquad f_{ab} := R''''_{ab}(1-\delta_{ab})\\
p_{ab} := R^{(5)}_{ab}(1-\delta_{ab}) \qquad s_{ab} := R^{(6)}_{ab}(1-\delta_{ab})\ .
\end{aligned}
\tag{C.1}
$$

We also use $h_0 := R''_{aa}$ a.s.o. The notation is such that all summations (which are implicit) are restricted. An example is

$$h_{ab} := \sum_{ab} h_{ab} \equiv \sum_{a \neq b} h_{ab} = \sum_{ab} R''_{ab} - \sum_{a} R''_{aa} \tag{C.2}$$

We will write rather instistinguishably, in a little abuse of notation, $R(u_a - u_b) \equiv R_u \equiv R_{ab}$, whatever is more convenient or suggestive. Below, we will give all diagrams.

There is always an additional combinatorial factor. At n-loop order, denote the number of propagators between points i and j as $n_{i,j}$. Further denote the number of symmetries $\mathcal{S}$ as $N_{\mathcal{S}}$. Then the combinatorial factor for the contribution to R is

$$\text{Comb} = \left(\frac{1}{2}\right)^n \times \frac{1}{N_{\mathcal{S}}} \times \prod_{i,j} \frac{1}{n_{i,j}!} \tag{C.3}$$

at n-loop order, *written apart from the diagram.* We will give this factor at the beginning of each diagram with the same conventions as above.

C.1 1 loop

Here we give the 1-loop diagram. A (closed) dashed line represents a sloop. $\text{Comb} = \frac{1}{2} \times \frac{1}{2} \times \frac{1}{2}$.

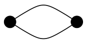 $= 4\, {h_{ab}}^2 + 4\, h_{ab}\, h_{ac}$ (C.4)

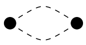 $= \sum_{a,b} 4\, R''_{ab}\, R''_{ac} = 4\, {h_0}^2 + 8\, h_0\, h_{ab} + 4\, h_{ab}\, h_{ac}$ (C.5)

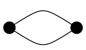 $-$ 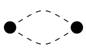 $= -4\, {h_0}^2 - 8\, h_0\, h_{ab} + 4\, {h_{ab}}^2 = 4 \sum_{a,b} \left[{R''_{ab}}^2 - 2\, R''_0\, R''_{ab} \right] + \text{const}$ (C.6)

C.2 2 loops

C.2.1 The hat-diagram

$\text{Comb} = \frac{1}{2^2} \times \frac{1}{2} \times \frac{1}{2}$

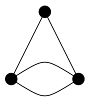 $= 8\, \left(2\, g_{ab}^2\, h_{ab} + 3\, g_{ab}^2\, h_{bc} - g_{ab}\, g_{ac}\, h_{bc} + 2\, g_{ac}\, g_{bc}\, h_{bc} + g_{ac}\, g_{bc}\, h_{cd} \right)$ (C.7)

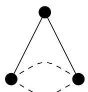 $= 8\, \left(g_{ab}^2\, h_{bc} - g_{ab}\, g_{ac}\, h_{bc} + 2\, g_{ac}\, g_{bc}\, h_{bc} + g_{ac}\, g_{bc}\, h_{cd} \right)$ (C.8)

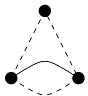 $= 8\, \left(h_0\, g_{ab}^2 + h_0\, g_{ab}\, g_{ac} + g_{ab}^2\, h_{bc} + g_{ac}\, g_{bc}\, h_{cd} \right)$ (C.9)

The simplest combination is

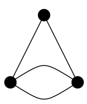 $-$ 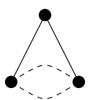 $= 16\, g_{ab}^2\, \left(h_{ab} + h_{bc} \right)\ .$ (C.10)

C.2.2 The bubble-chain

The bubble-chain has $\mathrm{Comb} = \frac{1}{2^2} \times \frac{1}{2} \times (\frac{1}{2})^2$, and reads

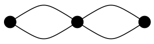 $$= 16\, f_{ab}\, h_{ab}^2 + 32\, f_{ab}\, h_{ab}\, h_{bc} + 8\, f_{ac}\, h_{ab}\, h_{cd} + 8\, f_{ac}\, h_{bc}\, h_{cd} \tag{C.11}$$

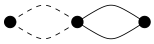 $$= 16\, h_0\, f_{ab}\, h_{ab} + 16\, h_0\, f_{ab}\, h_{bc} + 16\, f_{bc}\, h_{ab}\, h_{bc} + 8\, f_{ac}\, h_{ab}\, h_{cd} + 8\, f_{ac}\, h_{bc}\, h_{cd} \tag{C.12}$$

Now two sloops are a little bit more complicated, and in fact to be specific, we set

 $$:= \frac{1}{2} \Big[$$ 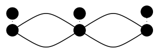 $$+$$ 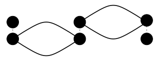 $$\Big] \tag{C.13}$$

We have

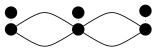 $$= 16\, h_0^2\, f_{ab} + 32\, h_0\, f_{ab}\, h_{ac} + 16\, f_{ab}\, h_{ac}\, h_{ad} \tag{C.14}$$

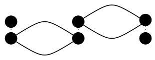 $$= 16\, h_0^2\, f_{ab} + 32\, h_0\, f_{ab}\, h_{ac} + 16\, f_{ab}\, h_{ac}\, h_{bd} \tag{C.15}$$

 $$= 16\, h_0^2\, f_{ab} + 32\, h_0\, f_{ab}\, h_{ac} + 8\, f_{ab}\, h_{ac}\, h_{ad} + 8\, f_{ab}\, h_{ac}\, h_{bd} \tag{C.16}$$

Note that we have dropped the term f_0, which naively would be there in the calculations. This can be done, since $f_0 \sum_{abc} R''_{ab} R''_{ac}$ is itself a 3-replica-term.

Then the simplest combination is

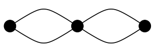 $$-\, 2$$ 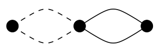 $$+$$ 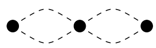 $$= 16 f_{ab}\, (h_{ab} - h_0)^2 = 16 \sum_{a,b} R''''_{ab}\, (R''_{ab} - R''_0)^2\ . \tag{C.17}$$

C.3 3 loops

C.3.1 Diagram (h)

Diagram (h) has $\mathrm{Comb} = \frac{1}{2^3} \times \frac{1}{2} \times (\frac{1}{2})^3$.

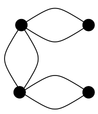
$$\begin{aligned} &= 64\, f_{ab}^2\, h_{ab}^2 + 128\, {f_{ab}}^2\, h_{ab}\, h_{bc} + 64\, f_{ab}\, f_{bc}\, h_{ab}\, h_{bc} + 64\, f_{ab}\, f_{bc}\, h_{ab}\, h_{cd} + 32\, {f_{bc}}^2\, h_{ab}\, h_{cd} \\ &\quad +64\, f_{ac}\, f_{bc}\, h_{ac}\, h_{cd} + 32\, {f_{bc}}^2\, h_{ac}\, h_{cd} + 16\, f_{ac}\, f_{cd}\, h_{ab}\, h_{de} + 32\, f_{ac}\, f_{cd}\, h_{bc}\, h_{de} \\ &\quad +16\, f_{ad}\, f_{cd}\, h_{bd}\, h_{de} \end{aligned} \tag{C.18}$$

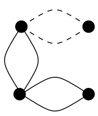
$$\begin{aligned} &= 64\, h_0\, {f_{ab}}^2\, h_{ab} + 64\, h_0\, {f_{ab}}^2\, h_{bc} + 64\, h_0\, f_{ab}\, f_{bc}\, h_{bc} + 64\, {f_{bc}}^2\, h_{ab}\, h_{bc} + 32\, h_0\, f_{ab}\, f_{bc}\, h_{cd} \\ &\quad +32\, h_0\, f_{ac}\, f_{bc}\, h_{cd} + 32\, {f_{bc}}^2\, h_{ab}\, h_{cd} + 32\, f_{ac}\, f_{cd}\, h_{ab}\, h_{cd} + 32\, {f_{bc}}^2\, h_{ac}\, h_{cd} \\ &\quad +32\, f_{ac}\, f_{cd}\, h_{bc}\, h_{cd} + 16\, f_{ac}\, f_{cd}\, h_{ab}\, h_{de} + 32\, f_{ac}\, f_{cd}\, h_{bc}\, h_{de} + 16\, f_{ad}\, f_{cd}\, h_{bd}\, h_{de} \end{aligned} \tag{C.19}$$

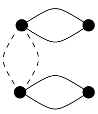
$$\begin{aligned} &= 64\, f_{ab}\, f_{bc}\, h_{ab}\, h_{bc} + 64\, f_{ab}\, f_{ac}\, h_{ab}\, h_{cd} + 64\, f_{ac}\, f_{bc}\, h_{ac}\, h_{cd} + 16\, f_{ab}\, f_{ad}\, h_{bc}\, h_{de} \\ &\quad +32\, f_{ab}\, f_{bd}\, h_{bc}\, h_{de} + 16\, f_{ad}\, f_{cd}\, h_{bd}\, h_{de} \end{aligned} \tag{C.20}$$

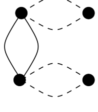
$$\begin{aligned} &= 64\, {h_0}^2\, {f_{ab}}^2 + 64\, {h_0}^2\, f_{ab}\, f_{ac} + 128\, h_0\, {f_{ab}}^2\, h_{ac} + 64\, h_0\, f_{ab}\, f_{ac}\, h_{ad} + 32\, {f_{ab}}^2\, h_{ac}\, h_{ad} \\ &\quad +16\, f_{ab}\, f_{ad}\, h_{ac}\, h_{ae} + 32\, {f_{ab}}^2\, h_{ac}\, h_{bd} + 64\, h_0\, f_{ab}\, f_{ac}\, h_{cd} + 32\, f_{ab}\, f_{ad}\, h_{ac}\, h_{de} \\ &\quad +16\, f_{ab}\, f_{bd}\, h_{ac}\, h_{de} \end{aligned} \tag{C.21}$$

For two intersecting 2-loops, there are 2 possibilities, and we define:

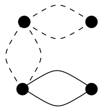 $$= \frac{1}{2} \Bigg[$$ 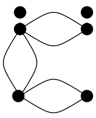 $$+$$ 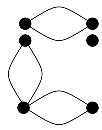 $$\Bigg] \qquad \text{(C.22)}$$

The terms are

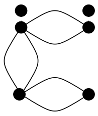 $$= 64\, h_0\, f_{ab}\, f_{bc}\, h_{bc} + 32\, h_0\, f_{ab}\, f_{ac}\, h_{cd} + 32\, h_0\, f_{ac}\, f_{bc}\, h_{cd} + 64\, f_{ac}\, f_{cd}\, h_{bc}\, h_{cd}$$
$$+32\, f_{ab}\, f_{ad}\, h_{ac}\, h_{de} + 32\, f_{ad}\, f_{cd}\, h_{bd}\, h_{de} \qquad \text{(C.23)}$$

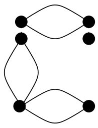 $$= 64\, h_0\, f_{ab}\, f_{bc}\, h_{bc} + 32\, h_0\, f_{ab}\, f_{bc}\, h_{cd} + 32\, h_0\, f_{ac}\, f_{bc}\, h_{cd} + 64\, f_{ac}\, f_{cd}\, h_{ab}\, h_{cd}$$
$$+32\, f_{ad}\, f_{cd}\, h_{ab}\, h_{de} + 32\, f_{ab}\, f_{bd}\, h_{ac}\, h_{de} \qquad \text{(C.24)}$$

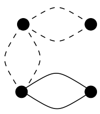 $$= 64\, h_0\, f_{ab}\, f_{bc}\, h_{bc} + 32\, h_0\, f_{ab}\, f_{ac}\, h_{cd} + 32\, h_0\, f_{ac}\, f_{bc}\, h_{cd} + 32\, f_{ac}\, f_{cd}\, h_{ab}\, h_{cd}$$
$$+32\, f_{ac}\, f_{cd}\, h_{bc}\, h_{cd} + 32\, f_{ab}\, f_{ad}\, h_{ac}\, h_{de} + 16\, f_{ab}\, f_{bd}\, h_{ac}\, h_{de} + 16\, f_{ad}\, f_{c,d}\, h_{bd}\, h_{de} \qquad \text{(C.25)}$$

Now 3 intersecting sloops. They can intersect in 3 different manners, and we take the average, with the weight proportional to their combinatorial factor,

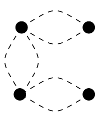 $$= \frac{1}{4} \Bigg[$$ 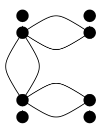 $$+ 2$$ 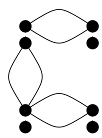 $$+$$ 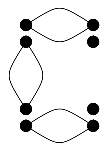 $$\Bigg]. \qquad \text{(C.26)}$$

The respective contributions are:

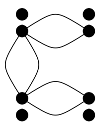 $$= 64\, {h_0}^2\, f_{ab}\, f_{ad} + 128\, h_0\, f_{ab}\, f_{ad}\, h_{ac} + 64\, f_{ab}\, f_{ad}\, h_{ac}\, h_{ae} \qquad \text{(C.27)}$$

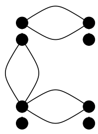 $$= 64\, {h_0}^2\, f_{ab}\, f_{ad} + 64\, h_0\, f_{ab}\, f_{ad}\, h_{ae} + 64\, h_0\, f_{ab}\, f_{ad}\, h_{bc} + 64\, f_{ab}\, f_{ad}\, h_{ae}\, h_{bc} \qquad \text{(C.28)}$$

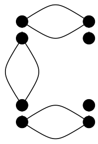 $$= 64\, {h_0}^2\, f_{ab}\, f_{ad} + 128\, h_0\, f_{ab}\, f_{ad}\, h_{bc} + 64\, f_{ab}\, f_{ad}\, h_{bc}\, h_{de} \qquad \text{(C.29)}$$

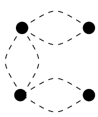 $$= 64\, {h_0}^2\, f_{ab}\, f_{ad} + 64\, h_0\, f_{ab}\, f_{ad}\, h_{ac} + 16\, f_{ab}\, f_{ad}\, h_{ac}\, h_{ae} + 64\, h_0\, f_{ab}\, f_{ad}\, h_{bc}$$
$$+32\, f_{ab}\, f_{ad}\, h_{ae}\, h_{bc} + 16\, f_{ab}\, f_{ad}\, h_{bc}\, h_{de} \qquad \text{(C.30)}$$

The final combination is

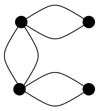 $-\,2$ 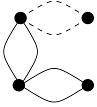 $-$ 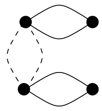 $+$ 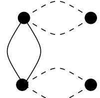 $+\,2$ 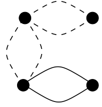 $-$ 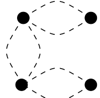

$$= 64 f_{ab}^2\,(h_{ab}-h_0)^2 = 64\sum_{a,b} f_{ab}^2\,(h_{ab}-h_0)^2 \tag{C.31}$$

Note that each sloop comes with a factor of (-1) and furthermore one has taken into account the proper combinatorial factor. This result is confirmed by the recursive-construction algorithm.

C.3.2 Diagram (*i*)

$\mathrm{Comb} = \frac{1}{2^3}\times\frac{1}{4!}\times 1$. For a given order of the contractions, we have:

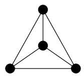 $$= 16\left(6\,g_{ab}^4 + 16\,g_{ab}^3\,g_{ac} + 3\,g_{ab}^2\,g_{ac}^2 + 6\,g_{ab}^2\,g_{ac}\,g_{ad} + g_{ab}\,g_{ac}\,g_{ad}\,g_{ae} + 12\,g_{ab}^2\,g_{ac}\,g_{bc}\right) \tag{C.32}$$

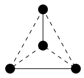 $$= 16\left(g_{ab}^2\,g_{ac}^2 + 2\,g_{ab}^2\,g_{ac}\,g_{ad} + g_{ab}\,g_{ac}\,g_{ad}\,g_{ae}\right) \tag{C.33}$$

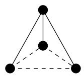 $$= 16\left(4\,g_{ab}^3\,g_{ac} + 3\,g_{ab}^2\,g_{ac}\,g_{ad} + g_{ab}\,g_{ac}\,g_{ad}\,g_{ae} + 3\,g_{ab}^2\,g_{ac}\,g_{bc}\right)\ . \tag{C.34}$$

The simplest combination is

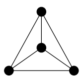 $+\,3$ 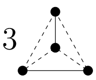 $-\,4$ 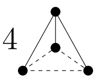 $$= 96\left(g_{ab}^4 + g_{ab}^2\,g_{ac}^2\right) = \text{1-rep} + 96\sum_{a,b}\left(R_{ab}'''^{\,4} - 2R_{ab}'''^{\,2}R_0'''^{\,2}\right) + \text{3-reps}\ . \tag{C.35}$$

Note that the factors are combinatorial factors for the number of possibilities to chose the sloop, while the signs are less intuitive. The diagram is supercusp-free.

C.3.3 Diagram (*j*)

Diagram (*j*) has $\mathrm{Comb} = \frac{1}{2^3}\times\frac{1}{4}\times\frac{1}{2}$. We number 1 to 4 for points x_1 to x_4,

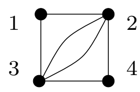

$$\tag{C.36}$$

We have performing, the contractions in the order (23)(23)(13)(12)(34)(24) or (13)(12)(34)(24)(23)(23)

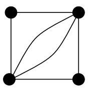 $$\begin{aligned} = 16\big(&4\,f_{ab}^2\,h_{ab}^2 + 12\,f_{ab}^2\,h_{ab}\,h_{bc} - 4\,f_{ab}\,f_{ac}\,h_{ab}\,h_{bc} + 2\,f_{ab}\,f_{bc}\,h_{ab}\,h_{bc} + f_{ab}\,f_{ac}\,h_{bc}^2 \\ &+2\,f_{ab}\,f_{bc}\,h_{bc}^2 + 4\,f_{ab}\,f_{bc}\,h_{ab}\,h_{bd} + 3\,f_{ab}^2\,h_{bc}\,h_{bd} + 4\,f_{ac}^2\,h_{ab}\,h_{c,d} - 2\,f_{ac}\,f_{ad}\,h_{ab}\,h_{c,d} \\ &+f_{ad}\,f_{cd}\,h_{bd}\,h_{de}\big) \end{aligned} \tag{C.37}$$

Sloops: The 2-sloop contracted as (23)(23)(13)(12)(34)(24) gives

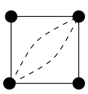 $$\begin{aligned} = 16\big(&4\,f_{ab}^2\,h_{ab}\,h_{bc} - 4\,f_{ab}\,f_{ac}\,h_{ab}\,h_{bc} + 2\,f_{ab}\,f_{bc}\,h_{ab}\,h_{bc} + f_{ab}\,f_{ac}\,h_{bc}^2 + 2\,f_{ab}\,f_{bc}\,h_{bc}^2 \\ &+4\,f_{ab}\,f_{bc}\,h_{ab}\,h_{bd} + f_{ab}^2\,h_{bc}\,h_{bd} + 2\,f_{ac}^2\,h_{ab}\,h_{c,d} - 2\,f_{ac}\,f_{ad}\,h_{ab}\,h_{c,d} + f_{ad}\,f_{cd}\,h_{bd}\,h_{de}\big) \end{aligned} \tag{C.38}$$

The 3-sloop is

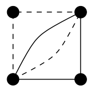

$$= 16\big(2\,h_0\,f_{ab}^2\,h_{ab} + h_0\,f_{ac}\,f_{ad}\,h_{ab} + 3\,h_0\,f_{ab}^2\,h_{bc} - h_0\,f_{ab}\,f_{ac}\,h_{bc} + 2\,h_0\,f_{ac}\,f_{bc}\,h_{bc}$$
$$+2\,f_{ab}^2\,h_{ab}\,h_{bc} + 2\,f_{ab}\,f_{bc}\,h_{ab}\,h_{bd} + f_{ab}^2\,h_{bc}\,h_{bd} + 2\,{f_{ac}}^2\,h_{ab}\,h_{cd} - f_{ac}\,f_{ad}\,h_{ab}\,h_{cd}$$
$$+f_{ad}\,f_{cd}\,h_{bd}\,h_{de}\big). \tag{C.39}$$

The 4-sloop(13)(12)(34)(24), then contracted (23)(23) gives

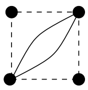

$$= 16\,\left(3\,h_0^2\,f_{ab}^2 + h_0^2\,f_{ab}\,f_{ac} + 2\,h_0\,f_{ac}\,f_{ad}\,h_{ab} + 6\,h_0\,f_{ab}^2\,h_{bc} + 3\,f_{ab}^2\,h_{bc}\,h_{bd} + f_{ad}\,f_{cd}\,h_{bd}\,h_{de}\right). \tag{C.40}$$

We can study another configuration, which we do not know how to draw, so call it S

$$S = 16(h_{ab}(x_1) + h_0)g_{ac}(x_2)g_{ac}(x_3)R_{de}(x_4)\;, \tag{C.41}$$

where we have already dropped the term $a = c$, which will disappear after the next contraction. Contracting (34) and then (24) gives

$$64\,h_0\,{f_{ab}}^2\,h_{ab} + 64\,h_0\,{f_{ab}}^2\,h_{bc} + 64\,{f_{bc}}^2\,h_{ab}\,h_{bc} + 32\,{f_{ac}}^2\,h_{ab}\,h_{cd} + 32\,{f_{bc}}^2\,h_{ac}\,h_{cd}\;. \tag{C.42}$$

A simple combination seems to be

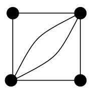 $-$ 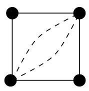

$$= 32\,\left(2\,f_{ab}^2\,h_{ab}^2 + 4\,f_{ab}^2\,h_{ab}\,h_{bc} + f_{ab}^2\,h_{bc}\,h_{bd} + f_{ac}^2\,h_{ab}\,h_{cd}\right)\;. \tag{C.43}$$

A still simpler configuration is

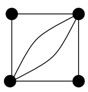 $-$ 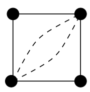

$$\begin{aligned} - S &= 64(-h_0{f_{ab}}^2h_{ab} + {f_{ab}}^2{h_{ab}}^2 - h_0{f_{ab}}^2h_{bc} + {f_{ab}}^2h_{ab}h_{bc}) \\ &= 64[{f_{ab}}^2h_{ab}(h_{ab} - h_0) + {f_{ab}}^2h_{bc}(h_{ab} - h_0)] \\ &= 64[{f_{ab}}^2(h_{ab} - h_0)](h_{ab} + h_{bc})\;. \end{aligned} \tag{C.44}$$

The trivial de-slooping gives (confirmed by the recursive-construction algorithm)

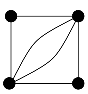 $-$ 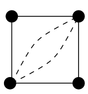

$$= 64f_{ab}^2(h_{ab} - h_0)^2 = 64\sum_{ab} R_{ab}^{''''2}\,(R''_{ab} - R''_0)^2\;. \tag{C.45}$$

C.3.4 Diagram (*k*)

Next is diagram (*k*). It has $\mathrm{Comb} = \frac{1}{2^3} \times \frac{1}{2} \times \frac{1}{3!}$. With contractions (13)(13)(13)(12)(34)(24) we have

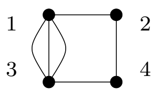

$$= 16\,\big(12\,f_{ab}^2\,h_{ab}\,h_{bc} - 6\,{f_{ac}}^2\,h_{ab}\,h_{bc} + 6\,{f_{ac}}^2\,h_{bc}^2 + 2\,f_{ab}\,f_{bc}\,h_{ab}\,h_{bd} + 7\,f_{ab}^2\,h_{bc}\,h_{bd}$$
$$+f_{ad}\,f_{cd}\,h_{bd}^2 - 2\,f_{ab}\,f_{ac}\,h_{bc}\,h_{cd} + f_{ab}\,f_{ad}\,h_{bc}\,h_{cd} + 2\,f_{ab}\,f_{bc}\,h_{bc}\,h_{cd} - 2\,f_{ab}\,f_{bd}\,h_{bc}\,h_{cd}$$
$$+f_{ad}\,f_{cd}\,h_{bd}\,h_{de}\big) \tag{C.46}$$

The 2-sloop (13)(13), then (13)(12)(34)(24)

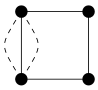

$$= 16 \left(4\, f_{ab}^2\, h_{ab}\, h_{bc} - 2\, f_{ac}{}^2\, h_{ab}\, h_{bc} + 2\, f_{ac}{}^2\, h_{bc}^2 + 2\, f_{ab}\, f_{bc}\, h_{ab}\, h_{bd} + 3\, f_{ab}^2\, h_{bc}\, h_{bd} \right.$$
$$+ f_{ad}\, f_{cd}\, h_{bd}^2 - 2\, f_{ab}\, f_{ac}\, h_{bc}\, h_{cd} + f_{ab}\, f_{ad}\, h_{bc}\, h_{cd} + 2\, f_{ab}\, f_{bc}\, h_{bc}\, h_{cd} - 2\, f_{ab}\, f_{bd}\, h_{bc}\, h_{cd}$$
$$\left. + f_{ad}\, f_{cd}\, h_{bd}\, h_{de}\right) \tag{C.47}$$

We find that the difference is

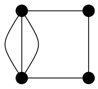 $-$ 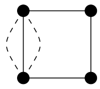

$$= 64 \left(2\, f_{ab}^2\, h_{ab}\, h_{bc} - f_{ac}^2\, h_{ab}\, h_{bc} + f_{ac}^2\, h_{bc}^2 + f_{ab}^2\, h_{bc}\, h_{bd}\right) \tag{C.48}$$

Trivial deslooping gives

$$0 \tag{C.49}$$

This is important since there is no counter-term in the theory for the divergence between the two leftmost vertices.

C.3.5 Diagram (*l*)

Diagram (*l*) has $\mathrm{Comb} = \frac{1}{2^3} \times 1 \times \frac{1}{2}$. We use the notation

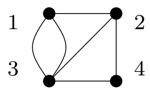

(C.50)

Diagram (l) is

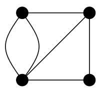

$$= 16\Big(4f_{ab}g_{ab}^2h_{ab} + 8f_{ab}g_{ab}^2h_{bc} - 3f_{ab}g_{ab}g_{ac}h_{bc} + f_{bc}g_{ab}g_{ac}h_{bc} - f_{ab}g_{ac}^2h_{bc} + f_{bc}g_{ac}^2h_{bc}$$
$$-3f_{ab}g_{ab}g_{bc}h_{bc} - 5f_{bc}g_{ab}g_{bc}h_{bc} + f_{ab}g_{bc}^2h_{bc} + f_{bc}g_{ac}^2h_{cd} - f_{ac}g_{ab}g_{bc}h_{cd} - 2f_{bc}g_{ab}g_{bc}h_{cd}$$
$$+4f_{ac}g_{ac}g_{bc}h_{cd} + f_{bc}g_{ab}g_{bd}h_{cd} + f_{cd}g_{ad}g_{bd}h_{cd} - f_{bc}g_{ac}g_{cd}h_{cd} + f_{cd}g_{ad}g_{bd}h_{de}\Big)\,. \tag{C.51}$$

The 2-sloop is

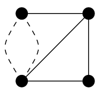

$$= 16\Big(2f_{ab}g_{ab}^2h_{bc} - f_{ab}g_{ab}g_{ac}h_{bc} + f_{bc}g_{ab}g_{ac}h_{bc} - f_{ab}g_{ac}^2h_{bc} + f_{bc}g_{ac}^2h_{bc} - f_{ab}g_{ab}g_{bc}h_{bc}$$
$$-3f_{bc}g_{ab}g_{bc}h_{bc} + f_{ab}g_{bc}^2h_{bc} + f_{bc}g_{ac}^2h_{cd} - f_{ac}g_{ab}g_{bc}h_{cd} - 2f_{bc}g_{ab}g_{bc}h_{cd} + 2f_{ac}g_{ac}g_{bc}h_{cd}$$
$$+f_{bc}g_{ab}g_{bd}h_{cd} + f_{cd}g_{ad}g_{bd}h_{cd} - f_{bc}g_{ac}g_{cd}h_{cd} + f_{cd}g_{ad}g_{bd}h_{de}\Big)\,. \tag{C.52}$$

There is the special sloop configuration, which is obtained by starting from $16g_{ab}(1)g_{ab}(2)h_{ac}(2)R_{de}(4)$. It is denoted and reads

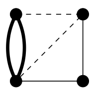

$$= 32\Big(-f_{ab}\, g_{ab}\, g_{ac}\, h_{bc} - f_{ab}\, g_{ab}\, g_{bc}\, h_{bc} + f_{bc}\, g_{ac}\, g_{bc}\, h_{bc} + f_{ac}\, g_{ac}\, g_{bc}\, h_{cd}\Big)\,. \tag{C.53}$$

Now diagram (l) is with the 2-sloop subtracted

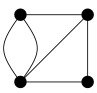 $-$ 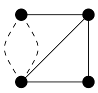

$$= 32\,\Big(2\, f_{ab}\, g_{ab}^2\, h_{ab} + 3\, f_{ab}\, g_{ab}^2\, h_{bc} - f_{ab}\, g_{ab}\, g_{ac}\, h_{bc} - f_{ab}\, g_{ab}\, g_{bc}\, h_{bc}$$
$$+ f_{bc}\, g_{ac}\, g_{bc}\, h_{bc} + f_{ac}\, g_{ac}\, g_{bc}\, h_{cd}\Big)\,. \tag{C.54}$$

An even simpler configuration is

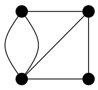 $-$ 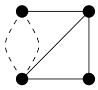 $-$ 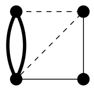

$$= 64\Big(f_{ab}\, g_{ab}^2\, h_{ab} + f_{ab}\, g_{ab}^2\, h_{bc}\Big)\ . \tag{C.55}$$

There are of course much more possible sloops, involving three or four vertices. However, we did not use them here, and thus do not display them.

The recursive-construction algorithm gives, consistent with the above

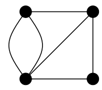

$$= 64\left[R''_u (R'''_u)^2 R''''_u - R''_0 (R'''_u)^2 R''''_u - R''_u (R'''_0)^2 R''''_0\right]\ . \tag{C.56}$$

C.3.6 Diagram (*m*)

Diagram (*m*) has $\mathrm{Comb} = \frac{1}{2^3}\times\frac{1}{4}\times(\frac{1}{2})^2$. It is not independent of the path of contractions. We number

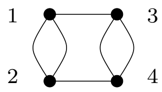

$$\tag{C.57}$$

The simplest result is obtained by using contractions (12)(12)(34)(34)(13)(24)

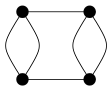

$$\begin{aligned} &= 16\Big(4\, g_{ab}^4 + 8\, g_{ab}^3\, g_{ac} + 8\, g_{ab}^2\, g_{ac}^2 + 8\, g_{ab}^2\, g_{ac}\, g_{ad} + g_{ab}\, g_{ac}\, g_{ad}\, g_{ae} - 4\, g_{ab}^2\, g_{ac}\, g_{bc} \\ &\quad -2\, g_{ab}^2\, g_{ac}\, g_{bd} - g_{ab}\, g_{ad}\, g_{bc}\, g_{cd}\Big)\ . \end{aligned} \tag{C.58}$$

Another result is obtained using (12)(12)(13)(24)(34)(34) instead of (12)(12)(34)(34)(13)(24). The difference is

$$(12)(12)(13)(24)(34)(34) - (12)(12)(34)(34)(13)(24) = 32\, g_{ab}\, g_{ac}\, g_{bc}\, g_{cd} \tag{C.59}$$

We check that this projects to 0.

Now the sloops give

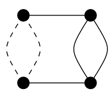

$$\begin{aligned} &= 16\Big(4\, g_{ab}^3\, g_{ac} + 2\, g_{ab}^2\, g_{ac}^2 + 6\, g_{ab}^2\, g_{ac}\, g_{ad} + g_{ab}\, g_{ac}\, g_{ad}\, g_{ae} - 2\, g_{ab}^2\, g_{ac}\, g_{bc} - 2\, g_{ab}^2\, g_{ac}\, g_{bd} \\ &\quad - g_{ab}\, g_{ad}\, g_{bc}\, g_{cd}\Big) \end{aligned} \tag{C.60}$$

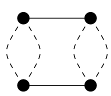

$$= 16\left(4\, g_{ab}^2\, g_{ac}\, g_{ad} + g_{ab}\, g_{ac}\, g_{ad}\, g_{ae} - 2\, g_{ab}^2\, g_{ac}\, g_{bd} - g_{ab}\, g_{ad}\, g_{bc}\, g_{cd}\right)\ . \tag{C.61}$$

The following combination is simple

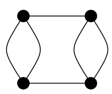 $-\,2$ 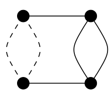 $+$ 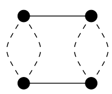

$$\begin{aligned} &= 64\, g_{ab}^4 + 64\, g_{ab}^2\, g_{ac}^2 \\ &= \text{1-rep} + 64 \sum_{a,b}\left({R'''_{ab}}^4 - 2{R'''_{ab}}^2 {R'''_0}^2\right) + \text{3-reps}\ . \end{aligned} \tag{C.62}$$

C.3.7 Diagram (n)

Comb $= \frac{1}{2^3} \times \frac{1}{3!} \times (\frac{1}{2})^3$. We have with the choice of contractions (13)(13)(23)(23)(34)(34)

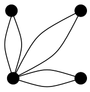

$$= 16(4{h_{ab}}^3 s_{ab} + 12{h_{ab}}^2 h_{bc} s_{ab} + 6h_{ab}h_{ac}h_{cd}s_{ac} + 6h_{ac}h_{bc}h_{cd}s_{ac} + 3h_{ab}h_{cd}h_{de}s_{ad} + h_{ad}h_{bd}h_{de}s_{cd}) \ . \tag{C.63}$$

A single sloop is

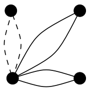

$$= 16(4h_0{h_{ab}}^2 s_{ab} + 8h_0 h_{ab}h_{bc}s_{ab} + 2h_0 h_{ab}h_{cd}s_{ac} + 2h_0 h_{bc}h_{cd}s_{ac} + 3h_{ab}h_{cd}h_{de}s_{ad} + 4h_{ab}{h_{bc}}^2 s_{bc} + 4h_{ab}h_{bc}h_{cd}s_{bc} + 4h_{ac}h_{bc}h_{cd}s_{bc} + h_{ad}h_{bd}h_{de}s_{cd}) \ . \tag{C.64}$$

Double and triple sloops yield

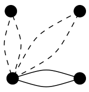 $= \frac{1}{2}\Big[$ 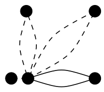 $+$ 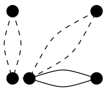 $\Big]$ (C.65)

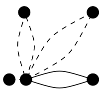

$$= 32(2h_0^2 h_{ab}s_{ab} + 2h_0^2 h_{bc}s_{ab} + 2h_0 h_{ab}h_{cd}s_{ac} + h_{ab}h_{ac}h_{de}s_{ad} + 4h_0 h_{ab}h_{bc}s_{bc} + 2h_0 h_{ac}h_{cd}s_{bc} + 2h_{ac}h_{bc}h_{cd}s_{cd} + h_{ad}h_{bd}h_{de}s_{cd}) \tag{C.66}$$

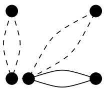

$$= 32(2h_0^2 h_{ab}s_{ab} + 2h_0^2 h_{bc}s_{ab} + 2h_0 h_{ab}h_{cd}s_{ac} + 2h_0 h_{bc}h_{cd}s_{ac} + 2h_{ab}h_{cd}h_{de}s_{ad} + 4h_0 h_{ab}h_{bc}s_{bc} + 2h_{ad}h_{bc}h_{cd}s_{cd}) \tag{C.67}$$

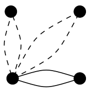

$$= 16(4h_0^2 h_{ab}s_{ab} + 4h_0^2 h_{bc}s_{ab} + 4h_0 h_{ab}h_{cd}s_{ac} + 4h_0 h_{bc}h_{cd}s_{ac} + 3h_{ab}h_{ac}h_{de}s_{ad} + 8h_0 h_{ab}h_{bc}s_{bc} + 2h_{ac}h_{bc}h_{cd}s_{cd} + 2h_{ad}h_{bc}h_{cd}s_{cd} + h_{ad}h_{bd}h_{de}s_{cd}) \ . \tag{C.68}$$

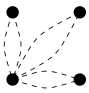 $= \frac{1}{4}\Big[$ 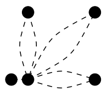 $+\,3$ 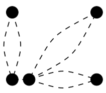 $\Big]$ (C.69)

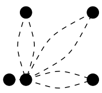

$$= 16(h_0^3 s_{ab} + 3h_0^2 h_{ab}s_{ac} + 3h_0 h_{ab}h_{ac}s_{ad} + h_{ab}h_{ac}h_{ae}s_{ad}) \tag{C.70}$$

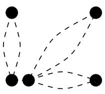

$$= 16(h_0^3 s_{ab} + 3h_0^2 h_{ab}s_{ac} + 2h_0 h_{ab}h_{cd}s_{ac} + h_0 h_{ab}h_{ac}s_{ad} + h_{ab}h_{ac}h_{de}s_{ad}) \tag{C.71}$$

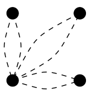

$$= 4(4h_0^3 s_{ab} + 12h_0^2 h_{ab}s_{ac} + 6h_0 h_{ab}h_{cd}s_{ac} + 6h_0 h_{ab}h_{ac}s_{ad} + h_{ab}h_{ac}h_{ae}s_{ad} + 3h_{ab}h_{ac}h_{de}s_{ad}) \tag{C.72}$$

The final result is

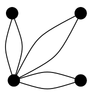 $-\,3$ 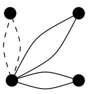 $+\,3$ 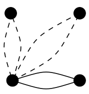 $-\,4$ 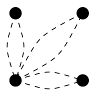 $= 64(h_{ab} - h_0)^3 s_{ab}$ (C.73)

This is confirmed by the recursive-construction algorithm.

C.3.8 Diagram (*o*)

Comb $= \frac{1}{2^3} \times \frac{1}{2} \times (\frac{1}{2})^2$.

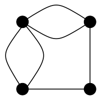

$$= 64\, f_{ab}\, {g_{ab}}^2\, h_{ab} + 128\, f_{ab}\, {g_{ab}}^2\, h_{bc} - 64\, f_{ab}\, g_{ab}\, g_{ac}\, h_{bc} - 64\, f_{ab}\, g_{ab}\, g_{bc}\, h_{bc}$$
$$-64\, f_{bc}\, g_{ab}\, g_{bc}\, h_{bc} + 16\, f_{ab}\, g_{ac}\, g_{bc}\, h_{cd} + 96\, f_{bc}\, g_{ac}\, g_{bc}\, h_{cd} - 16\, f_{ab}\, g_{ad}\, g_{bc}\, h_{cd}$$
$$-32\, f_{ac}\, g_{ad}\, g_{bc}\, h_{cd} - 16\, f_{cd}\, g_{ad}\, g_{bc}\, h_{cd} + 16\, f_{ab}\, {g_{bc}}^2\, h_{cd} - 16\, f_{ab}\, g_{bc}\, g_{bd}\, h_{cd}$$
$$-32\, f_{ac}\, g_{bc}\, g_{cd}\, h_{cd} + 16\, f_{ad}\, g_{bd}\, g_{cd}\, h_{de} \tag{C.74}$$

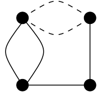

$$= 32\, f_{ab}\, {g_{ab}}^2\, h_{bc} - 32\, f_{ab}\, g_{ab}\, g_{ac}\, h_{bc} - 32\, f_{ab}\, g_{ab}\, g_{bc}\, h_{bc} + 32\, f_{bc}\, g_{ac}\, g_{bc}\, h_{bc}$$
$$+16\, f_{ab}\, g_{ac}\, g_{bc}\, h_{cd} + 64\, f_{bc}\, g_{ac}\, g_{bc}\, h_{cd} - 16\, f_{ab}\, g_{ad}\, g_{bc}\, h_{cd} - 32\, f_{ac}\, g_{ad}\, g_{bc}\, h_{cd}$$
$$-16\, f_{cd}\, g_{ad}\, g_{bc}\, h_{cd} + 16\, f_{ab}\, {g_{bc}}^2\, h_{cd} - 16\, f_{ab}\, g_{bc}\, g_{bd}\, h_{cd} - 32\, f_{ac}\, g_{bc}\, g_{cd}\, h_{cd}$$
$$+16\, f_{ad}\, g_{bd}\, g_{cd}\, h_{de} \tag{C.75}$$

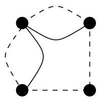

$$= 4\, h_0\, f_{ab}\, {g_{ab}}^2 + 8\, h_0\, f_{ab}\, g_{ab}\, g_{ac} + 4\, h_0\, f_{ab}\, g_{ac}\, g_{ad} + 4\, f_{ab}\, {g_{ab}}^2\, h_{ac} + 8\, f_{ab}\, g_{ab}\, g_{ac}\, h_{ad}$$
$$+4\, f_{ab}\, g_{ac}\, g_{ad}\, h_{ae} \tag{C.76}$$

For 2 touching loops, intersections are possible:

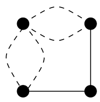 $= \frac{1}{2} \Bigg[$ 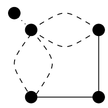 $+$ 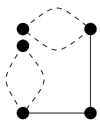 $\Bigg]$ (C.77)

The terms are

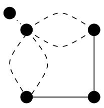

$$= 32\, f_{ab}\, {g_{ac}}^2\, h_{cd} - 32\, f_{ab}\, g_{ac}\, g_{ad}\, h_{cd} - 64\, f_{ac}\, g_{bc}\, g_{cd}\, h_{cd} + 32\, f_{ad}\, g_{bd}\, g_{cd}\, h_{de} d1 \tag{C.78}$$

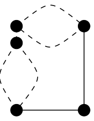

$$= 32\, f_{ab}\, g_{ac}\, g_{bc}\, h_{cd} + 64\, f_{ac}\, g_{ac}\, g_{bc}\, h_{cd} - 64\, f_{ac}\, g_{ad}\, g_{bc}\, h_{cd} - 32\, f_{ab}\, g_{ac}\, g_{bd}\, h_{cd}$$
$$-32\, f_{cd}\, g_{ac}\, g_{bd}\, h_{cd} \tag{C.79}$$

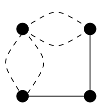

$$= 16\, f_{ab}\, {g_{ac}}^2\, h_{cd} - 16\, f_{ab}\, g_{ac}\, g_{ad}\, h_{cd} + 16\, f_{ab}\, g_{ac}\, g_{bc}\, h_{cd} + 32\, f_{ac}\, g_{ac}\, g_{bc}\, h_{cd}$$
$$-32\, f_{ac}\, g_{ad}\, g_{bc}\, h_{cd} - 16\, f_{ab}\, g_{ac}\, g_{bd}\, h_{cd} - 16\, f_{cd}\, g_{ac}\, g_{bd}\, h_{cd} - 32\, f_{ac}\, g_{bc}\, g_{cd}\, h_{cd}$$
$$+16\, f_{ad}\, g_{bd}\, g_{cd}\, h_{de} \tag{C.80}$$

The simplest combination is

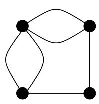 $-\, 2$ 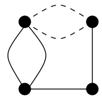 $+$ 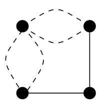 $= 64 f_{ab} g_{ab}^2\, (h_{ab} + h_{bc})$

$$= 64 \sum_{a,b} R^{(4)}_{ab}\, {R'''_{ab}}^2\, R''_{ab} - R''_0\, R''''_{ab}\, {R'''_{ab}}^2 - R''''_0\, R'''^2_0\, R''_{ab} \tag{C.81}$$

This is confirmed by recursive construction.

C.3.9 Diagram (*p*)

The diagram (*p*) has $\mathrm{Comb} = \frac{1}{2^3} \times 1 \times (\frac{1}{2})^2$ and is

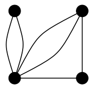

$$= 16(4g_{ab}{h_{ab}}^2p_{ab} + 10g_{ab}h_{ab}h_{bc}p_{ab} - 2g_{ac}h_{ab}h_{bc}p_{ab} - 2g_{bc}h_{ab}h_{bc}p_{ab} - g_{cd}h_{ab}h_{cd}p_{ac}$$
$$+3g_{bc}h_{ac}h_{cd}p_{ac} + g_{cd}h_{ab}h_{de}p_{ad} + 2g_{ac}{h_{bc}}^2p_{bc} + 3g_{bc}h_{ab}h_{cd}p_{bc} - g_{bd}h_{ab}h_{cd}p_{bc}$$
$$+3g_{bc}h_{ac}h_{cd}p_{bc} - g_{bd}h_{ac}h_{cd}p_{bc} - g_{cd}h_{ac}h_{cd}p_{bc} + g_{bd}h_{ac}h_{cd}p_{cd} + g_{bd}h_{ad}h_{de}p_{cd})\ . \quad (C.82)$$

The two 1-sloop terms are

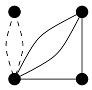

$$= 16(4h_0g_{ab}h_{ab}p_{ab} + 6h_0g_{ab}h_{bc}p_{ab} - 2h_0g_{ac}h_{bc}p_{ab} - 2h_0g_{bc}h_{bc}p_{ab} + h_0g_{bc}h_{cd}p_{ac}$$
$$-g_{cd}h_{ab}h_{cd}p_{ac} + g_{cd}h_{ab}h_{de}p_{ad} + 2h_0g_{ac}h_{bc}p_{bc} + 4g_{bc}h_{ab}h_{bc}p_{bc} + h_0g_{ac}h_{cd}p_{bc}$$
$$+3g_{bc}h_{ab}h_{cd}p_{bc} - g_{bd}h_{ab}h_{cd}p_{bc} + 3g_{bc}h_{ac}h_{cd}p_{bc} - g_{bd}h_{ac}h_{cd}p_{bc} - g_{cd}h_{ac}h_{cd}p_{bc}$$
$$+g_{bd}h_{ac}h_{cd}p_{cd} + g_{bd}h_{ad}h_{cd}p_{cd} + g_{bd}h_{ad}h_{de}p_{cd}) \quad (C.83)$$

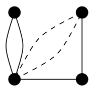

$$= 16(2g_{ab}h_{ab}h_{bc}p_{ab} - 2g_{ac}h_{ab}h_{bc}p_{ab} - 2g_{bc}h_{ab}h_{bc}p_{ab} + g_{ac}h_{ab}h_{cd}p_{ac} - g_{ad}h_{ab}h_{cd}p_{ac}$$
$$-g_{cd}h_{ab}h_{cd}p_{ac} + 3g_{bc}h_{ac}h_{cd}p_{ac} + g_{cd}h_{ab}h_{de}p_{ad} + 2g_{ac}{h_{bc}}^2p_{bc} + g_{bc}h_{ac}h_{cd}p_{bc}$$
$$-g_{bd}h_{ac}h_{cd}p_{bc} - g_{cd}h_{ac}h_{cd}p_{bc}$$
$$+g_{bd}h_{ac}h_{cd}p_{cd} + g_{bd}h_{ad}h_{de}p_{cd})\ . \quad (C.84)$$

There are again the 2-sloop terms,

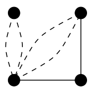 $= \frac{1}{2}\Big[$ 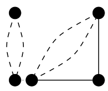 $+$ 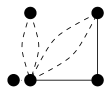 $\Big]$ (C.85)

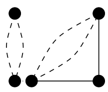

$$= 16(2h_0g_{ab}h_{bc}p_{ab} - 2h_0g_{ab}h_{bc}p_{ac} + 2h_0g_{bc}h_{bc}p_{ac} + 2g_{ac}h_{ab}h_{cd}p_{ac} - 2g_{ac}h_{ab}h_{cd}p_{ad}$$
$$-2h_0g_{ab}h_{bc}p_{bc} + 2h_0g_{ac}h_{cd}p_{bc} + 2g_{cd}h_{ad}h_{cd}p_{bd} - 2g_{bc}h_{ac}h_{cd}p_{cd} + 2g_{bd}h_{ad}h_{de}p_{cd}) \quad (C.86)$$

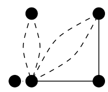

$$= 16(2h_0g_{ab}h_{bc}p_{ab} - 2h_0g_{ab}h_{bc}p_{ac} + 2h_0g_{bc}h_{bc}p_{ac} + 2h_0g_{bc}h_{cd}p_{ac} + 2g_{cd}h_{ab}h_{cd}p_{ad}$$
$$+2g_{cd}h_{ab}h_{de}p_{ad} - 2h_0g_{ab}h_{bc}p_{bc} + 2g_{bc}h_{ac}h_{cd}p_{bc} - 2g_{bc}h_{ad}h_{cd}p_{bd} - 2g_{bc}h_{ad}h_{cd}p_{cd}) \quad (C.87)$$

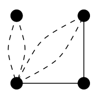

$$= 16(2h_0g_{ab}h_{bc}p_{ab} - 2h_0g_{ab}h_{bc}p_{ac} + 2h_0g_{bc}h_{bc}p_{ac} + h_0g_{bc}h_{cd}p_{ac} + g_{ac}h_{ab}h_{cd}p_{ac}$$
$$-g_{ac}h_{ab}h_{cd}p_{ad} + g_{cd}h_{ab}h_{cd}p_{ad} + g_{cd}h_{ab}h_{de}p_{ad} - 2h_0g_{ab}h_{bc}p_{bc} + h_0g_{ac}h_{cd}p_{bc}$$
$$+g_{bc}h_{ac}h_{cd}p_{bc} - g_{bc}h_{ad}h_{cd}p_{bd} + g_{cd}h_{ad}h_{cd}p_{bd} - g_{bc}h_{ac}h_{cd}p_{cd} - g_{bc}h_{ad}h_{cd}p_{cd}$$
$$+g_{bd}h_{ad}h_{de}p_{cd}) \quad (C.88)$$

There are more sloops, but we find a simple expression with only the above. It is

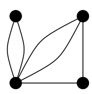 $-$ 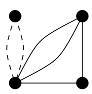 $-$ 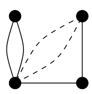 $+$ 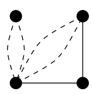

$$= -64h_0g_{ab}h_{ab}p_{ab} + 64g_{ab}{h_{ab}}^2p_{ab} - 64h_0g_{ab}h_{bc}p_{ab} + 64g_{ab}h_{ab}h_{bc}p_{ab} \quad (C.89)$$

Trivially deslooping gives, as with the recursive-construction algorithm,

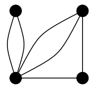

$$= 64\, R_u''' R_u^{(5)} (R_u'' - R_0'')^2 \; . \tag{C.90}$$

C.3.10 Diagram (*q*)

Diagram (q) has $\mathrm{Comb} = \frac{1}{2^3} \times \frac{1}{2} \times (\frac{1}{2})^2$. We make contractions (13)(13)(24)(24)(23)(34)

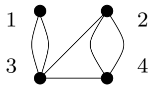

$$\begin{aligned} &= 16(4 f_{ab} {g_{ab}}^2 h_{ab} + 4 f_{ab} g_{ab} g_{ac} h_{ab} + 6 f_{ab} {g_{bc}}^2 h_{ab} + 4 f_{bc} {g_{bc}}^2 h_{ab} + 3 f_{bd} {g_{bc}}^2 h_{ab} \\ &\quad + 2 f_{ab} g_{bc} g_{bd} h_{ab} + 2 f_{bc} g_{bc} g_{bd} h_{ab} + f_{bd} g_{bc} g_{be} h_{ab} + 3 f_{ac} {g_{cd}}^2 h_{ab} + f_{ac} g_{cd} g_{ce} h_{ab} \\ &\quad + 2 f_{bc} g_{bc} g_{bd} h_{ac} - 2 f_{cd} g_{bc} g_{bd} h_{ac} - 2 f_{bc} g_{ab} g_{ac} h_{bc}) \; . \end{aligned} \tag{C.91}$$

Sloop (13)(13), then (24)(24)(23)(34) gives

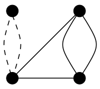

$$\begin{aligned} &= 16(4 h_0 f_{ab} {g_{ab}}^2 + 4 h_0 f_{ab} g_{ab} g_{ac} - 2 h_0 f_{bc} g_{ab} g_{ac} + 2 h_0 f_{ac} g_{ab} g_{ad} + 6 h_0 f_{ab} {g_{bc}}^2 \\ &\quad + 4 f_{bc} {g_{bc}}^2 h_{ab} + 3 f_{bd} {g_{bc}}^2 h_{ab} + 2 f_{bc} g_{bc} g_{bd} h_{ab} + f_{bd} g_{bc} g_{be} h_{ab} + 3 f_{ac} {g_{cd}}^2 h_{ab} \\ &\quad + f_{ac} g_{cd} g_{ce} h_{ab} + 2 f_{bc} g_{bc} g_{bd} h_{ac} - 2 f_{cd} g_{bc} g_{bd} h_{ac}) \; . \end{aligned} \tag{C.92}$$

Sloop (24)(24), then (13)(13)(34)(24) yields

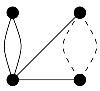

$$\begin{aligned} &= 16(4 f_{ab} g_{ab} g_{ac} h_{ab} + 2 f_{ab} g_{bc} g_{bd} h_{ab} + 2 f_{bc} g_{bc} g_{bd} h_{ab} + f_{bd} g_{bc} g_{be} h_{ab} + f_{ad} {g_{cd}}^2 h_{ab} \\ &\quad + f_{ac} g_{cd} g_{ce} h_{ab} + 2 f_{ac} {g_{bc}}^2 h_{ac} + 2 f_{bc} g_{bc} g_{bd} h_{ac} - 2 f_{cd} g_{bc} g_{bd} h_{ac} + f_{cd} {g_{bd}}^2 h_{ad} \\ &\quad - 2 f_{bc} g_{ab} g_{ac} h_{bc}) \; . \end{aligned} \tag{C.93}$$

Sloops (13)(13)and (24)(24), then (23) (34) gives

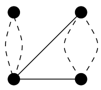

$$\begin{aligned} &= 16(4 h_0 f_{ab} g_{ab} g_{ac} - 2 h_0 f_{bc} g_{ab} g_{ac} + 2 h_0 f_{ac} g_{ab} g_{ad} + 2 h_0 f_{ac} {g_{bc}}^2 + 2 f_{bc} g_{bc} g_{bd} h_{ab} \\ &\quad + f_{bd} g_{bc} g_{be} h_{ab} + f_{ad} {g_{cd}}^2 h_{ab} + f_{ac} g_{cd} g_{ce} h_{ab} + 2 f_{bc} g_{bc} g_{bd} h_{ac} - 2 f_{cd} g_{bc} g_{bd} h_{ac} \\ &\quad + f_{cd} {g_{bd}}^2 h_{ad}) \; . \end{aligned} \tag{C.94}$$

There are more sloops, but our now acquired experience tells us that the simplest combination should be

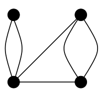 $-$ 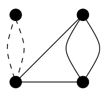 $-$ 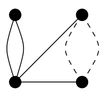 $+$ 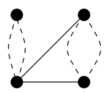

$$= 64(f_{ab} {g_{ab}}^2 h_{ab} + f_{ab} {g_{bc}}^2 h_{ab} - h_0 f_{ab} {g_{ab}}^2 - h_0 f_{ab} {g_{bc}}^2) \tag{C.95}$$

Trivial de-slooping yields in agreement with recursive construction

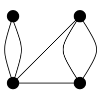

$$= 64\,[R_u'''^2 - R_0'''^2] R_u'''' (R_u'' - R_0''). \tag{C.96}$$

D 2-loop integral for the 2-point correlation function

We consider the following 2-loop contribution to the 2-point correlation function

$$\Phi_{2,\varepsilon}(q) = I_A(q) - I_A + I_1^2 - I_1 I_1(q) = \tfrac{1}{m^{2\varepsilon}}\tilde{\Phi}_{2,\varepsilon}(\tfrac{q}{m})\,, \tag{D.1}$$

which can be written as

$$\tilde{\Phi}_{2,\varepsilon}(z) = \mathcal{N}^2\big[F_\varepsilon(z,1) - F_\varepsilon(0,1) - F_\varepsilon(z,0) + F_\varepsilon(0,0)\big] \tag{D.2}$$

with

$$F_\varepsilon(z,b) = \Gamma(\varepsilon)\int_{x_1,x_2,x_3>0} \frac{\Big[1 + x_1 + x_2 + x_3 + z^2\frac{x_1(x_2+x_3)+x_2x_3b^2}{(x_2+x_3)(1+x_1)+x_2x_3b^2}\Big]^{-\varepsilon}}{\Big[(x_2+x_3)(1+x_1)+x_2x_3b^2\Big]^{2-\frac{\varepsilon}{2}}}\,. \tag{D.3}$$

Although each individual term is of order $\frac{1}{\varepsilon^2}$, the limit $\varepsilon \to 0$ of $\tilde{\Phi}_{2,\varepsilon}$ exists and is given by

$$\tilde{\Phi}_{2,0}(z) = \mathcal{N}^2\int_{x_1,x_2,x_3>0}\left\{\frac{\ln\Big(1+\frac{z^2x_1}{(1+x_1)(1+x_1+x_2+x_3)}\Big)}{(1+x_1)^2(x_2+x_3)^2} - \frac{\ln\Big(1+\frac{z^2x_1(x_2+x_3)+x_2x_3}{\big[(1+x_1)(x_2+x_3)+x_2x_3\big](1+x_1+x_2+x_3)}\Big)}{\big[(x_2+x_3)(1+x_1)+x_2x_3\big]^2}\right\}. \tag{D.4}$$

We were not able to obtain a closed analytical expression for the three-dimensional integral. Using the variable transformations $x_1 = \frac{1}{x}-1$, $x_3 = \frac{y}{x}$, and $x_2 = \frac{y_2}{x}$ helps to determine the Taylor expansion $\tilde{\Phi}_{2,0}(z) \approx \mathcal{N}^2\sum_n \alpha_n z^{2n}$ with the first four coefficients

$$\alpha_1 = -\frac{2}{9} - \frac{8\pi^2}{243} + \frac{1}{81}\left[\psi'(\tfrac{1}{3}) + \psi'(\tfrac{1}{6})\right] \approx 0.03821\,, \tag{D.5}$$

$$\alpha_2 = \frac{193}{3240} + \frac{16\pi^2}{2187} - \frac{2}{729}\left[\psi'(\tfrac{1}{3}) + \psi'(\tfrac{1}{6})\right] \approx 0.00169\,, \tag{D.6}$$

$$\alpha_3 \approx -0.00039\,, \tag{D.7}$$

$$\alpha_4 \approx 0.00007\,. \tag{D.8}$$

Since the coefficients are small, a Taylor expansion to fourth order compares well with the full function up to $z \approx 3$, see Fig. 11.

To render the integral numerically well-behaved, it is convenient to perform a variable transformation to $s = x_2 + x_3$, $ds = x_2 - x_3$, $x = x_1$. The integral to be calculated then is (using the symmetry $d \to -d$)

$$\tilde{\Phi}_{2,0}(z) = \mathcal{N}^2\int_{0<d<1}\int_{s,x>0}\frac{\ln\Big(\frac{xz^2}{(x+1)(s+x+1)}+1\Big)}{s\,(x+1)^2} - \frac{16\ln\Big(\frac{z^2\big[\big(d^2-1\big)s-4x\big]}{(s+x+1)[(d^2-1)s-4(x+1)]}+1\Big)}{s\,(d^2s-s-4x-4)^2}\,. \tag{D.9}$$

In order to calculate the asymptotics for large z we consider $z^2\frac{\mathrm{d}}{\mathrm{d}z^2}\tilde{\Phi}_{2,0}(z)$, which helps to solve the integrals but eliminates the constant part. Using again the variable transformations $x_1 = \frac{1}{x} - 1$,

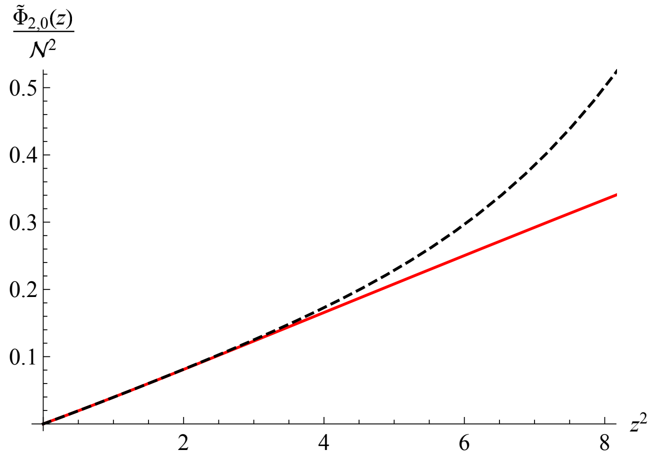

Figure 11: Taylor expansion to 8th order as given in Eq. (D.5)–(D.8) (dashed curve) of $\tilde{\Phi}_{2,0}(z)$ (red, solid line).

$x_3 = \frac{y}{x}$, and $x_2 = \frac{y_2}{x}$ the integral reads

$$z^2 \tfrac{\mathrm{d}}{\mathrm{d}(z^2)} \tilde{\Phi}_{2,0}(z) = \mathcal{N}^2 \int_0^1 \mathrm{d}x \int_0^\infty \mathrm{d}y \int_0^\infty \mathrm{d}y_2 \, \left[F_z^{(1)}(x,y,y_2) + F_z^{(2)}(x,y,y_2)\right] \tag{D.10}$$

$$F_z^{(1)}(x,y,y_2) = \frac{xz^2(1-x)}{(y+y_2)^2(1+y+y_2+(1-x)xz^2)} \tag{D.11}$$

$$F_z^{(2)}(x,y,y_2) = \frac{-xz^2[y(1-x+y_2)+(1-x)y_2]}{(y+y_2+yy_2)^2\big[(1+y+y_2)(y+y_2+yy_2)+xz^2(y_2-xy_2+y(1-x+y_2))\big]} \tag{D.12}$$

We distinguish the cases $y<1$ and $y>1$ and split $z^2 \frac{\mathrm{d}}{\mathrm{d}z^2} \tilde{\Phi}_{2,0}(z) = A_< + A_>$ accordingly. For $y<1$ the limit $z\to\infty$ exists and can be taken in the integrand. This integration gives a constant,

$$\lim_{z\to\infty} A_< = \int_0^1 \mathrm{d}x \int_0^\infty \mathrm{d}y \int_0^1 \mathrm{d}y_2 \, \left[\frac{1}{(y+y_2)^2} - \frac{1}{(y+y_2+yy_2)^2}\right] = \ln 2 \, . \tag{D.13}$$

For $y>1$ we perform the y and y_2 integration over the first term in Eq. (D.4), then expand to lowest orders in $\frac{1}{z}$ and integrate over x. This gives the logarithm

$$\int_0^1 \mathrm{d}x \int_0^\infty \mathrm{d}y \int_0^\infty \mathrm{d}y_2 \, F_z^{(1)}(x,y,y_2) = -3 + 2\ln z + \mathcal{O}(z \ln z). \tag{D.14}$$

Obtaining the next order is more delicate than expanding in $\frac{1}{z}$ before the x-integration. The second term gives again only a constant, and the limit $z\to\infty$ can be taken in the integrand

$$\lim_{z\to\infty} \int_0^1 \mathrm{d}x \int_0^\infty \mathrm{d}y \int_0^\infty \mathrm{d}y_2 \, F_z^{(2)}(x,y,y_2) = -\ln 2 \, . \tag{D.15}$$

In summary, we find

$$z^2 \frac{\mathrm{d}}{\mathrm{d}z^2} \tilde{\Phi}_{2,0}(z) = \mathcal{N}^2 \big[2\ln z - 3 + \mathcal{O}(\tfrac{1}{z} \ln z)\big] \, . \tag{D.16}$$

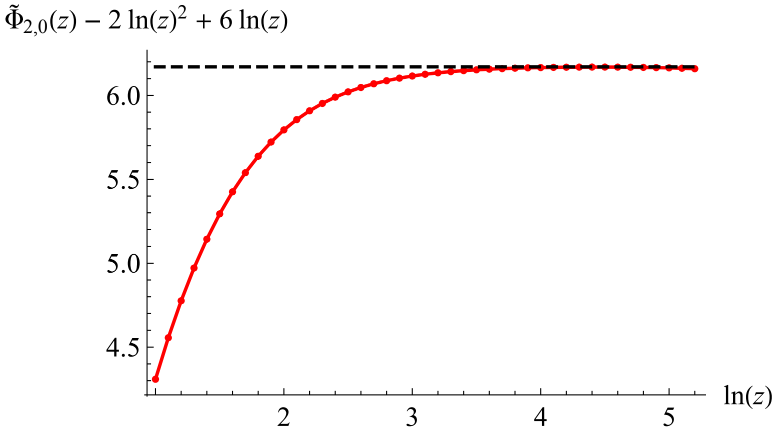

Figure 12: Asymptotics of $\tilde{\Phi}_{2,0}(z) - 2\ln(z)^2 + 6\ln(z)$ for large z. The dashed line is the asypmptotic value 6.17.

And consequently after integration

$$\tilde{\Phi}_{2,0}(z) = \mathcal{N}^2\big[2(\ln z)^2 - 6\ln z + \alpha_0 + \mathcal{O}(\tfrac{1}{z}\ln z)\big]. \tag{D.17}$$

We plot the asymptotics in Fig. 12 and find numerically $\alpha_0 \approx 6.17(2)$.

References

[1] G. Parisi and N. Sourlas, *Random magnetic fields, supersymmetry, and negative dimensions*, Phys. Rev. Lett. **43** (1979) 744–5.

[2] M. Mézard, G. Parisi and M.A. Virasoro, *Spin Glas Theory and Beyond*, World Scientific, Singapore, 1987.

[3] K. Wilson and J. Kogut, *The renormalization group and the ε-expansion*, Phys. Rep. **12** (1974) 75–200.

[4] F.J. Wegner and A. Houghton, *Renormalization group equation for critical phenomena*, Phys. Rev. A **8** (1973) 401–12.

[5] D.S. Fisher, *Random fields, random anisotropies, nonlinear sigma models and dimensional reduction*, Phys. Rev. B **31** (1985) 7233–51.

[6] O. Narayan and D.S. Fisher, *Dynamics of sliding charge-density waves in 4-epsilon dimensions*, Phys. Rev. Lett. **68** (1992) 3615–18.

[7] O. Narayan and D.S. Fisher, *Critical behavior of sliding charge-density waves in 4-epsilon dimensions*, Phys. Rev. B **46** (1992) 11520–49.

[8] T. Nattermann, S. Stepanow, L.-H. Tang and H. Leschhorn, *Dynamics of interface depinning in a disordered medium*, J. Phys. II (France) **2** (1992) 1483–8.

[9] L. Balents, J.P. Bouchaud and M. Mézard, *The large scale energy landscape of randomly pinned objects*, J. Phys. I (France) **6** (1996) 1007–20, cond-mat/9601137.

[10] P. Le Doussal, *Finite temperature Functional RG, droplets and decaying Burgers turbulence*, Europhys. Lett. **76** (2006) 457–463, cond-mat/0605490.

[11] A.A. Middleton, P. Le Doussal and K.J. Wiese, *Measuring functional renormalization group fixed-point functions for pinned manifolds*, Phys. Rev. Lett. **98** (2007) 155701, cond-mat/0606160.

[12] P. Le Doussal and K.J. Wiese, *How to measure Functional RG fixed-point functions for dynamics and at depinning*, EPL **77** (2007) 66001, cond-mat/0610525.

[13] A. Rosso, P. Le Doussal and K.J. Wiese, *Numerical calculation of the functional renormalization group fixed-point functions at the depinning transition*, Phys. Rev. B **75** (2007) 220201, cond-mat/0610821.

[14] P. Le Doussal, K.J. Wiese, S. Moulinet and E. Rolley, *Height fluctuations of a contact line: A direct measurement of the renormalized disorder correlator*, EPL **87** (2009) 56001, arXiv:0904.4156.

[15] P. Le Doussal and K.J. Wiese, *2-loop functional renormalization for elastic manifolds pinned by disorder in N dimensions*, Phys. Rev. E **72** (2005) 035101 (R), cond-mat/0501315.

[16] P. Le Doussal, K.J. Wiese and P. Chauve, *2-loop functional renormalization group analysis of the depinning transition*, Phys. Rev. B **66** (2002) 174201, cond-mat/0205108.

[17] AA. Middleton, *Asymptotic uniqueness of the sliding state for charge-density waves*, Phys. Rev. Lett. **68** (1992) 670–673.

[18] P. Chauve, P. Le Doussal and K.J. Wiese, *Renormalization of pinned elastic systems: How does it work beyond one loop?*, Phys. Rev. Lett. **86** (2001) 1785–1788, cond-mat/0006056.

[19] P. Le Doussal, K.J. Wiese and P. Chauve, *Functional renormalization group and the field theory of disordered elastic systems*, Phys. Rev. E **69** (2004) 026112, cond-mat/0304614.

[20] P. Chauve and P. Le Doussal, *Exact multilocal renormalization group and applications to disordered problems*, Phys. Rev. E **64** (2001) 051102/1–27, cond-mat/0006057.

[21] S. Scheidl and Y. Dincer, *Interface fluctuations in disordered systems: Universality and non-gaussian statistics*, (2000), cond-mat/0006048.

[22] P. Le Doussal, *Exact results and open questions in first principle functional RG*, Annals of Physics **325** (2009) 49–150, arXiv:0809.1192.

[23] K. Johansson, *Shape fluctuations and random matrices*, Communications in Mathematical Physics **209** (2000) 437–76, math/9903134.

[24] M. Prähofer and H. Spohn, *Universal distributions for growth processes in 1 + 1 dimensions and random matrices*, Phys. Rev. Lett. **84** (2000) 4882–4885, cond-mat/9912264.

[25] M. Prähofer and H. Spohn, *Statistical self-similarity of one-dimensional growth processes*, Physica A **279** (2000) 342–52, cond-mat/9910273.

[26] M. Kardar, G. Parisi and Y.-C. Zhang, *Dynamic scaling of growing interfaces*, Phys. Rev. Lett. **56** (1986) 889–892.

[27] E. Frey and U.C. Täuber, *Two-loop renormalization group analysis of the Burgers-Kardar-Parisi-Zhang equation*, Phys. Rev. E **50** (1994) 1024–1045.

[28] M. Lässig, *On the renormalization of the Kardar-Parisi-Zhang equation*, Nucl. Phys. **B 448** (1995) 559–574, cond-mat/9501094.

[29] E. Frey, U.C. Täuber and T. Hwa, *Mode coupling and renormalization group results for the noisy Burgers equation*, Phys. Rev. E **53** (1996) 4424.

[30] K.J. Wiese, *Critical discussion of the 2-loop calculations for the KPZ-equation*, Phys. Rev. **E 56** (1997) 5013–5017, cond-mat/9706009.

[31] K.J. Wiese, *On the perturbation expansion of the KPZ-equation*, J. Stat. Phys. **93** (1998) 143–154, cond-mat/9802068.

[32] E. Marinari, A. Pagnani and G. Parisi, *Critical exponents of the KPZ equation via multi-surface coding numerical simulations*, J. Phys. A **33** (2000) 8181–92.

[33] M. Prähofer and H. Spohn, *An exactly solved model of three-dimensional surface growth in the anisotropic KPZ regime*, J. Stat. Phys. **88** (1997) 999–1012, cond-mat/9612209.

[34] J. Krug, *Origins of scale invariance in growth processes*, Advances in Physics **46** (1997) 139–282.

[35] M. Mezard, *Disordered systems and Burger's turbulence*, J. Phys. IV (France) **8** (1997) 27–38, cond-mat/9801029.

[36] E. Medina, T. Hwa, M. Kardar and Y.C. Zhang, *Burgers equation with correlated noise: Renormalization-group analysis and applications to directed polymers and interface growth*, Phys. Rev. **A 39** (1989) 3053.

[37] T. Hwa and D.S. Fisher, *Anomalous fluctuations of directed polymers in random media*, Phys. Rev. B **49** (1994) 3136–54, cond-mat/9309016.

[38] R. Bundschuh and T. Hwa, *An analytic study of the phase transition line in local sequence alignment with gaps*, Discrete Applied Mathematics **104** (2000) 113–42.

[39] R. Bundschuh and T. Hwa, *RNA secondary structure formation: a solvable model of heteropolymer folding*, Phys. Rev. Lett. **83** (1999) 1479–82, cond-mat/9903089.

[40] T. Hwa and M. Lässig, *Optimal detection of sequence similarity by local alignment*. RECOMB 98, pages 109–16, 1998, cond-mat/9712081.

[41] T. Nattermann, *Theory of the random field Ising model*, in A.P. Young, editor, *Spin glasses and random fields*, World Scientific, Singapore, 1997.

[42] S. Lemerle, J. Ferré, C. Chappert, V. Mathet, T. Giamarchi and P. Le Doussal, *Domain wall creep in an Ising ultrathin magnetic film*, Phys. Rev. Lett. **80** (1998) 849.

[43] G. Grüner, *The dynamics of charge-density waves*, Rev. Mod. Phys. **60** (1988) 1129–81.

[44] G. Blatter, M.V. Feigel'man, V.B. Geshkenbein, A.I. Larkin and V.M. Vinokur, *Vortices in high-temperature superconductors*, Rev. Mod. Phys. **66** (1994) 1125.

[45] T. Giamarchi and P. Le Doussal, *Statics and dynamics of disordered elastic systems*, in A.P. Young, editor, *Spin glasses and random fields*, World Scientific, Singapore, 1997, cond-mat/9705096.

[46] T. Giamarchi and P. Le Doussal, *Elastic theory of flux lattices in the presence of weak disorder*, Phys. Rev. B **52** (1995) 1242–70, cond-mat/9501087.

[47] T. Giamarchi and P. Le Doussal, *Elastic theory of pinned flux lattices*, Phys. Rev. Lett. **72** (1994) 1530–3.

[48] T. Nattermann and S. Scheidl, *Vortex-glass phases in type-II superconductors*, Advances in Physics **49** (2000) 607–704, arXiv:cond-mat/0003052.

[49] A. Prevost, E. Rolley and C. Guthmann, *Dynamics of a helium-4 meniscus on a strongly disordered cesium substrate*, Phys. Rev. B **65** (2002) 064517/1–8.

[50] A. Prevost, PhD thesis, Orsay, 1999.

[51] D. Ertas and M. Kardar, *Critical dynamics of contact line depinning*, Phys. Rev. E **49** (1994) 2532.

[52] P. Le Doussal and K.J. Wiese, *Elasticity of a contact-line and avalanche-size distribution at depinning*, Phys. Rev. E **82** (2010) 011108, arXiv:0908.4001.

[53] M. Kardar, *Lectures on directed paths in random media*, in F. David, P. Ginsparg and J. Zinn-Justin, editors, *Fluctuating Geometries in Statistical Mechanics and Field Theory*, Volume *LXII* of *Les Houches, école d'été de physique théorique 1994*, Elsevier Science, Amsterdam, 1996.

[54] L.E. Aragon, A.B. Kolton, P. Le Doussal, K.J. Wiese and E. Jagla, *Avalanches in tip-driven interfaces in random media*, EPL **113** (2016) 10002, arXiv:1510.06795.

[55] G. Durin, F. Bohn, M.A. Correa, R.L. Sommer, P. Le Doussal and K.J. Wiese, *Quantitative scaling of magnetic avalanches*, Phys. Rev. Lett. **117** (2016) 087201, arXiv:1601.01331.

[56] L. Laurson, X. Illa, S. Santucci, K.T. Tallakstad, K.J. Måløy and M.J. Alava, *Evolution of the average avalanche shape with the universality class*, Nat. Commun. **4** (2013) 2927.

[57] G. Durin and S. Zapperi, *Scaling exponents for Barkhausen avalanches in polycrystalline and amorphous ferromagnets*, Phys. Rev. Lett. **84** (2000) 4705–4708.

[58] O. Perkovic, K. Dahmen and JP. Sethna, *Avalanches, Barkhausen noise, and plain old criticality*, Phys. Rev. Lett. **75** (1995) 4528–4531.

[59] P. Le Doussal and K.J. Wiese, *Avalanche dynamics of elastic interfaces*, Phys. Rev. E **88** (2013) 022106, arXiv:1302.4316.

[60] A. Dobrinevski, P. Le Doussal and K.J. Wiese, *Statistics of avalanches with relaxation and Barkhausen noise: A solvable model*, Phys. Rev. E **88** (2013) 032106, arXiv:1304.7219.

[61] A. Dobrinevski, P. Le Doussal and K.J. Wiese, *Non-stationary dynamics of the Alessandro-Beatrice-Bertotti-Montorsi model*, Phys. Rev. E **85** (2012) 031105, arXiv:1112.6307.

[62] P. Le Doussal, M. Müller and K.J. Wiese, *Equilibrium avalanches in spin glasses*, Phys. Rev. B **85** (2012) 214402, arXiv:1110.2011.

[63] P. Le Doussal and K.J. Wiese, *Driven particle in a random landscape: disorder correlator, avalanche distribution and extreme value statistics of records*, Phys. Rev. E **79** (2009) 051105, arXiv:0808.3217.

[64] P. Le Doussal, M. Müller and K.J. Wiese, *Cusps and shocks in the renormalized potential of glassy random manifolds: How functional renormalization group and replica symmetry breaking fit together*, Phys. Rev. B **77** (2007) 064203, arXiv:0711.3929.

[65] P. Le Doussal and K.J. Wiese, *First-principle derivation of static avalanche-size distribution*, Phys. Rev. E **85** (2011) 061102, arXiv:1111.3172.

[66] P. Le Doussal, A.A. Middleton and K.J. Wiese, *Statistics of static avalanches in a random pinning landscape*, Phys. Rev. E **79** (2009) 050101 (R), arXiv:0803.1142.

[67] P. Le Doussal and K.J. Wiese, *Size distributions of shocks and static avalanches from the functional renormalization group*, Phys. Rev. E **79** (2009) 051106, arXiv:0812.1893.

[68] A. Rosso, P. Le Doussal and K.J. Wiese, *Avalanche-size distribution at the depinning transition: A numerical test of the theory*, Phys. Rev. B **80** (2009) 144204, arXiv:0904.1123.

[69] J. Berges, N. Tetradis and C. Wetterich, *Non-perturbative renormalization flow in quantum field theory and statistical physics*, Phys. Rep. **363** (2002) 223–386.

[70] N.N. Bogoliubov and O.S. Parasiuk, *Über die Multiplikation der Kausalfunktionen in der Quantentheorie der Felder*, Acta Math. **97** (1957) 227.

[71] K. Hepp, *Proof of the Bogoliubov-Parasiuk theorem on renormalization*, Comm. Math. Phys. **2** (1966) 301–326.

[72] W. Zimmermann, *Convergence of Bogoliubov's method of renormalization in monmentum space*, Commun. Math. Phys. **15** (1969) 208–234.

[73] M.C. Bergere and Y.-M.P. Lam, *Bogoliubov-Parasiuk theorem in the α-parametric representation*, J. Math. Phys. **17** (1976) 1546–1557.

[74] F. David, B. Duplantier and E. Guitter, *Renormalization theory for interacting crumpled manifolds*, Nucl. Phys. **B 394** (1993) 555–664, hep-th/9211038.

[75] F. David, B. Duplantier and E. Guitter, *Renormalization theory for the self-avoiding polymerized membranes*, (1997), cond-mat/9702136.

[76] K.J. Wiese, *Polymerized membranes, a review*, Volume *19* of *Phase Transitions and Critical Phenomena*, Acadamic Press, London, 1999.

[77] J.C. Collins, *Renormalization*, Cambridge University Press, 1984.

[78] L. Balents and P. Le Doussal, *Thermal fluctuations in pinned elastic systems: field theory of rare events and droplets*, Annals of Physics **315** (2005) 213–303, cond-mat/0408048.

[79] P. Grassberger, D. Dhar and P. K. Mohanty, *Oslo model, hyperuniformity, and the quenched Edwards-Wilkinson model*, Phys. Rev. E **94** (2016) 042314.

[80] Ezequiel E. Ferrero, Sebastián Bustingorry and Alejandro B. Kolton, *Non-steady relaxation and critical exponents at the depinning transition*, Phys. Rev. E **87** (2013) 032122, arXiv:1211.7275.

[81] M. Kardar, D.A. Huse, C.L. Henley and D.S. Fisher, *Roughening by impurities at finite temperatures (comment and reply)*, Phys. Rev. Lett. **55** (1985) 2923–4.

[82] A.A. Middleton, *Numerical results for the ground-state interface in a random medium*, Phys. Rev. E **52** (1995) R3337–40.

[83] P. Le Doussal and C. Monthus, *Exact solutions for the statistics of extrema of some random 1d landscapes, application to the equilibrium and the dynamics of the toy model*, Physica A **317** (2003) 140–98, cond-mat/0204168.

[84] P. Le Doussal and K.J. Wiese, *Higher correlations, universal distributions and finite size scaling in the field theory of depinning*, Phys. Rev. E **68** (2003) 046118, cond-mat/0301465.

[85] P. Le Doussal and K.J. Wiese, *Functional renormalization group at large N for random manifolds*, Phys. Rev. Lett. **89** (2002) 125702, cond-mat/0109204.

[86] P. Le Doussal and K.J. Wiese, *Functional renormalization group at large N for disordered elastic systems, and relation to replica symmetry breaking*, Phys. Rev. B **68** (2003) 174202, cond-mat/0305634.

[87] P. Le Doussal and K.J. Wiese, *Derivation of the functional renormalization group β-function at order $1/N$ for manifolds pinned by disorder*, Nucl. Phys. B **701** (2004) 409–480, cond-mat/0406297.

Contents